1.0 Introduction

In aerospace and electronics industries, the demand for high performance adhesives and composites exhibiting a wider range of mechanical and physical properties results in the continuous evaluation of applicable materials. Solutions to these barriers and technical needs have yielded an increase in the use of polymers for aerospace design and construction, and aided the electronics industry in expanding circuit board technologies. The continual demand for new and better products has led to the development of many novel material systems beyond those that exist today, such as epoxies, vinyl esters, and bismaleimides. These traditional solutions either lack thermal stability in high temperature applications or require narrow processing windows for application. Some cyanate ester resins, a novel class of thermosetting materials, are systems which exhibit enhanced physical and thermal properties when compared to the existing polymer systems. These cyanate esters display features including high glass transition temperatures, low dielectric loss, low moisture absorption, low corrosion potential, and easy processing, and thus show promise in these technical applications.

AroCy cyanate esters are a family of aryl dicyanate monomers and their prepolymer resins containing the reactive cyanate (-O-CN) functional group. When heated, this cyanate functionality undergoes an exothermic cyclotrimerization reaction to form triazine ring connecting units, eventually

resulting in gelation and the formation of thermoset polycyanurate plastics. These ester resins provide thermoset performance far beyond the range of epoxies (glass transition temperatures much greater than epoxies), while retaining the best easy-processing features of those materials. The blending of cyanate esters with high performance thermoplastics offers an additional or broader range of performance properties. Generally, performance is increased as a result of the phase structure of the phase domains in these blends can differ depending on the cure cycle, and these differences afford performance property separated morphology that is produced by the blending process. Furthermore, the size and differentiation.

Since cyanate esters are still novel in their development, little is known about the time-temperature behavior of these resins, or the effects thermoplastic toughening has on their properties. The objectives of this research are to characterize the long term mechanical properties of these materials, develop a method for determining the effects physical and chemical aging exert on these properties, and evaluate a specific cyanate ester resin for use in high temperature applications.

A major characteristic of isothermal aging on materials in the glassy state is the decrease in volume, enthalpy, and entropy over time. This reversible process is known as physical aging. Due to the time dependent nature of this event, this densification process may affect the long-term properties of a material and an increase in material stiffness may be observed. Chemical aging or degradation

also has great significance on the behavior of polymers, as it is an irreversible process that usually causes substantial changes in polymer properties. This research, while incorporating cyanate ester thermosets, has developed a method of understanding these properties and separated each phenomenon in the long-term mechanical regime of these materials by varying the aging atmosphere and exposure times.

Added to this understanding, is an examination of the physical changes, which occur during the cure of these materials. The ability to measure these cure properties is an invaluable asset in determining the processing capabilities of a material, and to that end, two novel approaches to obtaining these measurements were developed using dynamic mechanical and dielectric instrumentation. The development of sample preparation, instrument testing and data analysis methods were examined.

Concurrent with the laboratory investigations was a literature search covering the attributes of cyanate esters and includes a brief history of the synthesis of the resins, as well as the reactions of cyanate esters and the development of the cyanate ester network thermoset. Certain areas of intensive investigation were identified that applied the theory of physical aging and the concept of chemical degradation. An intensive discussion of laboratory results follows the literature review and the work is concluded by determining the utility of the commercially available AroCy B-10 cyanate ester resin in high temperature applications.

2.0 Background and Literature Review

2.1 Introduction

The physical and mechanical properties of a material determine the behavior of that material and its subsequent application in a particular environment. If these properties change abruptly or as a function of exposure to that environment, the expected performance features of the material will also be directly affected in the specified application. Therefore, it is important to understand these property changes and possess the ability to predict their effect in a specified application. In such a spirit, this chapter will discuss, in increasing detail, the synthesis, reactivity and use of cyanate esters. Included will be the theory of physical aging along with the methods to detect and measure this event in polymers. Finally, the kinetics, mechanisms and methods of examining chemical degradation in polymeric materials are reviewed.

Cyanate ester thermosetting polymers are a novel addition to the ever-growing number of materials for aerospace applications. They provide[1] excellent high performance characteristics such as a high T_g, solvent resistance, and a low dielectric constant. However, an inherent brittleness exists in these materials due to their highly cross-linked structure. As a result of this brittleness, a thermoplastic or rubber is needed as an additive to increase the toughness of the material. Unfortunately, choosing the proper toughener is difficult since an optimization of all thermal and mechanical properties of the blended material is

desired. It has also been shown[2] that to obtain the best results for toughening cyanate esters, while retaining their high performance properties, incorporation of thermoplastic polymers with similar glass transition temperatures to the cyanate ester resins was desirable. These blends decrease the brittleness of the material while retaining the high temperature properties of the thermoset. The present research concentrated its effort on the examination of the long-term properties of the untoughened cyanate network. The thermoplastic toughened blend was also examined as well, and provided insight on the effect created by the toughener on the time-temperature behavior of the material. A short discussion of the techniques employed and relevant literature is contained in this chapter.

Physical aging is an event that occurs in all glass forming materials. It is the gradual process of material densification that is believed to be thermodynamically driven and kinetically controlled below the T_g. It may greatly affect many properties in a way dependent on the temperature of the aging. The mechanical and physical properties of the polymer are the most significantly affected. Consequently, it is important to understand these property changes to predict the material behavior in (or under) the application conditions. In addition, knowledge of the aging behavior is indispensable to the prediction of long term properties using short-term tests. One example involves the concept of time-temperature superposition.

The time-temperature-superpositon principle (TTSP) was developed to aid in the prediction of the long-term behavior of a material using short-term experiments. Williams, Landel and Ferry[79] developed a relation known as the WLF equation which equates the amount of shift required in log time, log a_T, of any polymer material property to the temperature of interest. The procedure gave a foundation to the empirically based "Master Curve" construction of Tobolsky and Leaderman[174-175]. This TTSP principle can be further extended to doubly shift information and create master-master curves. This scheme may apply to almost any material property that can be measured isothermally over a range of temperatures as long as certain assumptions apply (i.e. continued curing of the material, chemical degradation, or conflicting physical behavior). The result is a family of isothermal curves that can be shifted horizontally along the log time axis. The resultant master curve displays the predictive long-term behavior of the material from short-term experiments. The major assumption is that the changes in temperature do not alter the mechanisms of the processes being observed.

Besides physical aging, chemical degradation is also an important change to consider when characterizing polymeric materials at elevated temperatures. Random thermal degradation is accompanied by the random reduction of the molecular weight of the polymer. This process tends to occur through chain rupture or scission at different points along the chain leaving large fragments in comparison to the monomer unit[3]. This type of aging is irreversible and can be

initiated not only thermally, but also by UV light, oxygen or ozone, or catalyzed by other foreign material in the polymer matrix. It may occur entirely at random or be initiated at chain ends or through other weak links in the polymer backbone. This aging process tends to have an opposite effect on material properties to those observed in physical aging. In polymer networks, chain fragments are separated from the network yielding more free volume in the material and this is in direct contrast to the densification process.

Throughout this chapter, several comparisons between the results encountered in this investigation and literature report are made. Most notably are those related to the competing processes of chemical and physical aging.

2.2 Cyanate Esters

2.2.1 Introduction

This section of the literature review discusses the overall development of cyanate ester materials. A brief historical background and the synthetic challenges that were originally faced in the development process are discussed as well as the efforts that led to commercial monomer synthesis. Other challenges such as functionalized monomers, cure cycle investigations, and kinetic analyses with mechanistic observations are also discussed. Finally, the development and comparison of toughening agents is also included.

The term "cyanate ester resin" is used to describe both prepolymers and cured resins, the former containing the reactive ring forming cyanate (-O-C≡N) functional group. To fully examine cyanate esters, it is important to understand the development history of cyanate ester monomers, how these monomers are reacted, and the recent activities of developing thermosetting materials from cyanate esters.

Problems were soon encountered during the initial attempts to synthesize cyanate esters; including cyanic acid difficulties {cyanic acid (HOCN) tends to exist predominantly in the iso form (HNCO), the resultant major product was an isocyanate [4] (Scheme 2-1)}, the inability to convert mineral acid esters to the desired monomer[5], or displacement reactions on cyanogen halides with alkoxides[6].

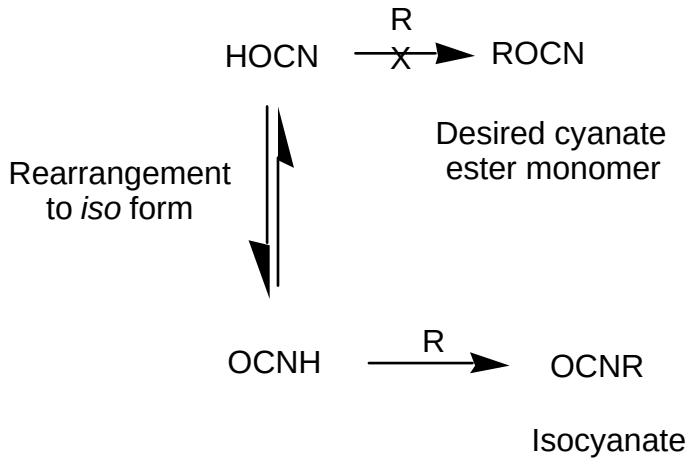

Scheme 2-1. Attempted Cyanate Ester Synthesis from Cyanic Acid

Grigat and Putter [7-9], were among the first to report a simple synthesis of cyanate esters by reaction of a phenol with cyanogen halides (Scheme 2-2). This method is reportedly successful with mono- and poly-phenolic compounds as well as a number of aliphatic hydroxyl compounds.

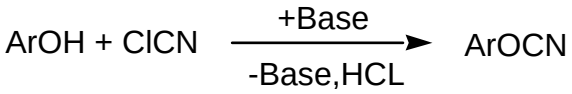

Scheme 2-2. Synthesis of Cyanate Esters as Reported by Grigat and Putter[7-9]

Martin,[10] and Jensen, and Holm[11] were also among the first to report the synthesis of cyanate esters; however, their methods were not quite as simple and resulted in relatively low yields. The research presented in this manuscript employed a commercially available dicyanate monomer (AroCy B-10). This monomer is a bisphenol A based dicyanate developed by Ciba-Geigy Corporation.

2.2.2 Reactions of Cyanate Esters

Aryl cyanates (unlike their aliphatic counterparts), do not rearrange to form aryl isocyanates, thus allowing for many further reactions[12]. The carbon atom of the -OCN group is strongly electrophilic because of its electronegative neighbors, O

and N. Consequently, nucleophilic reagents readily react with cyanates even under mild conditions. Acid catalysis of the nucleophilic addition reaction occurs by activation of the -OCN group by protonation, while base catalysis occurs by enhancement of the nucleophilic strength of the incoming nucleophile. Alternatively, nucleophilic addition on the oxygen atom of the -OCN group of aryl cyanates has also been reported[64].

Electrophilic addition to the -OCN group of aryl cyanates (Ar-OCN) proceeds less readily than the corresponding addition to aryl nitriles (Ar-CN). No reaction occurred in attempted alkylations with alkyl halides, sulfonates and dialkyl sulfates [12-13]. However, a few types of electrophilic addition reactions proceed smoothly[14], but are not relevant to our investigation.

The possible reactions of cyanate esters can be classified in the following outline:[2]

1) Nucleophilic reactions
    a) To the carbon atom of the -OCN group
        i) Nucleophiles having one acidic H on the O, S, or N atom (E.g. ROH, ArOH, RSH, R'RNH, ketoximes (HON=CRR'), etc.)
        ii) Reagents having a nucleophilic carbon atom, C* (E.g. $C^*H_2(CN)_2$, C^*H_3MgX (RMgX), H*CN, etc.)

iii) Nucleophiles having two or more acidic hydrogens on the total O, S, or N atoms of the nucleophile

(E.g. H_2O, H_2S, NH_3, RNH_2, NH_2OH, semi-carbazides H_2N-NR-CO-NHR, cyanamides H_2NCN, amidocarboxylic acids H_2N CHR-COOH, sulfonamides H_2N-SO_2R, hydrazines H_2N-NH_2 and HRN-NRH, sulfonylhydrazines H_2N-NH-SO_2R, etc.)

iv) Ring closure to form triazines by self-condensation via N as the nucleophile

v) Aryl cyanates can act as agents for the elimination of water from aldoximes HON=CH-R, amides $RCONH_2$, hydroxamic acids HON=C(OH)R, carboxylic acids RCOOH, etc.

vi) Aryl cyanates can act as agents for the elimination of H_2S from organic compounds like thioureas, dithiocarbonates, thiocarboxylic acids, etc.

b) To the O of the -OCN group

(E.g. dialkyl phosphites $(RO)_2P=O$)

2) Electrophilic addition reactions (as previously discussed)

3) 1,3-dipolar addition to the -OCN group

(E.g. sodium azide NaN_3, diazomethane $CH_2=N=N$, diazoacetic ester C_2H_5COO-CH=N=N, nitrones R-CH=N($\rightarrow$O)-R', nitrilimines C_6H_5-C(Cl)=N-NH-C_6H_5, nitrile oxides $Ar-C\equiv N\rightarrow O$, etc.)

Reactions of Cyanate Esters with Aromatic Phenolic Compounds

Phenols add smoothly to aryl cyanates in the presence of bases to give symmetrical or unsymmetrical bisaryl imidocarbonates[15]. (Scheme 2.3)

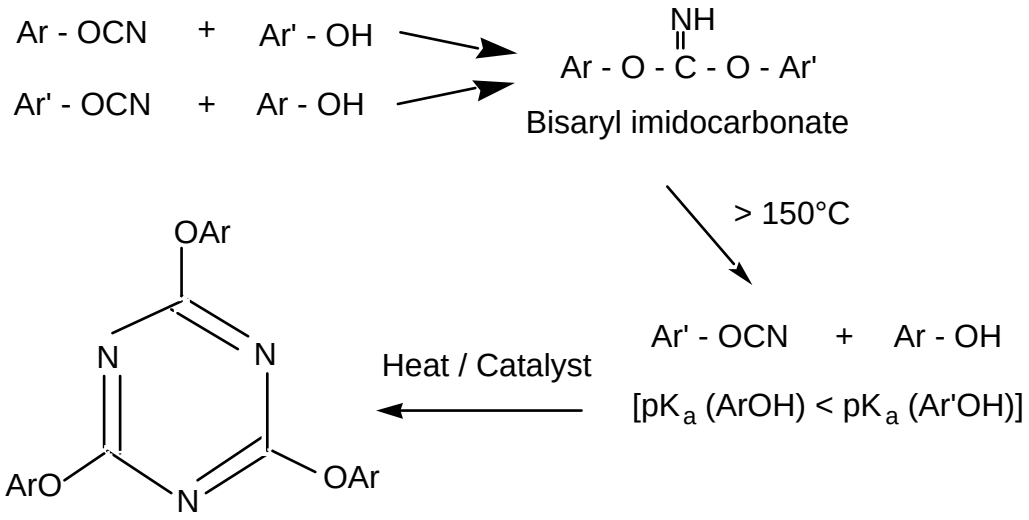

Scheme 2-3. Reaction of Aryl Cyanates with Aromatic Phenols

When Ar and Ar' are different, the decomposition of the imidocarbonate leads to the formation of the more acidic phenol[15], and ultimately the cyclic cyanate ester network.

Direct Ring Closure to form s-Triazines

A number of reactions of aryl cyanates lead to direct ring closure and formation of s-triazine derivatives. Tris-aryloxy-s-triazines are formed almost quantitatively by the trimerization of aryl cyanates[10, 17]. The trimerization is promoted by acids, bases, and phenolic compounds.

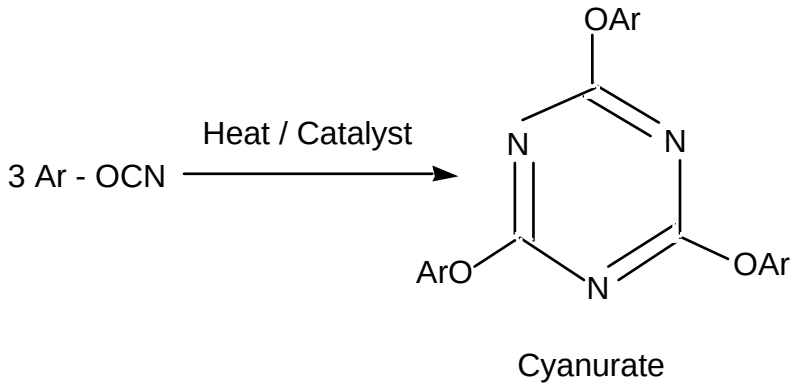

Scheme 2-4. Direct Ring Closure to form s-Triazines

2.2.3 Cyanate Ester Resin Networks

Cyanate ester resins are bisphenolic or polyphenolic derivatives containing the ring forming cyanate (-OCN) functional group. Chemically, this family of thermosetting monomers and their pre-polymers are esters of bisphenol (or polyphenol) and cyanic acid. The esters cyclotrimerize to form substituted triazine rings on heating[18]. Crosslinking of cyanate esters occurs via cyclotrimerization to form 3-dimensional networks of oxygen linked triazine rings. The curing reaction is classified as an addition polymerization and occurs without emission of volatile by-products. (Scheme 2.5)

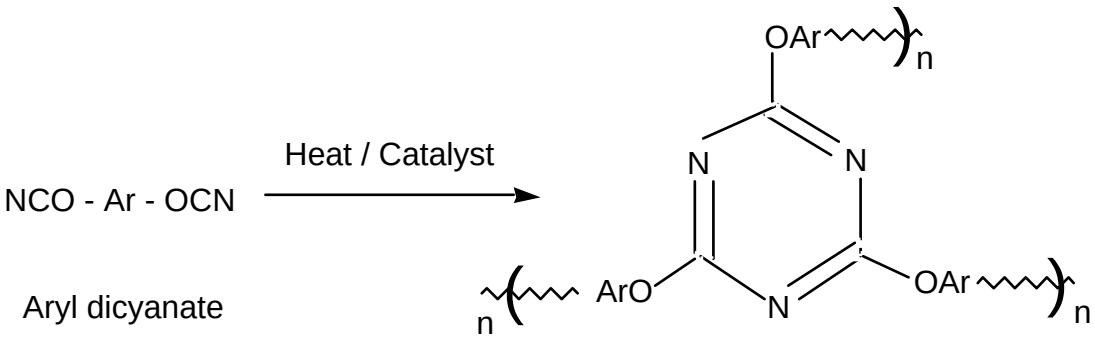

Scheme 2-5. Formation of Three-dimensional Networks by Cyclotrimerization

Several different companies have increasingly explored the commercial utility of cyanate ester resins over the past 15 years. The development of a clean synthetic route to cyanate ester monomers[19] led to the first commercially available Bayer/Mobay 'Triazine A' dicyanate pre-polymer resin in 1976. However, 'Triazine A' performed inconsistently and had to be withdrawn in 1978[18]. The Bayer technology was licensed to Mitsubishi Gas Chemical who introduced 'BT Resins' which were blends of bismaleimide and cyanate ester resins.

Rhone-Poulenc licensed Bayer-AG patents and manufacturing rights in 1984[21]. Research at Rhone-Poulenc focused on producing high purity monomers from a variety of bisphenol precursors. This evolved into an 'AroCy® family' of O-alkylated, fluorinated, sulfur-linked and asymmetrical cyanate resins with expanded versatility. These developments were commercialized by Rhone-Poulenc from 1985-89[20-22]. The Rhone-Poulenc cyanate ester business was

recently (1992-93) purchased by Ciba-Geigy, Inc. Finally, Dow Chemical Company introduced an experimental cyanate ester 'XU 71787' based on an cyclo-aliphatic linked bisphenol[23-24]. (Table 2.1) The AroCy® B-10 monomer was chosen for study because its structure suggested mechanistic explanations of physical aging and chemical degradation would be straightforward. It is also of lower cost than other cyanate resins and because of this, is considered a preferred candidate for industrial use.

Table 2-1. Commercially Available Dicyanate Monomers from Ciba-Geigy, Inc. and Dow Chemical Company

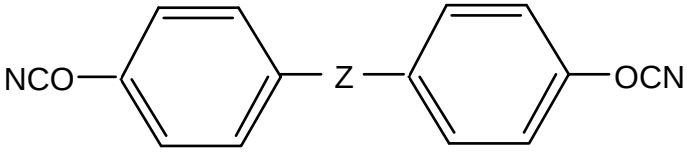

Structure - Z-	Trade Name	Physical Form (25°C)	M.P. (°C) or η_{melt}/ °C	Cured Tg °C TMA	TGA Onset (Air) °C
- $C(CH_3)_2$ -	AroCy B-10	solid	79°C	257	411
- CH_2 -	AroCy M-10	solid	106°C	244	403
- S -	AroCy T-10	solid	94°C	270	400
- $C(CF_3)_2$ -	AroCy F-10	solid	86°C	265	431
- $CH(CH_3)$ -	AroCy L-10	liquid	140cps/25°C	259	408
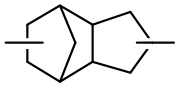	XU-71787	liquid	700cps/85°C	223	405

Pure cyanate ester monomers will cure relatively slowly. However, the addition of a catalyst exponentially increases the cure rate. Effective catalysts

recommended by Rhone-Poulenc for cyclotrimerization were a combination of transition metal complexes and active hydrogen; non-volatile, liquid phenolic compounds, e.g. nonyl phenol, that serve as co-catalysts. The latter also promoted enhanced solubility of the metal catalyst in the cyanate resin. In general, organic soluble compounds of most coordination metals serve as potent trimerization accelerators. Zinc, copper, manganese and cobalt compounds were preferred over the more reactive transition metals of iron, tin, titanium, lead and antimony. This solution is consistent with the observation that the latter group promotes the undesirable hydrolysis of an otherwise stable cyanate ester linkage. Specifically, chelated metals of acetylacetonates are less active hydrolysis catalysts (relative to the metal carboxylates, octoates and naphthenates) and also have the added advantage of increased latency (less trimerization activity at room temperature per unit of elevated temperature activity) due to the lower activity of the chelate[18].

In 1989, Allied Signal, Inc. patented a family of phenolic-triazine resins[25], the basic backbone structure of which is derived from 'phenolic resins' such as 'Novolac'. This was enabled by means of a cyanation reaction between the phenolic salt (usually a trialkyl amine salt) and cyanogen halide (chloride or bromide) in a suitable organic solvent. By adjusting the value of 'n' and lowering the extent of hydrogen bonding through the cyanation reaction, the physical form of 'cyanated phenolic resin' (the precursor of 'PT resins') can be tailored [26-27] to exhibit a range of physical properties from a low viscosity fluid to a low melting

solid. (Scheme 2-6) The 'PT resins' offer low shrinkage and do not emit volatiles during cure. They exhibit glass transition temperatures in excess of 300°C and the onset of thermal degradation in air is
440-450°C. This was the first evidence that cyanate esters could be developed to compete in high temperature applications.

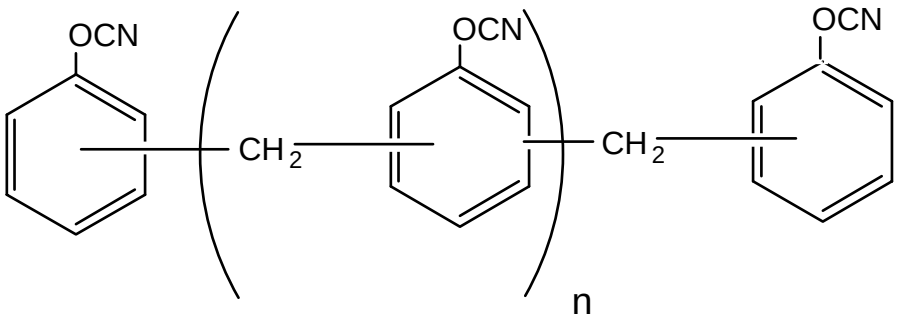

Scheme 2-6. General Structure of Phenolic Triazine PT Resins from Allied Signal, Inc.

The synthesis of several other cyanate esters has been reported by Abed and McGrath[28-29]. Particularly noteworthy are the novel phosphine oxide containing dicyanate ester monomers, and when polymerized, form crosslinked networks which exhibit good thermo-oxidative properties and afford superior char yields indicative of flame retardant characteristics. This work also demonstrated interesting trends between the 'glass transition - crystalline melting point' process window and the electron withdrawing / donating characteristics of the linking groups, *para* to the -OCN group. In general, it was demonstrated that electron-withdrawing groups promoted enhanced reactivities of the -OCN group toward cyclotrimerization[29] (Table 2-2). This observation is consistent with the

nucleophilic self-condensation trimerization discussed earlier, whereby electron-withdrawing groups para to the reactive sites increase the electrophilic nature of the carbon atom or each cyanate ester group.

Table 2-2. Novel Dicyanate Monomers Reported by Abed and McGrath.[28-29]

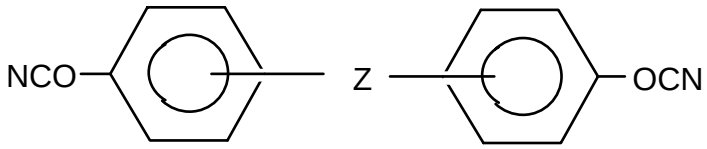

- Z -	Para/Meta to -OCN	MP °C	T_g °C DSC	TGA 5% (Air)	% Char 750°C
- SO2 -	para	-	212	355	-
- CO -	para	105	268	286	-
- C(Ph) (CF3) -	para	102	280	443	-
- O - (pAr) - SO2 - (pAr) - O -	para	107	254	448	-
- PO (Ar) -	para	-	-	371	32
- O - (pAr) - PO (Ar) - (pAr) - O -	para	45-50	282	444	38
- O - (pAr) - PO (Ar) - (pAr) - O -	meta	40-50	278	425	34

where '-(pAr)-' is a 1,4-phenylene linkage and 'Ar' is a phenyl group.

Several variations of modified cyanate ester monomers and their utility have been reported in the literature. Modifications include additional polymerizable

functionalities, homopolymerization or copolymerization techniques. For example, an extension of dicyanate ester monomer synthesis has been reported by Barton and coworkers[32] with the synthesis of several functionalized aryl cyanate esters bearing reactive allyl groups. (Scheme 2-7)

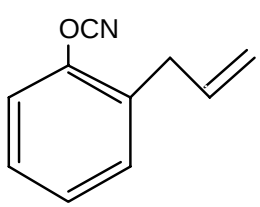

1-allyl-2-cyanatidobenzene

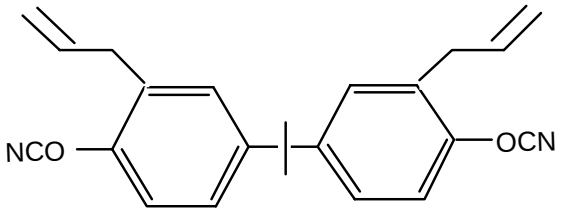

2,2'-Bis(3-allyl-4-cyanatidophenyl)isopropylidene

Scheme 2-7. Allyl Functionalized Aryl Dicyanate Ester Monomers Reported by Barton and coworkers[32]

These monomers are capable of undergoing quantitative homopolymerization and have been postulated as potential co-monomers for bismaleimide resins[31]. The co-reaction (Scheme 2-8) between the cyanate ester and the maleimide functional group forms the basis of Mitsubishi's commercial 'BT resin'.

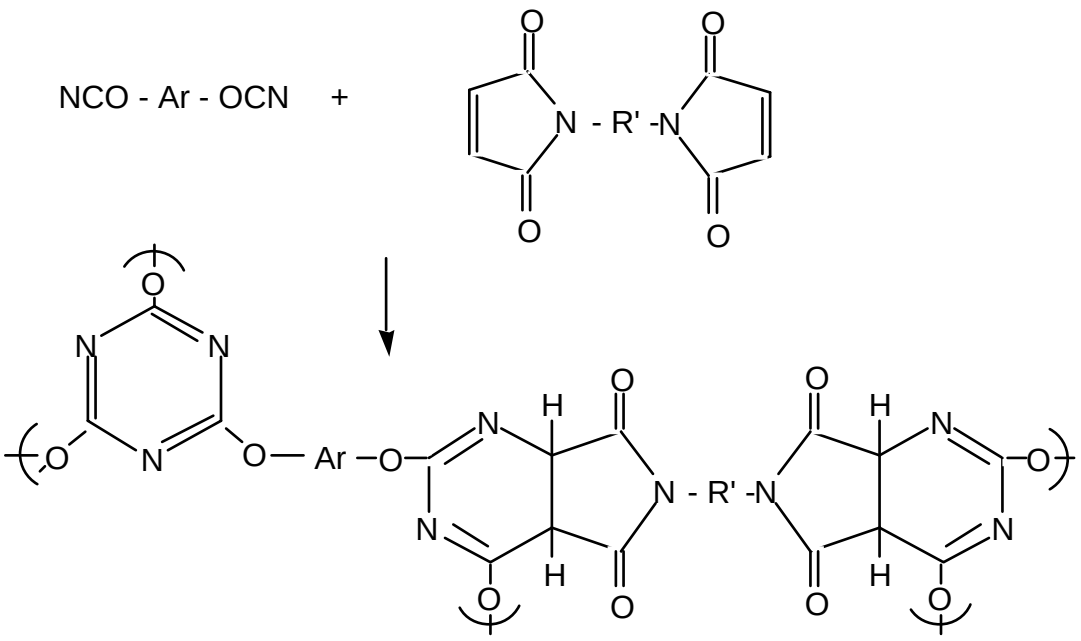

Scheme 2-8. Reaction scheme for Mitsubishi's Commercial 'BT Resin'

Although Scheme 2-8 shows a pyrimidine type structure for the proposed product, no evidence has been presented to confirm the existence of such a reaction.

Cyanate esters have also been used commercially as a co-monomer along with epoxies[35]. The four primary steps in the curing process have been identified as cyanate trimerization, epoxide insertion into the cyanurate, isomerization to the isocyanurate and further epoxide reaction to form chain extending oxazolidinone ring linkages[34,36].

Barclay et al.[33], have reported the formation of liquid crystalline (LC) thermosets by the thermal cyclotrimerization of dicyanate compounds of ring substituted

bis(4-hydroxyphenyl)terephthalate. The resulting triazine networks formed a mesophase during cure, and thereby enabled alignment in applied magnetic fields to yield oriented triazine networks with smectic-like molecular organization. Well-oriented triazine networks were reportedly obtained with low values of thermal expansion (17 ppm/°C) in the direction of the applied field. The networks had a T_g • 190 °C and exhibited little thermal decomposition until 440 °C. The LC alignment is thermally stable to 100 °C above their T_g.

Fyfe et al.[37] have investigated the mechanism of curing reactions of cyanate resins based on Bisphenol-A dicyanate, in solution and in the solid state by NMR spectroscopy. They employed high resolution ^{13}C and ^{15}N NMR to aid their investigations. Their studies suggested that, in solution, the main reaction is the formation of triazine rings as identified by NMR and MS techniques. Further characterization was accomplished by single crystal X-ray diffraction on an isolated crystalline compound from the mono-cyanate model compound. The cyclotrimerization process was rationalized in terms of very strong intermolecular intercyanate bonding interactions in the crystal structure of Bisphenol-A dicyanate monomer. Side products were formed by the reaction of cyanate functionalities with trace water found in the solvent. Interestingly, there was no NMR evidence for the formation of dimeric or other intermediate species prior to triazine ring formation. The curing reaction in the molten state was verified to be exclusively one of quantitative trimerization. Certainly, this is consistent with a 6π

electron transition state driven by aromatization. In addition, in the molten state, side reactions with water were minimized.

Owusu et al.[38] analyzed the curing behavior of cyanate ester systems using FTIR, DSC and rheological measurements to elucidate the role of transition metal catalysts employed to catalyze the cure reaction. The Bisphenol-A dicyanate was cured with octoates and naphthenates of zinc and manganese and with cobalt acetylacetonate at concentrations up to 750 parts per million (ppm) metal. Nonyl phenol at concentrations between 0-8 parts per hundred (phr) was used as a co-catalyst. Their results showed the final T_g's were significantly influenced by the catalyst/co-catalyst systems employed. They[39] further suggested that the kinetics of the uncatalyzed cyanate ester systems could be described by an autocatalytic rate law, while the rate of decrease of cyanate concentration in the catalyzed systems could be described by a second order rate law. Their investigations also suggested that the thermal stability of the network by thermal gravimetric analysis (TGA), with a zinc catalyst, decreases with increasing catalyst concentrations, whereas, no concentration effect was observed for samples cured with manganese.

Gupta[40] has reported a solution for describing the kinetics of polymerization of dicyanates. Using the 'kinetic solution approach' of the 'Flory-Stockmayer statistical theory', Gupta based his solution on the assumption that the trimerization reaction is the only reaction. (Later experiments by Gupta and

Macosko suggested that such an approximation was not an over-estimation as was also seen with Fyfe[37]). Accordingly,

$$3A \longrightarrow A_3 \quad (\text{ with a rate constant, } k \tag{2-1}$$

the kinetic solution involved a reaction kinetic equation for the time rate evolution of a typical polymeric molecule in terms of other polymeric species. From the solution to the kinetic equation, Gupta[40], derived the equation for the weight average degree of polymerization:

$$<Dp_w> = (1 + 2\alpha) / (1 - 2\alpha) \tag{2-2}$$

where α is the gel point or fraction of the material that is gelled to form an infinite network. As follows from the above equation, the gel point, wherein ($<DP_w> \rightarrow \bullet$), is predicted at 50% conversion under the assumption that trimerization is the exclusive reaction.

This model was consistent with the experimental observations of Baur et al.[41-42]. Based on their investigations and modeling of the process, they reported good agreements between the theoretical analysis by Gupta and their experimental values of 50% (α_g = 0.5) conversion at the gel-point. However, their reports on the experimental gel-point values varied considerably from those reported by other research groups. Shimp et al.[43], Simon and Gillham[44], Barton et al.[45] and Gupta and Macosko[46] report a gel conversion of ~ 60-65% (α_g = 0.6 - 0.65) for

several different bifunctional cyanate ester monomers covering a range of reaction temperatures and catalyst concentrations. The value of 'α_g = 0.6 - 0.65' is now an accepted value for the experimental gelation of these materials.

The discrepancy between 'theoretical predictions' (α_g = 0.5) and experimentally obtained values (α_g = 0.6 - 0.65), is rationalized as a consequence of trimerization as the exclusive reaction. The reaction process has been sufficiently investigated by various research groups to suggest that the exclusive trimerization reaction was reasonable and side reactions if any, were < 1%[45]. Gupta and Macosko[46] re-examined the assumptions underlying the 'mean field theory' (which forms the very basis of the 'kinetic solution approach') for possible explanations to the contradicting α_g values. The 'mean field theory' for theoretical gel-point prediction assumes the entire process is a 'reaction controlled polymerization process' and such an assumption, according to Gupta and Macosko[46], is not valid for the 'cyanate polymerization' under the conditions studied. It has been suggested for this case that molecules typically react only in small "neighborhoods" (as expected for a diffusion-controlled polymerization), thereby resulting in smaller average structures at any conversion. Consequently, gelation is delayed. These diffusion limitations encourage growth of isolated clusters owing to the limited accessibility of molecules. Thus Gupta and Macosko[46-47] suggest that cyanate polymerization is most likely 'diffusion controlled' rather than 'reaction controlled' and this results from steric hindrances limiting reactions to local domains. Williams[48] considered such substitution

(steric) effects and introduced a parameter 'r' into the kinetic model, wherein 'r' decreases continuously with increasing cluster size (or molecular weight) due to diffusional restrictions. The justification being that the reactivity of a free '-OCN group' pertaining to any cluster P_{2n+1} (n>1) is 'r times' lower than the reactivity of an '-OCN group' of the unreacted monomer.

Earlier in this chapter, it was discussed that most cyanate ester networks are too brittle for practical application, and that toughening of these materials was required for potential utility. The work presented in this manuscript investigated some of the facets of toughened cyanate ester. Other researchers have investigated some of the facets of toughening materials and their results appear in the literature. Seferis et al.[49] investigated the degree of toughening of a dicyanate matrix composite with particulate modified resin rich layers. The particles used to modify the resin rich layers were semi-crystalline Nylon-6 particles of 20 micron average diameter. They reported that creation of such a layered composite structure resulted in no improvement in 'G_{IC}' but greatly increased 'G_{IIC} values'. Yang and coworkers[50-51] have investigated the degree of toughening of the Dow experimental cyanate ester resin, XU 71787.02, by incorporating an experimental core-shell rubber modifier and reportedly obtained significant enhancements in toughness. They attributed such improvements to a rubber-induced shear yielding mechanism. Similarly, Arnold et al.[52] reported their investigations of a number of siloxane modified cyanates of undisclosed chemistries. The siloxane modifications reportedly resulted in significant

improvements in properties such as toughness, micro-crack resistance and oxygen plasma resistance over the unmodified cyanates. Almen et al.[53-54] has reported studies into the use of engineering thermoplastics to toughen cyanates. Although they saw significant improvements, the resins and compositions were not revealed. Some limited work (and the successes obtained therein) on the thermoplastic modifications of cyanates have also been reported by Shimp and coworkers[55], and are promising. This was determined by a marked increase in toughness and micro-crack resistance. Pascault and co-workers[58] reported ways to control the morphologies and properties of rubber or thermoplastic modified systems. They[56] examined the phase separation process induced by the step growth polymerization of the cyanate ester networks in the presence of elastomeric (butadiene-acrylonitrile random copolymer) or thermoplastic (polyethersulfone) modifiers. Hedrick, Gotro and Viehbeck[57] have investigated the degree of toughening of a fluorine containing polycyanurate thermoset by the incorporation of a highly compatible engineering thermoplastic. They used of scanning force microscopy (SFM) to confirm the existence of microphase separation. Srinivasan et al.[58-65] focused investigations into the degree of toughening of Bisphenol-A based cyanate ester networks using a variety of thermoplastic backbone chemistries. The role of the solubility parameter as a tool for selection of thermoplastic toughener of appropriate backbone chemistry was promoted[58]. On this basis, they reported Bisphenol-A[59-61] and phenolphthalein[62-65] based polyarylene ether toughened cyanate ester networks. They also reported on the processing features of these modified systems

employing thermal and microwave radiation[63] to cure the materials. Like the work of Hedrick[57], Srinivasan reported that phase domains were widely varied depending on the cure technique.

2.3 PHYSICAL AGING

2.3.1 Introduction

It has been known for years[3] that amorphous materials in their glassy state are generally not in thermodynamic equilibrium. Temperature dependent properties such as volume, entropy and enthalpy are strongly influenced by the gradual approach to equilibrium of these materials below their T_g. This gradual approach to thermodynamic equilibrium is known as physical aging. The importance of this phenomenon in applications is that material performance, which is affected by change in volume, entropy and enthalpy, must be predictable to ensure compliance with design specifications throughout the expected service life of the product. Because of this importance, physical aging has been extensively explored through research as well as the appearance of review articles[66-69] and books[70-72] on the subject. Research efforts in this area are presently being directed in two areas: (1) development of a quantitative theory capable of accurately predicting aging behavior in polymers under different conditions, and (2) experimental studies of this phenomenon in various glassy polymer systems. The research scope of this dissertation is directed toward the latter effort.

2.3.2 Glass Transition and the Glassy State

An understanding of the origin and nature of the glass transition is necessary to reasonably understand nonequilibrium behavior. Several theories have been developed to describe the glass transition or the transition region. Two of these theories, free volume theory and thermodynamic theory, have gained major acceptance in recent review articles[68-69]. Therefore, a brief description of these theories is discussed to better understand nonequilibrium behavior in the glassy state.

2.3.2a Free Volume Theory

The structure of an amorphous liquid is simply modeled as shown in Figure 2-1. A quantity of liquid is considered to consist of a volume "occupied" by the liquid molecules, V_0, and some free volume, V_F. V_0 is associated with the Van der Waal's radii of the liquid molecules and the additional volume associated with vibrational motions. V_F is that volume not occupied by molecules and into which the molecules move as they undergo Brownian motion. Figure 2-2 displays the total and occupied specific volumes of a glass forming liquid as a function of temperature. This graphic representation shows a change in the slope of the total volume line, or change in the coefficient of thermal expansion (CTE) which

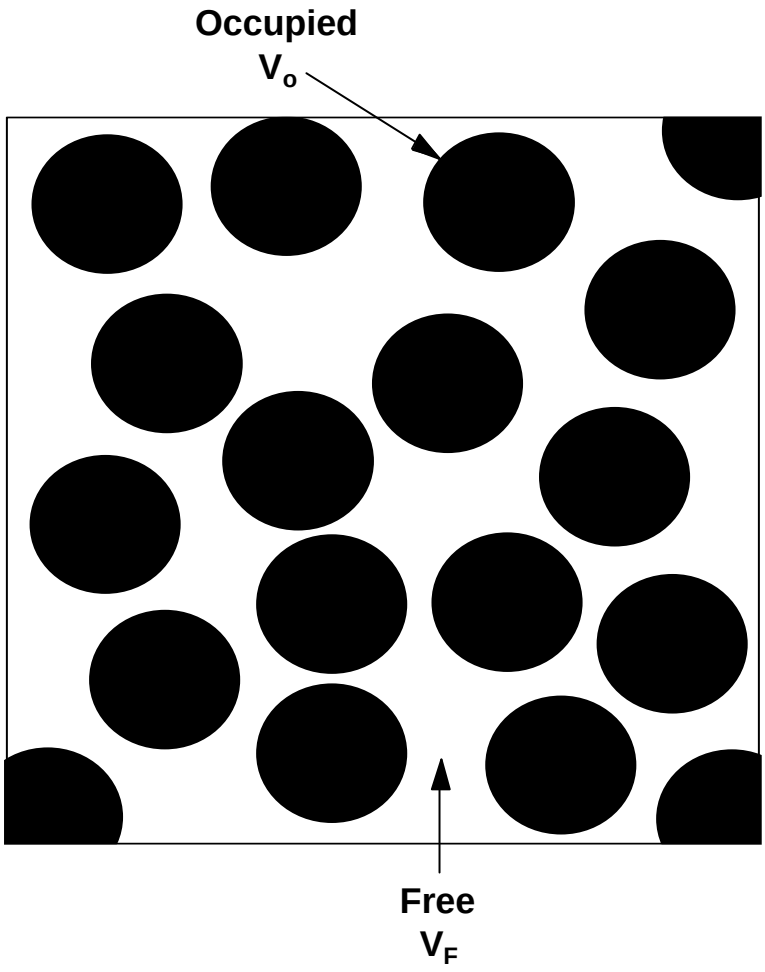

Figure 2-1. Simple model of a liquid showing occupied and free volume.(72)

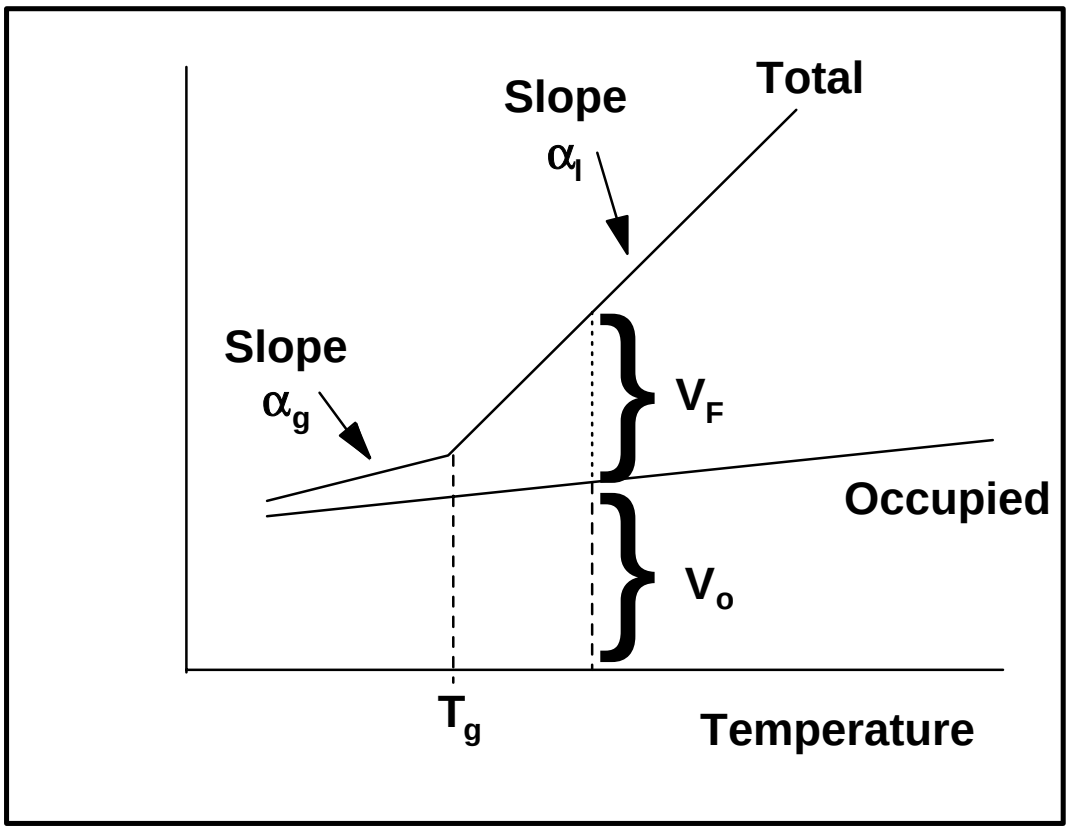

Figure 2-2. Total and occupied volumes of a glass forming liquid as a function of temperature.(72)

often defines the glass transition temperature.[74-75]. However, as is well known, the glass transition temperature may vary depending upon the rate of heating or cooling of the process used in the measurement. This kinetic effect will be discussed in detail later with respect to nonequilibrium behavior.

The concept of free volume first found utility in describing the transport properties of viscosity and diffusivity in liquids.[76] These properties are considered a function of the free volume or fractional free volume. The fractional free volume, f, is defined as the free volume divided by the total volume:

$$f = \frac{V_f}{V_f + V_0} \quad . \qquad (2\text{-}3)$$

In most cases $V_f << V_0$, therefore

$$f \approx \frac{V_f}{V_0} \qquad (2\text{-}4)$$

An expression for f at $T>T_g$ can be written[73]:

$$f = f_g + (\alpha_l - \alpha_g)(T - T_g) \qquad (2\text{-}5)$$

where f_g = fractional free volume at T_g

α_l = thermal expansion coefficient above T_g

α_g = thermal expansion coefficient below T_g.

This is seen graphically in Figure 2-2.

Taking, $\alpha \equiv \alpha_l - \alpha_g$ then:

$$f = f_g + \alpha(T - T_g). \qquad (2\text{-}6)$$

Doolittle's equation[78] relating the decrease in the viscosity of a liquid (•) as temperature increases with free volume theory yields:

$$\ln \eta = \ln A + \frac{V_0}{V_f} \qquad (2\text{-}7)$$

Alternatively, combining with Equation 2-4 gives:

$$\ln \eta = \ln A + \frac{1}{f} \qquad (2\text{-}8)$$

where A is a constant.

If Equation 2-8 is written for T and T_g then subtracted to solve the simultaneous equations, the resulting relationship becomes:

$$\log \left(\frac{\eta}{\eta_g}\right) = \frac{1}{2.303}\left(\frac{1}{f} - \frac{1}{f_g}\right) \qquad (2\text{-}9)$$

where η_g = viscosity at T_g.

The combination of Equations 2-6 and 2-9 leads to the following equation:

$$\log\left(\frac{\eta}{\eta_g}\right) = \frac{\frac{-1}{2.303 f_g}(T - T_g)}{\frac{f_g}{\alpha} + (T - T_g)} \quad . \qquad (2\text{-}10)$$

If f_g and α are constant and:

$$C_1 = \frac{1}{2.303 f_g} \qquad (2\text{-}11)$$

$$C_2 = \frac{f_g}{\alpha} \qquad (2\text{-}12)$$

then Equation 2-10 becomes:

$$\log\left(\frac{\eta}{\eta_g}\right) = \frac{-C_1 (T - T_g)}{C_2 + (T - T_g)} . \qquad (2\text{-}13)$$

Since viscosity, relaxation times and shift factors are related by the expression:

$$\log\left(\frac{\eta}{\eta_g}\right) = \log\left(\frac{\tau}{\tau_g}\right) = \log\left(\frac{a_T}{a_g}\right) \qquad (2\text{-}14)$$

Equation 2-13 can be re-written to generate the well-known Williams-Landel-Ferry (WLF) Equation:[79]

$$\log (a_T) = \frac{-C_1 (T - T_g)}{C_2 + (T - T_g)}. \qquad (2\text{-}15)$$

This equation was first introduced in 1955 as an empirical formula to relate mechanical and electrical relaxation times of a material at any temperature to their values at a reference temperature. It has also become an important component in examining free volume relaxation in polymers. One of the main concepts developed to determine long term behavior from short term experiments, namely time-temperature superposition, is encompassed in the Williams-Landel-Ferry (WLF) equation.[78-79]

The WLF equation can be expanded to include temperatures other than T_g:

$$\log (a_T) = \frac{-C_1'(T - T_R)}{C_2' + (T - T_R)}; \qquad (2\text{-}16)$$

which now relates time dependent properties to a reference temperature, T_R, of choice. The parameters (C_1, C_2) and (C_1', C_2') in Equations 2-11 and 2-12 are constants for a given polymer and reference temperature. If $T_R = T_g$, the values of C_1 and C_2 are close to so-called universal values[71]: $C_1^g = 17.4$ and $C_2^g = 51.6$.

Since $a_T = \eta_T/\eta_{Tg}$, the WLF equation suggests that at $T = T_g - 51.6$, the viscosity of the polymer material becomes infinite. Cohen and Turnbull (80-81) proposed one of the explanations for this anomaly. They modified the free volume theory so that changes in free volume with temperature relate to a discontinuity at a temperature, T_β, which was below the T_g. T_β was considered the secondary relaxation encountered first on cooling through the T_g. Furthermore they suggested that the free volume, V_F, corresponds to that part of the excess volume, $V - V_0$, which can be redistributed without a change in energy. (The fractional free volume, $f = V_F/V$, is typically around 0.025 for most polymers at their respective glass transition temperature.) In other words, only voids or "holes", which are larger than a certain volume, constitute the free volume that is related to mobility. Using this rationale, Cohen and Turnbull[81] showed that the viscosity can then be expressed as

$$\eta = a \exp\left(\frac{B'}{T - T_\beta}\right) \tag{2-17}$$

where a and B' are constants and

$$\tau = \tau_0 \exp\left(\frac{B'}{T - T_\beta}\right) \tag{2-18}$$

When $T_\beta = T_g - 51.6$, the WLF equation is again obtained. However, other research has shown[76] that C_1 and C_2 can vary significantly depending on the polymer system. Equation 2-18 is often referred to as the Vogel-Fulcher equation.

2.3.2b Thermodynamic Theory

The prediction by the WLF equation that viscosity becomes infinite at $T = T_g - 51.6$ has also been examined from a thermodynamic approach by Gibbs and DiMarzio[82-83], and Adam and Gibbs[84]. The previous authors proposed that the specific volume depiction of T_g (discussed earlier) is simply a kinetic manifestation of a true, equilibrium, second-order transition at T_β. A second-order transition is one in which the second partial derivative of the Gibbs free energy is discontinuous at the transition point. Ehrenfest[85] derived thermodynamic equations based upon this definition which clearly show that a second order transition occurs only when equilibrium exists on both sides of the transition[86]. Adam and Gibbs derived the WLF equation using the assumption of Gibbs and DiMarzio as a basis. They assumed the frequency of molecular jumps is expressed by:

$$\nu_c = A \exp\left(-\frac{n\Delta G^*}{kT}\right) \qquad (2\text{-}19)$$

where A is a constant, ΔG^* is the barrier height for internal rotation per segment, and n is the number of segments acting cooperatively to make a conformational rearrangement. The conformational entropy per mole of segments is

$$S = \left(\frac{N_A}{n}\right) s_n \tag{2-20}$$

where N_A is Avogadro's number and s_n is the entropy of a unit of n segments. The frequency of molecular jumps is then given by:

$$\nu_c = A \exp\left(\frac{- N_A s_n \Delta G^*}{SkT}\right) \tag{2-21}$$

The conformational entropy of the system, S, is assumed to be zero at the thermodynamic transition temperature T_β and therefore n becomes infinite. The conformational entropy may then be calculated by

$$S(T) = \Delta C_p \ln\left(\frac{T}{T_\beta}\right) \tag{2-22}$$

where $\bullet C_p$ is the difference in specific heat between the model liquid and the glass at T_g and is assumed constant. Substituting this into Equation 2-21 leads to

$$\nu_c = A \exp\left(\frac{-N_A s_n \Delta G^*}{k \Delta C_p (T - T_\beta)}\right) \qquad (2\text{-}23)$$

This gives a relaxation time of the form shown in Equation 2-18, which was previously shown to be equivalent to the WLF equation.

2.3.3 Physical Aging and Nonequilibrium Behavior

Nonequilibrium behavior of glassy polymers results from the inherently kinetic nature of the glass transition. What this means is that as a polymer is cooled at a finite rate through its T_g, the molecular mobility decreases to the point where the molecules are not able to reach their equilibrium conformation in the time frame of the observation. In this scenario, the glass transition would be detected at a lower temperature for a slower cooling rate, since the slower rate would allow the molecules more time to approach their equilibrium state.[71] The important relationship between the experimental time scale and the time scale required for molecular motion is well known in the examination of mechanical properties of polymers. The relationship is described by the Deborah number, N_{De}, such that

$$N_{De} = \frac{\lambda_c}{t_s} \qquad (2\text{-}24)$$

where λ_c is defined as a characteristic time for a material to reach 1/e of its ultimate elastic response to a step change, and t_s is the time scale of the experiment.[87] For example, a more elastic response will result in a high Deborah number, whereas viscous-like responses will be reflected by low Deborah numbers.

Since some relaxations may require experimentally inaccessible times at lower temperatures, at a finite cooling rate, the polymer molecules will in that case be frozen in a state of higher energy and volume relative to the equilibrium state. Over time, due to thermodynamic driving forces on the molecules to approach the state of lowest energy, the molecules may slowly rearrange in the glassy state. The rate of approach toward equilibrium is controlled by the mobility, M, of the molecules and the degree of packing or free volume. Figure 2-3 displays this concept graphically. The segmental mobility is considered the rate factor for changes in chain conformation. When a polymer is above its T_g, it behaves like a liquid or rubber. The segmental mobility is large relative to that in the glassy state, and so is the free volume. Upon cooling there is a simultaneous decrease in V_f and M until its T_g is reached. The changes in free volume are

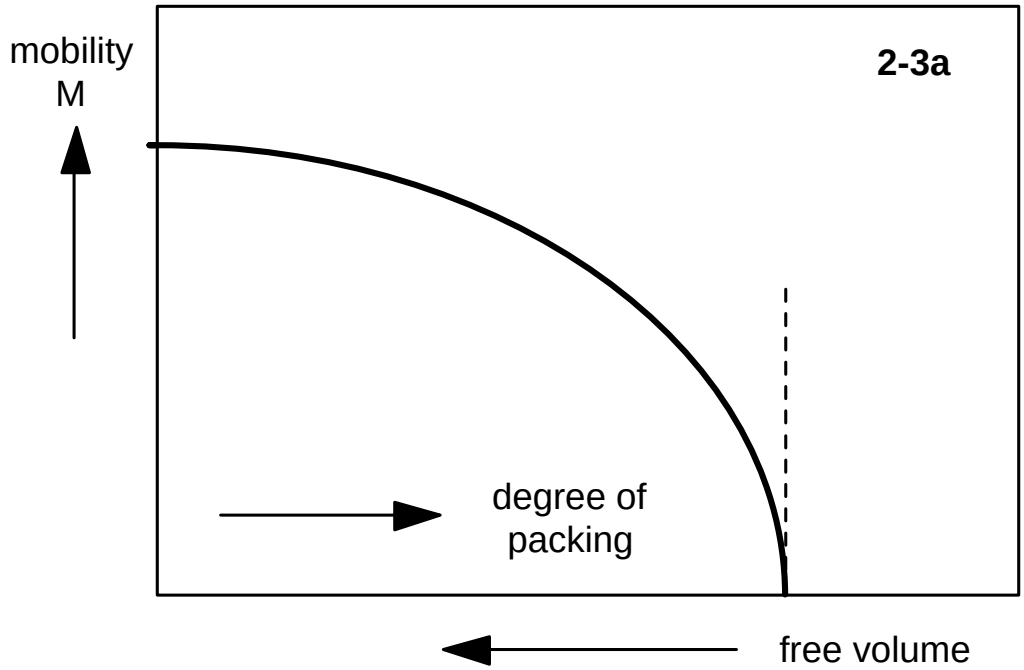

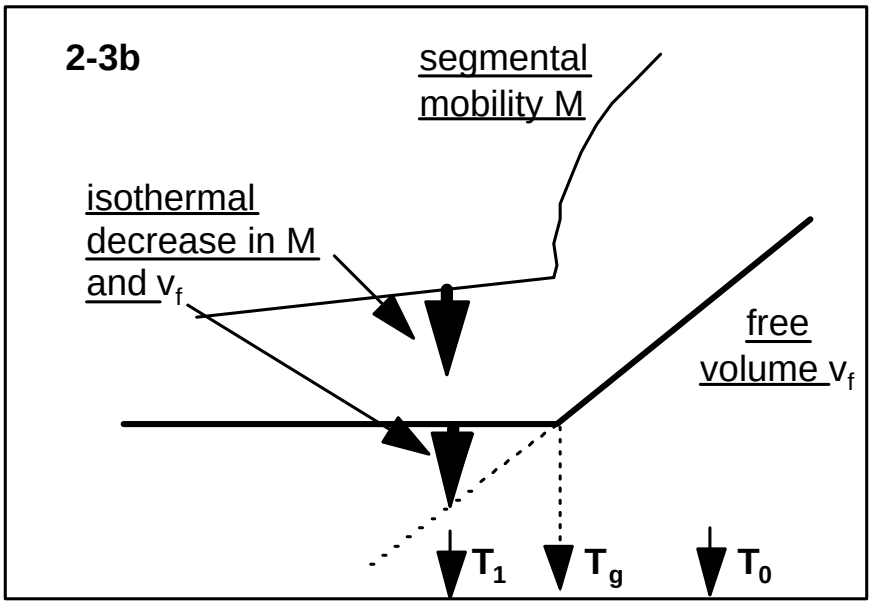

Figure 2-3. Illustration of the free-volume concept and its application to the aging problem.(70)
a.) Segmental mobility vs. volume
b.) Free volume and segmental mobility vs. temperature

brought about by a cooperative redistribution of space between molecules and the rate of this redistribution are determined by M. A closed loop scheme has been developed to explain this process:

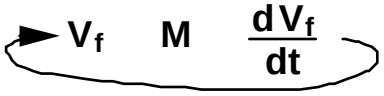

(2-25)

As the material drops below its T_g, the rapid decrease in free volume cannot continue because at the T_g, molecular mobility is drastically decreased and impacts the rate of change in free volume. However, mobility does not cease completely, and the free volume must still decrease, leading to physical aging.[70] The above relationship also suggests that volume relaxation is a non-linear process.

It is observed from the above relationship (Equation 2-25) that the basic property changing upon annealing below the T_g is the segmental mobility. This mobility is directly related to the relaxation times of the polymer, and therefore may be studied by using experiments that provide the relaxation spectrum of the polymer. Mainly creep[72] and stress relaxation[88-89] experiments have been used to study this phenomenon.

Figure 2-4 presents representative small strain creep curves as a function of annealing time below the T_g. One should note that the curves are shifted to the right by one decade for each tenfold increase in sub-T_g aging time when the

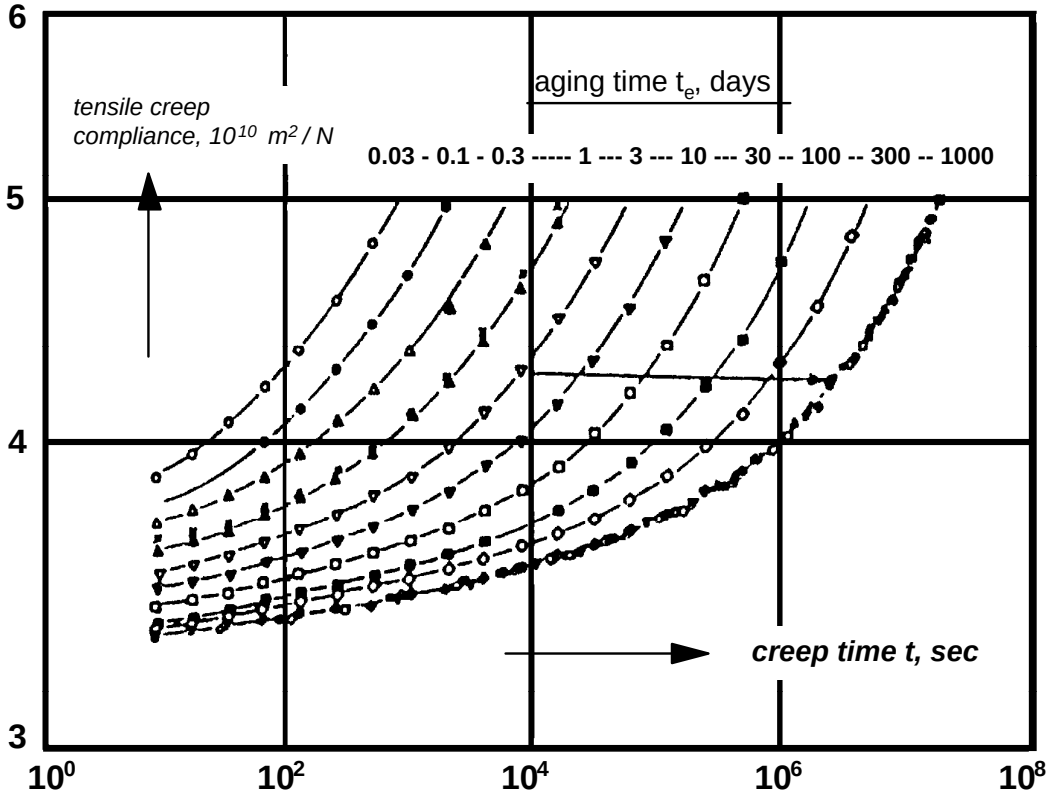

Figure 2-4. Small strain tensile creep curves of rigid PVC quenched from 90°C to 40°C and annealed at 40°C. (69,70)

annealing temperature is held constant. This suggests that under these conditions, aging is linear with respect to logarithmic time. As a note on the investigation of cyanate esters in this thesis, their curves do not necessarily conform to the expected physical aging vs. log time behavior observed. The addition of

thermal and oxidative degradation interferes with physical aging and greatly changes the expected behavior. This is displayed in Chapter 4 Section 4.3.3.

It can also be seen that the curves in Figure 2-4 can be approximately superimposed by a horizontal shift to form an expanded curve on the x-axis known as a master curve. This shifting is known as time-temperature superpositioning (TTSP). It obviously is related to frequency-temperature superposition or the method of reduced variables[(90)]. This concept is often applied to determine the temperature dependence of the rheological behavior of a polymeric liquid or to expand the time or frequency regime at a given temperature at which the mechanical response behavior is studied. According to Ferry[(75)], TTSP is valid when: (1) exact matching of shapes of adjacent (time or frequency dependent) curves is obtained; (2) the shift factor, a_T, has the same value for all viscoelastic functions; (3) the temperature dependence of a_T has a reasonable form (WLF, Arrhenius, or monatomic).

In practice, however, the TTSP scheme may not be justified. One example is the occurrence of more than one relaxation mechanism with distinct temperature

dependencies.[91] Polymers that are "thermo-rheologically" complex will not satisfy superposition restrictions. Also, near the glass transition, both energetically and entropically driven relaxations are probable, and in general, TTSP will not hold. Consequently, log a_T increases less rapidly with decreasing temperature than expected. This causes a shift in mechanical behavior that is inconsistent with WLF theory. Several papers have shown deviation below the T_g of a master curve shift factor plot.[92-93] This deviation stems from the material not being in the equilibrium state at these temperatures. Hunston et al[92] concluded that this deviation was caused by the variations of free volume in the glassy state. This also suggests that as the material physically ages, this deviation should approach an expected equilibrium curve. In addition, materials that change chemically during the rheological measurement will not obey TTSP. To some extent, deviation from the WLF theory is seen with the cyanate ester networks of this research as well. More importantly, the master curves in this study are discussed later and found to be shifted in unexpected ways due to chemical degradation.

One of the major extensions of superposition methods was the development of the doubly shifted or master-master curve.[94-96] This type of curve resulted from the realization that a group of time-temperature master curves which differed by a third variable could again be shifted to form one composite master curve. The resultant doubly reduced curve (master-master curve), with the assistance of the two shift factor plots produced, allows for the prediction of properties over a three

variable range. Such curves have been published in which varying volume fraction[94], weight percent filler content[95], humidity, and physical aging were employed. Crissman and McKenna[96] in a paper that is related to the present research, studied the effects of physical and chemical aging on the creep and creep rupture behavior of poly(methyl methacrylate). The PMMA samples of their study were aged at room temperature for varying times in air, and then tested to examine the effects of physical aging. The first (and unanticipated) observations were that the molecular weight and density of the material decreased with increasing aging time. They suggested this was caused by chemical degradation in the material during the annealing and aging process. Also their examination of the reduced creep curves (creep master curves) showed varying behavior inconsistent with observed physical aging behavior. Finally an interesting result was construction of a double shift plot, formed from the master-master curve development. This master-master curve exhibited a maximum instead of the expected linearity. This maximum occurred at the same time the material decreased in molecular weight and density suggesting there was an overwhelming competing mechanism to the physical aging, and this competition was caused by chemical degradation.

As stated earlier, aging primarily affects the retardation and/or the relaxation times of a material, and aging results from the inherently kinetic nature of the changes occurring in the non-equilibrium glass. A connection between creep (or stress relaxation) isothermal experiments is empirically accessible, and is defined

by the shift factors, log a_T, relative to a reference isotherm. The accepted convention is a positive shift factor for a shift to the left, and negative for a shift to the right. The aging rate may therefore be defined as:

$$\mu = \frac{\mathbf{d \log\ a_T}}{\mathbf{d \log\ t_e}} \qquad (2\text{-}26)$$

where log a_T is the horizontal shift required to superpose two viscoelastic curves of differing aging times, and t_e is the aging time.[72] This rate has been used to characterize the intensity of physical aging for many polymeric materials (Figure 2-5). According to Struik[72], no aging occurs above the T_g and μ is zero in that region. Of course this reflects the equilibrium behavior of a liquid. On cooling the liquid, at the T_g, or just below it, μ rises to a value of about unity for all polymers. From equation 2-26, the relaxation times will increase proportionally to aging time. At even lower temperatures, μ begins to decrease and asymptotically approaches zero as the beta transition temperature, T_β, is reached. This phenomenon is demonstrated graphically in Figure 2-5. Several researchers[97-98] have shown that aging rates, μ, may depart rather drastically from unity. Some attempt has been made to correlate the aging rate, μ, with molecular structure.[73]

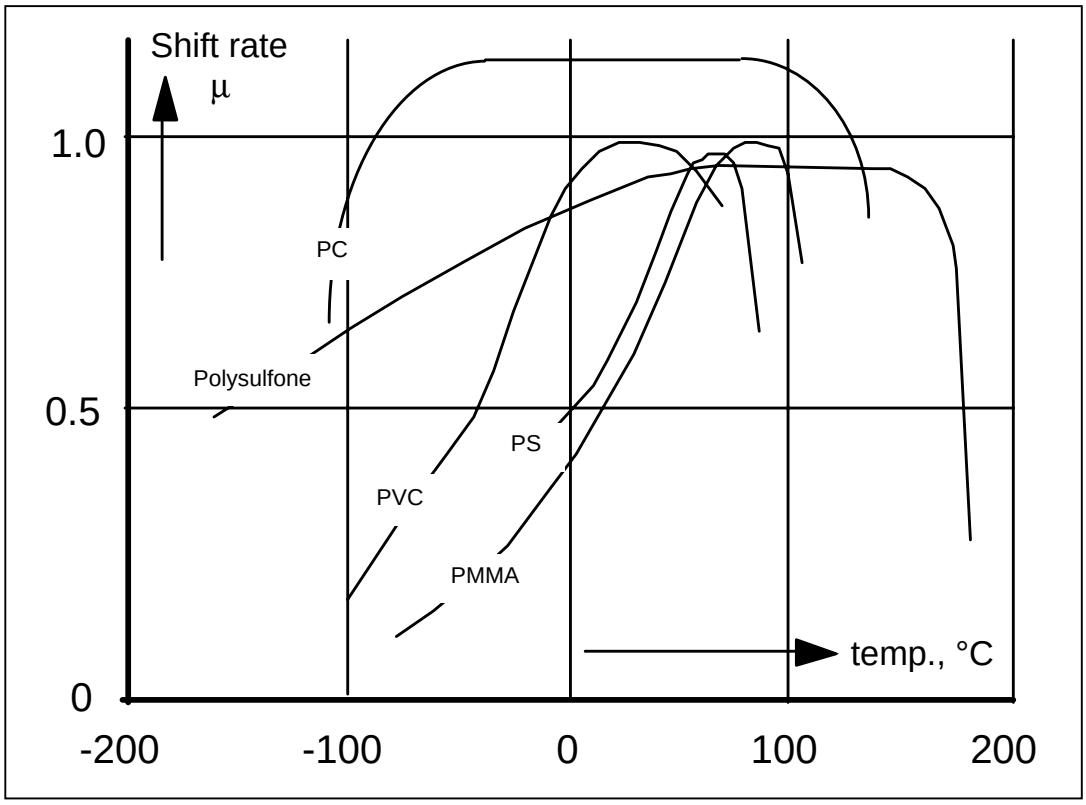

Figure 2-5. The shift rate, μ, vs. temperature for various polymers. [70]

Other scientists have investigated physical aging and made some interesting observations. One of these is that the behavior of a glass depends significantly upon its thermal history below T_g. Kovacs[99] demonstrated an unusual effect on the volume of a glass during physical aging using poly(vinyl acetate). The effect, known as the "memory effect", was originally found as a spontaneous expansion followed by a contraction of an annealed glass during isothermal measurements at a temperature T_A when the temperature was suddenly raised from T_B to T_A both below T_g. Pressure also had a similar effect on the material. Cavaille et al[100] showed that this memory effect had a pronounced impact on dynamic mechanical modulii. Examining the material under shear, these authors noticed that G'' decreased with physical aging and G' increased with physical aging. It was also observed that the slopes of the G" and G' results on increasing frequency were lower. When the temperature of the aged material was raised, G'' went through a maximum and G' a minimum on physical aging at that temperature. This was consistent with the memory effects observed by Kovacs, and was interpreted as the dynamic mechanical analog of his volume dilatometry experiments. These results are important to the conclusions of the present research.

2.3.4 Methods of Detecting and Measuring Physical Aging

Many properties of a polymer change as a result of physical aging. Therefore, a number of techniques have been utilized to follow these changes. Some of these

techniques include differential scanning calorimetry, infrared analysis, as well as creep compliance, stress relaxation, refractive index, and dynamic mechanical analysis. One of the more popular non-mechanical monitors of physical aging utilizes the differential scanning calorimeter (DSC). Typical DSC instruments yield the specific heat change in a material, with respect to a reference material, as the sample is heated over a specified temperature range. Considerable standard information determined by DSC includes the heat of crystallization, crystalline melt temperature, residual heat of curing, T_g, and other thermal properties. The use of DSC to examine physical aging has been reported extensively.[101-106] The physical aging process is manifested through an "overshoot" peak in the heat capacity (heat flow) response when the material is heated through its T_g (Figure 2-6a). As physical aging progresses, this endothermic peak area increases. This is due to continued densification and the associated enthalpy changes of the material over time. The area under this peak is known as the enthalpy of aging, and when plotted against log (aging time), a linear relationship over a certain time range and at certain temperatures is revealed. (Figure 2-6b).

2.3a

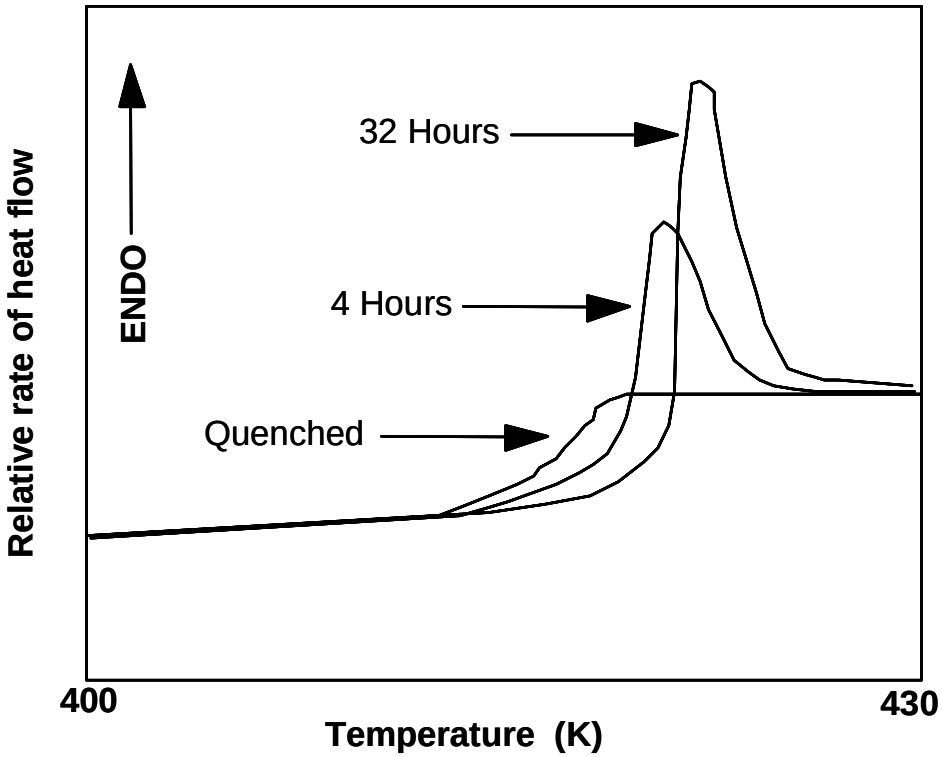

2.3b

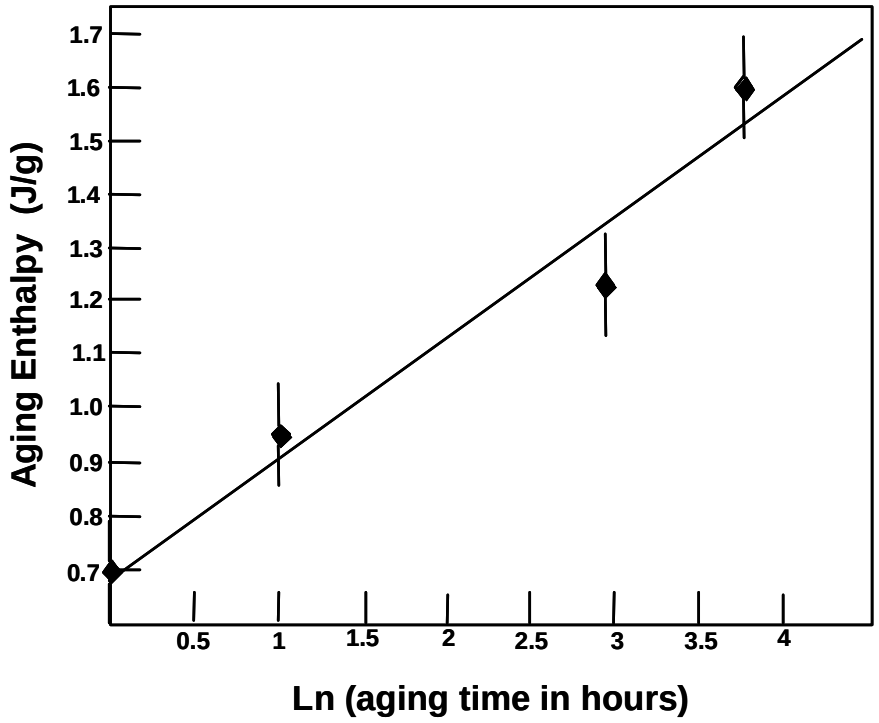

Figure 2-6. a) Changing heat capacity with aging.
b) Extent of aging at 12.6 K below T_g. (102)

Some researchers have investigated the use of infrared analysis to follow physical aging. Hay et. al.[107] used characteristic frequency bands for *trans* and *gauche* conformations to follow the progression of poly(ethylene terephthalate) relaxation as the material approached the equilibrium-glassy state. They concluded infrared spectral changes are consistent with the temperature dependent changes in chain conformation as thermodynamic equilibrium is approached.

One common method of examining physical aging is by observing changes occurring in the mechanical properties of a polymer. The most popular of these measurements have been the creep compliance studies. Creep investigations are performed by applying an instantaneous and constant stress to the sample. The change in strain of that material is measured over time, and generally follows the relationship:

$$J(t) = \frac{\gamma(t)}{\sigma_0} \qquad (2\text{-}27)$$

where $\gamma(t)$ is the time dependent strain, σ_0 is the applied stress, and J(t), the time dependent shear creep compliance.[108] Many studies have shown[109-116] that physical aging has a pronounced effect on creep measurements. With increased aging time, the material's response is a shifting of the creep compliance curve to longer relaxation times. This suggests that the material has densified, and this densification is part of the sequence that produces the longer relaxation times. In

a paper by Read[109], poly(methyl methacrylate), poly(vinyl chloride), and polycarbonate, all linear amorphous polymers, were examined for this aging behavior. Shifts to longer times were found on aging. Physical aging occurred in each sample, and the rates of aging were comparable.

Similar aging results were also obtained by Struik[110-113] in creep examinations of semi-crystalline polymers. This series of papers discussed, in depth, the effects physical aging has on the creep properties of semi-crystalline polymers. Struik studied nylons, high-density polyethylene, polypropylene and other known semi-crystalline polymers, and observed a similar behavior to that found for amorphous and cross-linked polymers. In addition, Sell and McKenna[117] evaluated epoxies of differing cross-link densities and found no change in physical aging behavior (as determined by yield stress measurements) between such samples.

Stress relaxation is another method employed in the examination of physical aging. In this test, a material is held at a constant strain, and the change in stress over time is measured. Maurer and coworkers[118] reported the relaxation aging study for a blend of poly(acrylonitrile-butadiene-styrene) and polycarbonate. They concluded that both phases of this phase-separated system were in good agreement with typical theoretical descriptions of relaxation behavior and they postulated that all glass forming materials followed a similar behavior. Furthermore, Mijovic et al.[119] used six different formulations of compatible polymer blends and, by examining their stress relaxation behavior,

they developed a single master curve relating blend composition, aging temperature and aging time.

In addition to the preceding techniques, many papers have been published which report dynamic mechanical tests to examine the physical aging process.[120-128] Many of the same materials were studied using DMA. These include linear amorphous polymers, thermosets, and semi-crystalline polymers and are available for comparative analysis. The conclusions from this body of work generally indicate that similar aging behavior occurs in all of these materials below their T_g. However, DMA allows for easier examination in sub-ambient conditions, and in some cases the β transition region of these materials was probed for aging response. The results of each of these studies were in agreement:[120-121] a decrease in the area under the tan δ curve at the β-relaxation region with increasing aging was discovered. It was suggested this phenomenon had predictive value in indicating a decrease in material toughness as molecular segmental mobility decreased. This seems to be an interesting and contradictory finding to Struik's earlier examinations, where aging ceased at T_β. Obviously, complex mechanisms are active in this range of a ploymer's temperature/property spectrum.

Some novel techniques have been developed to examine physical aging in polymers. Using mobility- or free volume-sensitive fluorescent molecules, researchers followed a fluorescence response to examine molecular relaxation during physical aging.[129-130] They found that the physical aging rate depended on

temperature in all the polymers studied, and the results agreed well with specific volume relaxation studies. Other studies[131-132] noticed an apparent reversal of physical aging due to electron beam irradiation. It was noted here that there was a significant decrease in physical aging with increasing radiation. There was also some reversal upon requenching the material, but overall, the properties had been irreversibly affected by the irradiation.

2.4 Chemical Aging

2.4.1 Introduction

All polymers will chemically age, or react, under certain environmental conditions such as temperature, humidity, and light. Depending on the combination of these conditions, degradation, or further reactions may occur very rapidly. To fully understand this occurrence, detailed investigation is required and usually complicated by the often insoluble nature of these solids. Frequently, the chemical processes are associated with polymer chain cleavage. In the case of crosslinked materials, a breakdown of the network may result. An immediate result of such a process is a reduction in molecular weight; and in most cases, this decrease leads to adverse and irreversible changes in physical and mechanical properties of the polymer. Although the chemical alteration of a polymer is frequently a destructive process, for some applications, further chemical reaction can be controlled and encouraged to achieve a specific

property. Examples include the adjustment of the molecular weight of a thermoplastic through controlled backbone scission during extrusion[133], and the controlled oxidative cross-linking of surface coatings[134]. Finally, an important societal concern is the recycling and disposal of polymers without severe consequences to the environment where degradation is required. Volatile gases (CO, CO_2, NO, NO_2, HC≡N, etc.) and insoluble by-products are usually a result of degradation.[135]

2.4.2 Kinetics of Chemical Aging

The most popular model for condensed phase rate processes is:

$$\frac{d\alpha}{dt} = f(\alpha)k(T), \qquad (2\text{-}28)$$

where the rate of change of a reaction parameter α with respect to time is $d\alpha/dt$, and $f(\alpha)$ and $k(T)$ are separable functions of conversion and temperature, respectively. At a constant heating rate with $\beta = dT/dt$, Equation 2-28 becomes:

$$\frac{d\alpha}{dT} = \beta^{-1} f(\alpha)k(T). \qquad (2\text{-}29)$$

Integrating with respect to α and T, Equation 2-29 becomes:

$$F(\alpha) = \int_0^{\alpha} \frac{d\alpha}{f(\alpha)} = \beta^{-1} \int_{T_0}^{T} k(T)\, dT \quad . \qquad (2\text{-}30)$$

The conventional model for k(T), the temperature dependence of the rate, is the Arrhenius equation,

$$k(T) = A \exp\left(-\frac{E}{RT}\right), \qquad (2\text{-}31)$$

where A is the preexponential factor, E is the energy of activation and R is the gas constant. Combining Equations (2-30) and (2-31) one obtains:

$$F(\alpha) = A\beta^{-1} \int_{T_0}^{T} \exp\left(-\frac{E}{RT}\right) dT \quad . \qquad (2\text{-}32)$$

If T_0 is well below the temperature where the reaction rate becomes measurable, the lower limit of the temperature integral may be ignored. Thus, defining x = -E/RT, Equation 2-32 becomes:

$$F(\alpha) = \left(\frac{AE}{\beta R}\right) \left\{ -\frac{e^x}{x} + \int_{-\infty}^{x} \left(\frac{e^x}{x}\right) dx \right\} = \left(\frac{AE}{\beta R}\right) p(x) \quad . \qquad (2\text{-}33)$$

The term in braces in Equation 2-33, symbolized by p(x) and containing the exponential integral, cannot be integrated in closed form. Doyle[131] was the first to utilize the near linearity of the logarithm of p(x) when plotted as a function of x, and proposed the approximating relationship:

$$\log p(x) \bullet -2.315 + 0.457\,x \qquad (-20 > x > -60) \qquad (2\text{-}34a)$$

or, in terms of natural logarithms,

$$\ln p(x) \bullet -5.3305 + 1.052\,x \qquad (-20 > x > -60) \qquad (2\text{-}34b)$$

These are the equations upon which Ozawa, Flynn and Wall[137-138] based the integral isoconversional method for calculating activation energies. They elucidated this relationship by a) taking the logarithm of Equation (2-33) and b) combining this with equations (2-34a) or (2-34b) to yield:

$$\log F(\alpha) \approx \log\left(\frac{AE}{R}\right) - \log\beta - 2.315 + 0.457\frac{E}{RT} \qquad (2\text{-}35a)$$

or

$$\ln F(\alpha) \approx \ln\left(\frac{AE}{R}\right) - \ln\beta - 5.3305 + 1.052\frac{E}{RT}. \qquad (2\text{-}35b)$$

Therefore, if a series of experiments are performed at heating rates, β_1, β_2, β_3, ..., β_j and $T_{k,j}$ is the temperature at which conversion fraction, α_k, was reached at

heating rate β_j, then a plot of log β_j (or ln β_j) vs. $1/T_{k,j}$ for each of k fractions of conversion, α_1, α_2, α_3, ..., α_k will yield k isoconversional lines whose slopes are, from equations (2-35a) or (2-35b)

$$\text{slope} \bullet 0.457 \text{ (for } \log \beta_j \text{ vs. } 1/T_{k,j}\text{);} \qquad \text{(2-36a)}$$

$$\text{slope} \bullet 1.052 \text{ (for } \ln \beta_j \text{ vs. } 1/T_{k,j}\text{);} \qquad \text{(2-36b)}$$

Thus, the activation energy at any degree of conversion, α_k, is calculated from a plot of log β_j (or ln β_j) vs. $1/T_{k,j}$. The linearity of three or more values of β in this analysis is the usually accepted criteria for obtaining a reliable value of the activation energy. Any change in the activation energy with respect to conversion may be observed by the comparison of slopes in the above plots at the respective α_k.

In a corollary to the linear assumption made above, Flynn[138] improved upon the Doyle approximation by disregarding the validity of a single linear approximation to log p(x) over the entire range of x found in kinetic experiments. Instead, the linear approximation is obtained in the region of x into which the data fall. Because this region depends on E, this technique is applied in an iterative fashion. Starting with the Doyle approximation, an estimate of E is obtained. This estimate is used to re-calculate a more accurate value for the slope of the log p(x) vs. x relationship in the region where the experimental points lie. This process is repeated until a self-consistent relationship is derived.

Alternatively, Equation 2-33 can be solved numerically without making the linear approximation. It is a two-parameter equation consisting of a linear [AE/RF(α)] and a non-linear [E in x = E/RT] component. The previous methods are used to establish a good initial estimate for the nonlinear parameter - a least squares technique can be utilized to refine the values. The activation energy is obtained directly from the second parameter, and the pre-exponential factor is computed from the first (linear) parameter

$$A = \frac{R\ F(\alpha)}{E} \tag{2-37}$$

For this calculation to be completed, F(α) must be known. This requires further assumptions regarding the original rate equation (Equation 2-28). The most common assumption is that the reaction follows first-order kinetics, which in this case yields:

$$A = \frac{R}{E} \ln(1 - \alpha) \tag{2-38}$$

Once the activation energy and pre-exponential factor are determined, other kinetic parameters can easily be obtained. Equation 2-31 is first calculated to get an accurate value for the temperature dependent rate constant. Also obtained is the time to half-life as a function of temperature:

$$t_{1/2} = \frac{\ln(2)}{k(T)} \tag{2-39}$$

This information is useful in following the reactions of a sample over a specified temperature range. The 60 minute half-life temperature $T_{t1/2} = 60$ is also determined:

$$T_{t1/2\,=\,60} = \frac{-E}{R \ln\left(\frac{\ln(2)}{60\ A}\right)} \tag{2-40}$$

Using this temperature, the validity of the kinetic calculations can be confirmed. Since one hour is a reasonable experimental time, material degradation at that temperature for 60 minutes should yield 50% weight loss. Deviations from this percentage indicate the amount of inaccuracy in the original experiments. The time to reach a specified conversion at temperature T is given as:

$$t(T,\alpha) = \frac{-\ln(1-\alpha)}{k(T)} \tag{2-41}$$

and the conversion that occurs at a specified time, t, and temperature, T is

$$\alpha(t,T) = \left(1 - e^{-k(T)\,t}\right) \tag{2-42}$$

If a certain amount of degradation is acceptable for an application, Equation 2-41 determines the time the material may encounter a certain temperature before that conversion is reached. Alternatively, if the time and temperature of the application are known, Equation 2-42 will predict the amount of degradation. These fundamental relationships will be applied, and in more detail, to the research in this manuscript on the degradation of cyanate ester networks. (see Chapter 4 Section 4.3)

2.4.3 Mechanisms of Chemical Aging

Reactions breaking the molecular skeleton during thermal and photooxidative aging have been extensively studied in linear polymers[3]. However, 3-dimensional networks are characteristically insoluble in organic solvents and therefore, much more difficult to examine[139]. In the case of most thermosets, a significant decrease in the T_g is observed via DSC or differential thermal analysis (DTA) measurements during the thermal[140] or photochemical oxidation[141-142] of these materials. Lin et al. found on examining epoxies (based on the diglycidyl ether of bisphenol A) using infrared measurements, that carbonyl groups were formed from ether linkage degradation in the polymer. It was hypothesized that complicated chemical rearrangements were occurring and were probably responsible for the observed degradation[143]. Bellenger and Verdu[144] verified the above hypothesis. They observed network breakdown at the ether linkages in the cured epoxy network, and correlated the chemical changes to thermal and mechanical property changes.

Ether linkages have been well documented with respect to their thermo- and oxidative stabilities; and for this reason, they provide a suitable model structure for comparison to the cyanate ester degradation studies of this work. These ether linkages are prone to oxidative[145-146] as well as hydrolytic attack. Presented below is a general view of the degradation processes of the ether linkage.

2.4.3a Oxidation

The hydrogen atom of the adjacent CH group to the ether link is rapidly abstracted by a peroxyl radical (Scheme 2-9).

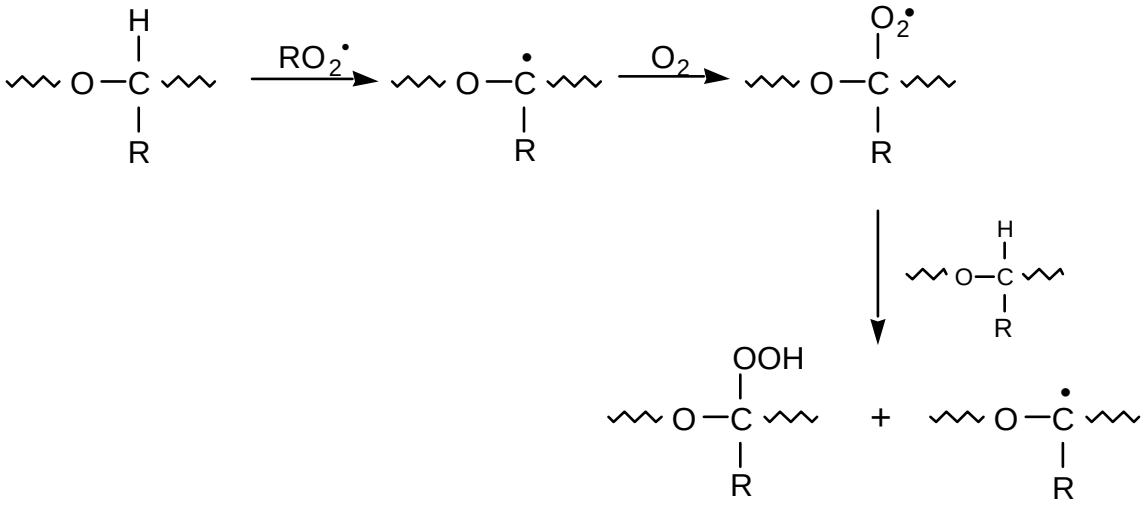

Scheme 2-9. Abstraction of CH Group by a Peroxyl Radical.

The hydroperoxy ether readily eliminates water in the case of polyoxymethylene (POM) to give a carbonate link (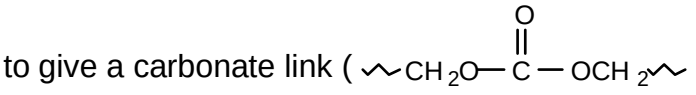).[146] Sequential attack on adjacent methylene sites yields anhydride-like linkages, and their presence is confirmed by infrared analysis. Surprisingly, POM is photo-oxidized even by quite long UV wavelengths, i.e., 365 nm. This degradation must result from UV absorption by impurities such as aldehyde groups or from residuals resulting from end-capping by groups such as toluene diisocyanate. Model ethers and extracted POM do not absorb beyond ca 210 nm.[147] Certainly, as unsaturation is introduced, the degradation is accelerated because of the ability of the double bond to absorb light (internal photo-sensitization).

Poly (vinyl butyral) contains cyclic ether rings along the backbone. It is widely used as the plastic interlayer in automotive safety glass. This resin is extremely photosensitive when irradiated in air as a thin film.[148] An infrared study shows that oxidative scission of the pendent rings can occur at wavelengths as long as 445 nm, presumably as a result of radical attack on the tertiary C – H group alpha to two ether linkages. (Scheme 2-10)

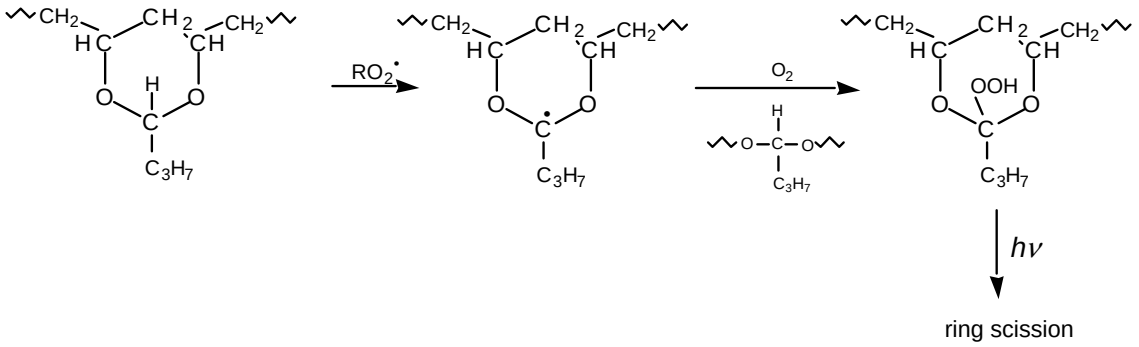

Scheme 2-10. Oxidative Ring Scission at Ether Linkages

The long wavelength sensitivity results from impurities in the polymer introduced during its synthesis from poly(vinyl alcohol). Additionally, cyclic ethers undergo very rapid oxidation. In this study of cyanate ester degradation, rapid oxidation also occurs when the ether linkage is directly attached to the triazine ring. This will be discussed in more detail in Chapter 4.

2.4.3b Hydrolysis

Polyoxymethylene (POM) undergoes random, acid-catalyzed hydrolysis, many orders of magnitude faster than simple ethers (Scheme 2-11). The acid catalyst employed is often formic acid, produced during the depolymerization, by chain cleavage to formaldehyde and subsequent oxidation to the acid.

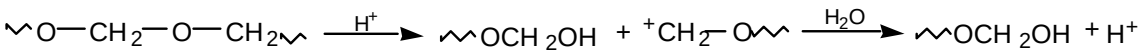

Scheme 2-11. Acid Catalyzed Degradation of Ether Linkages

Once a terminal alcohol group is formed, or if the original polymer is not end-capped, a rapid base-catalyzed depolymerization, i.e., unzipping, is possible (Scheme 2-12).[149]

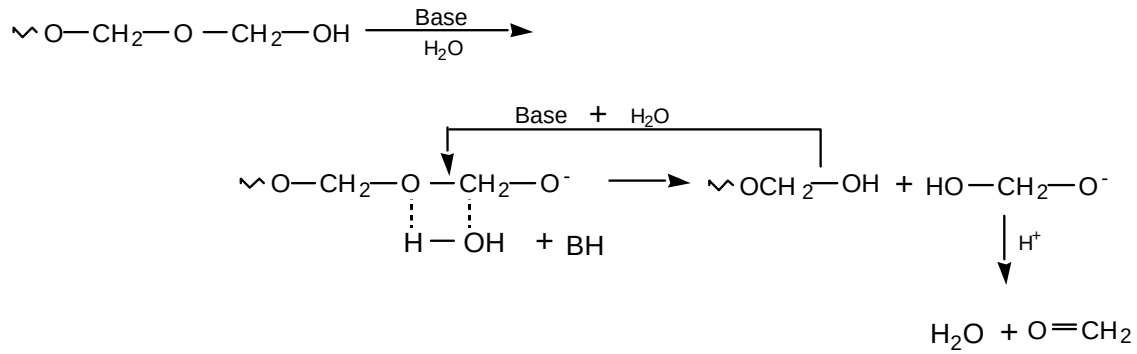

Scheme 2-12. Unzipping Process in Polyoxymethylene Under Basic Conditions

This undesired hydrolytic degradation can be significantly retarded, and the depolymerization blocked by co-polymerization with ethylene oxide. This increases the thermal hydrolytic stability by limiting the unzipping process via the additional carbon atom of ethylene oxide interfering with the mechanism proposed in Scheme 2-12.[145]

Oxidative polymer degradation is also affected by transition metals. As will be seen later, this effect may have profound significance in the research presented here since transition metal catalysts were used to accelerate the curing process of the cyanate ester thermosets. Traces of these metals accelerate thermal

oxidative degradation by inducing hydroperoxide decomposition (Scheme 2-13). For example, uncoated TiO_2 pigment particles cause melt degradation of PE.[150]

$$M^{n+} + ROOH \longrightarrow RO\bullet + OH^- + M^{(n+1)+}$$

$$M^{(n+1)+} + ROOH \longrightarrow RO_2\bullet + H^+ + M^{n+}$$

Scheme 2-13 Acceleration of Thermal Oxidative Polymer Degradation by Transition Metals

Polyolefins in contact with copper embrittle rapidly due to the formation of copper carboxylate salts. Surface spectroscopy shows that these salts migrate into the polymer and promote oxidation at distances > 1μm from the metal surface.[151] In contrast, many pigments are based on transition metals such as Zn, Fe, Cr, Cd, etc., but they often enhance the thermal stability of stabilizer-free polyolefins, rather than accelerate degradation.[152-153] The commercial benefits gained by this phenomenon are endless; however, each material is unique in its response. Hong et al[154] demonstrated that the incorporation of copper oxides (CuO and Cu_2O) catalytically increases the degradation process and even varies the kinetics of degradation from near zeroth order to an autocatalytic nature.

2.4.4 Methods of Detecting and Quantifying Chemical Aging

Most analytical methods for evaluating chemical aging of polymers in the past have been applied to changes in practical performance. The ASTM has well-

established test procedures for evaluating changes in physical properties, and several critical reviews of methods for evaluating the accompanying chemical degradation have appeared.[155-161]

Spectroscopic methods are most informative for characterizing the chemistry of degradation. UV-visible spectroscopy, although less definitive because of the usually broad nature of the absorption in the solid state, gives a direct correlation with polymer discoloration and can be very sensitive. The extinction coefficients are commonly 10^5 L/(mol•cm) in such UV studies. Derivatization can sometimes be used to allow the detection of weak UV absorbers. For example, hydrazone formation from ketones gives an intense absorption in the visible region [156]. Luminescence (fluorescence or phosphorescence) compliments UV-visible spectroscopy and has the added advantage that emission detection is more sensitive than absorption measurements. Furthermore, the absorption (excitation) spectrum corresponding to a specific emission is often more definitive than the overall absorption spectrum. An example of changes in emission and excitation spectra from a degraded aramid are shown in Figure 2-7.[162]

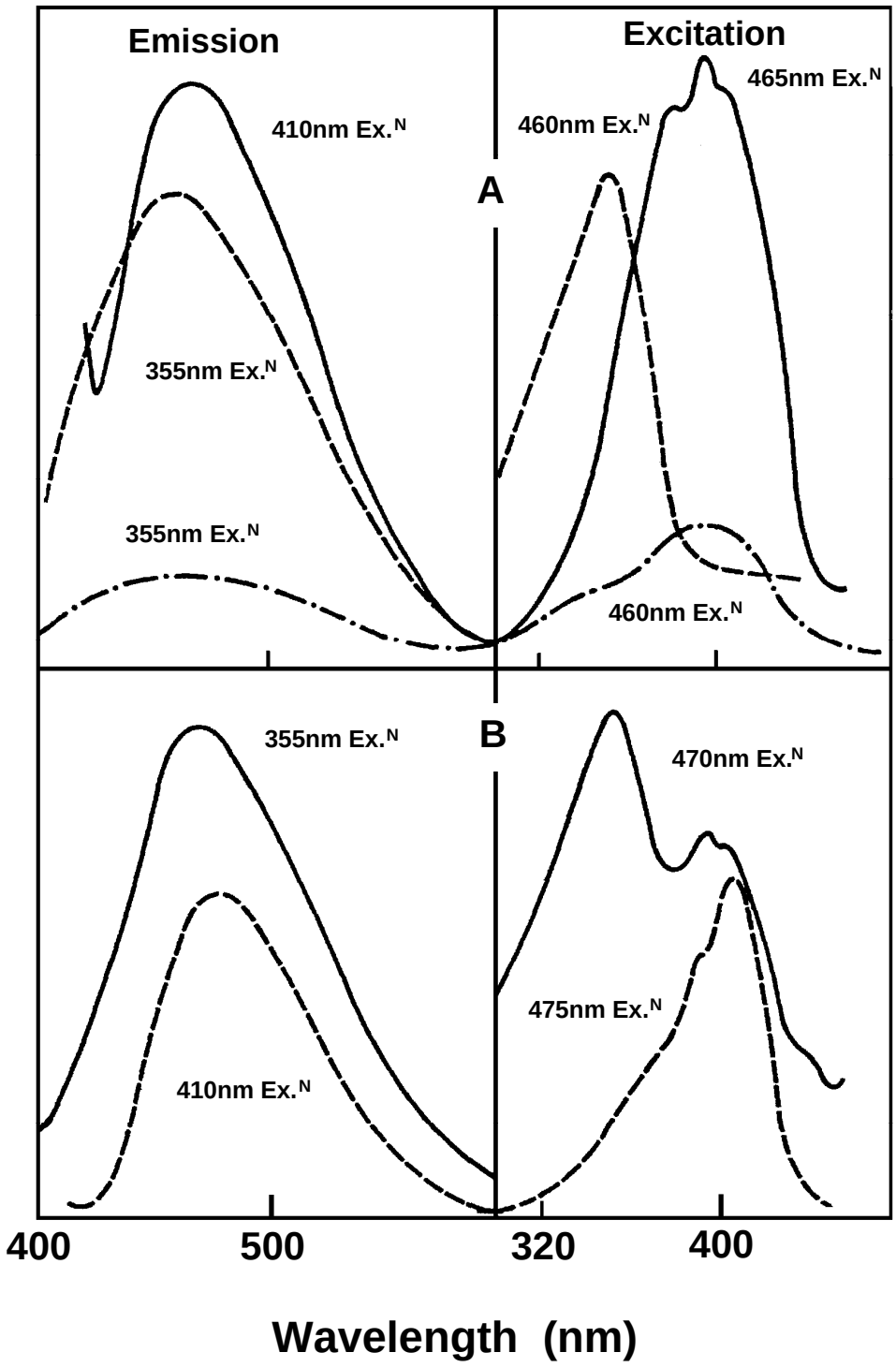

Figure 2-7. Luminescence emission from aramid films at 77K: poly(m-phenylene 1,3-phthalamide). (157)
a.) Irradiated at >310nm under vacuum for 0h (---), 20 h(-•-),and 100 h (–)
b.) Comparative samples containing 2-aminobenzophenone: unirradiated film (0.025 M) (–), 2-propanol solution (-----).

Chemiluminescence is another type of UV-visible emission spectroscopy, where the emission is stimulated by the degradative process itself (usually oxidative). This technique is capable of measuring the exceptionally slow processes that occur during the induction period of the thermal oxidation of polyolefins, polyamides, etc. The exact nature of the reactions leading to the emission process is still not established, although excited ketones from the self-termination of peroxyl radicals are frequently implicated.[163-164]

Infrared (IR) and nuclear magnetic resonance (NMR) spectroscopy are the most definitive techniques for the identification of degradation products. IR has a higher sensitivity than NMR, but less resolution. Fourier transform IR (FTIR) offers the power of computer manipulation of spectra and enhanced signal-to-noise ratios that allow detection of low concentrations of species.[161] The IR of polymer surfaces, i.e., ca. 0.1 •m or greater in thickness, may be recorded by internal reflectance spectroscopy. This technique is useful for thick samples or polymers that degrade exclusively at the irradiated surface, for example, in studying the weathering of many aromatic polymers and metal-surface-catalyzed oxidation processes.[151,165-166] Total internal reflectance IR is limited by the need for excellent polymer-reflection mirror contact. For IR spectroscopy in general, the limitation of overlapping IR absorbances, especially interference with –OH species (ca 3400cm^{-1}) and of carbonyl species (ca 1720 cm^{-1}) can be partially offset by chemical derivatization. For example, –OOH can be discriminated from –OH by SO_2 exposure, which destroys –OOH. Formation of sulfate groups is not

always clean as in oxidized polyethylene.[167] Carboxylic acid groups are smoothly converted to acid fluorides by SF_4 treatment, provided that the heat of reaction does not cause charring.[167-168]

In some instances, the characterization of polymer degradation is difficult to analyze. This is particularly true in highly crosslinked thermosets after cure, when thin films are not easily obtainable, or the lack of a characteristic spectral band is not present. In these cases, new approaches are required to characterize this system. Larrabee et al.[169] used radioisotope measurements to follow the degradation of thermoset blends of poly(methyl vinyl ether). By following the loss of radioactivity of certain isotope labels placed in the polymer, they determined that these materials undergo thermal oxidative degradation when maintained at elevated temperatures. Furthermore, they were able to identify the type of degradation as main chain scission, side chain scission, or a mixture of the two.

The NMR technique has superb structural discrimination, but is limited by low sensitivity. High resolution ^{13}C liquid-phase NMR has been used to study the oxidation of polyethylene.[170] Solid-state ^{13}C NMR also has great potential for the study of polymer degradation.[171]

3.0 Experimental Methods and Test Procedures

3.1 Introduction

This chapter explains the experimental procedures of the research. Several main topics are discussed and cover the synthesis and formulation of the materials employed, the aging profiles used, and the measurement techniques employed to collect the data. First, a brief description of the chemicals employed is given.

The next topic covers the resin chemistry and includes discussions on the various morphologies obtained in a toughened version of the resin. The understanding of cure cycle variations yielding the different morphologies is also described.

The instrumentation employed to obtain data is briefly outlined including the conditions and methods developed to facilitate the different measurements. Included in these discussions are the mechanical tests employed to obtain aging master curves and the methods used to determine the T_g of the samples including modulated DSC. Weight loss measurements over time due to degradation of the resins were obtained as well.

Finally, a brief summary of the aging experiments data is compiled in tabular form. These tables allow for a quick reference to the different observed behaviors.

3.2 Synthesis and Formulation of Cyanate Esters

3.2.1 Material Information

The following materials were employed in these investigations, and for ready reference, each chemical is described via a specification table.

2,2'-Bis(4-cyanatophenyl)propane [AroCy B-10®]

Supplier:	Ciba-Geigy, Inc.
Molecular Formula:	$C_{17}H_{14}O_2N_2$
Molecular Weight, g/mol:	278.312
Melting Point, °C:	79
Density, g/cc:	1.259
Chemical Structure:	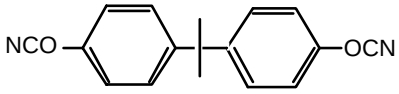
Appearance:	White crystalline powder with practically no odor
Environmental Health and Safety (EH&S):	contains some materials that may be slightly toxic
Comments:	material was used as received from the manufacturer.

Poly(1,4-phenylene ether sulfone-co-1,4-phenylene ether isobenzofuranone) [phenolphthalein based hydroxy functionalized poly(arylene ether sulfone)]

Supplier:	Virginia Tech Experimental Thermoplastic
Molecular Formula:	Thermoplastic polymer
Molecular Weight, g/mol:	M_N = 15,000
Glass Transition, °C:	259
Intrinsic Viscosity [•], dL/g:	0.26

Chemical Structure:

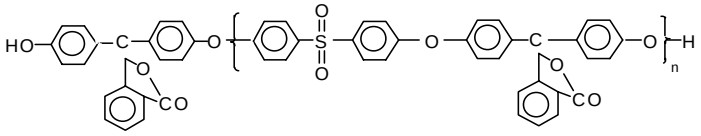

Appearance:	White, odorless flakes
EH&S:	undetermined
Comments:	material was synthesized by Srinivasan[2], recrystalized in chloroform and dried before blending with cyanate ester resin.

Aluminum 2,4-pentanedionate {Aluminum Acetyl Acetonate, [Al (ac ac)$_3$]}

Supplier:	Strem Chemicals
Molecular Formula:	$AlC_{15}H_{14}O_6$
Molecular Weight, g/mol:	324.31
Melting Point, °C:	190-193
Boiling Point, °C:	315

Chemical Structure: 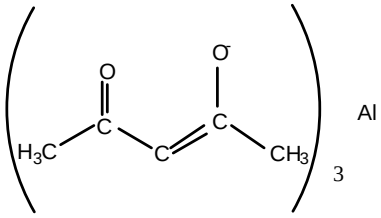

Appearance: White powder with no odor

EH&S: Non-toxic

Comments: material was blended with nonyl phenol and used as the catalyst for the cyanate ester cure

Nonyl Phenol

Supplier: Aldrich

Molecular Formula: $C_{15}H_{24}O$

Molecular Weight, g/mol: 220.36

Flash Point, °C: >110

Density, g/cc: 0.937

Chemical Structure: 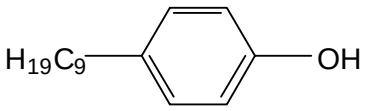

Appearance: Clear, viscous liquid with some odor

EH&S: IRRITANT

Comments: material was used as received from the manufacturer.

Chloroform

Supplier:	Fisher Scientific
Molecular Formula:	$CHCl_3$
Molecular Weight, g/mol:	119.38
Melting Point, °C:	-63
Density, g/cc:	1.492
Chemical Structure:	$CHCl_3$
Appearance:	Clear liquid with strong odor
EH&S:	HIGHLY TOXIC, CANCER SUSPECT AGENT
Grade:	Technical
Comments:	material was used as received from the manufacturer.

3.2.2 Neat Resin

The cyanate ester used in this research was AroCy® B-10 cyanate ester provided by Ciba Geigy Corporation. The monomer will be referred to as B-10 cyanate ester resin throughout the remainder of these discussions.

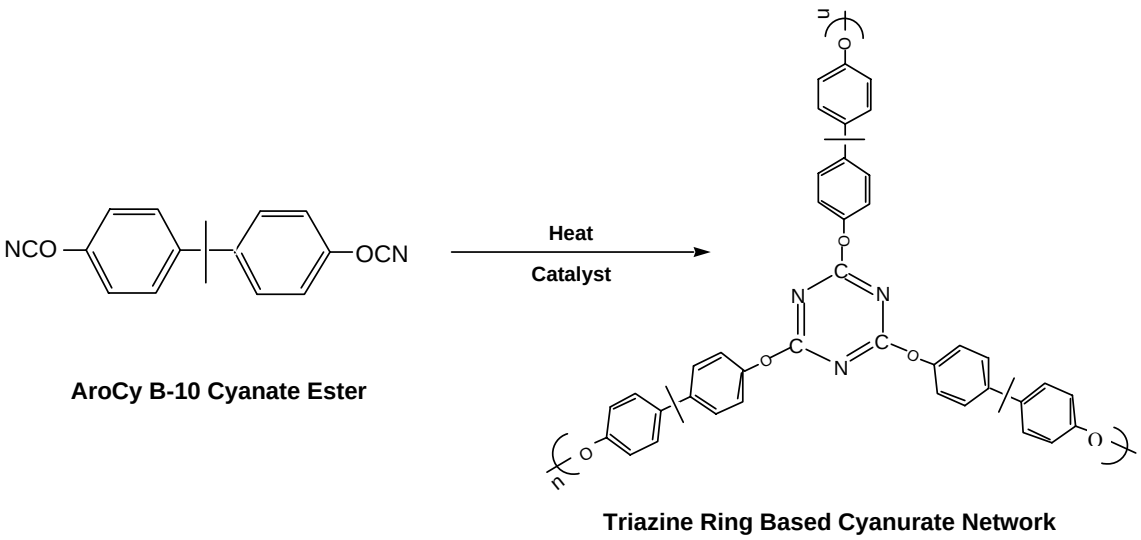

Scheme 3-1. Triazine Ring Based Cyanurate Network Formation

This monomer was chosen for its relatively high glass transition temperature (260 °C) after cure, its simplicity in chemical structure, and its possible uses in aerospace applications. The B-10 monomer was combined with a catalysis agent (250 parts per million (ppm) aluminum acetyl acetonate (AlAcAc) and 2 parts per hundred (phr) nonyl phenol) at 100 °C. The blending temperature was 10 °C above the melting point of the cyanate monomer, yet insufficient to induce polymerization during the time period employed.

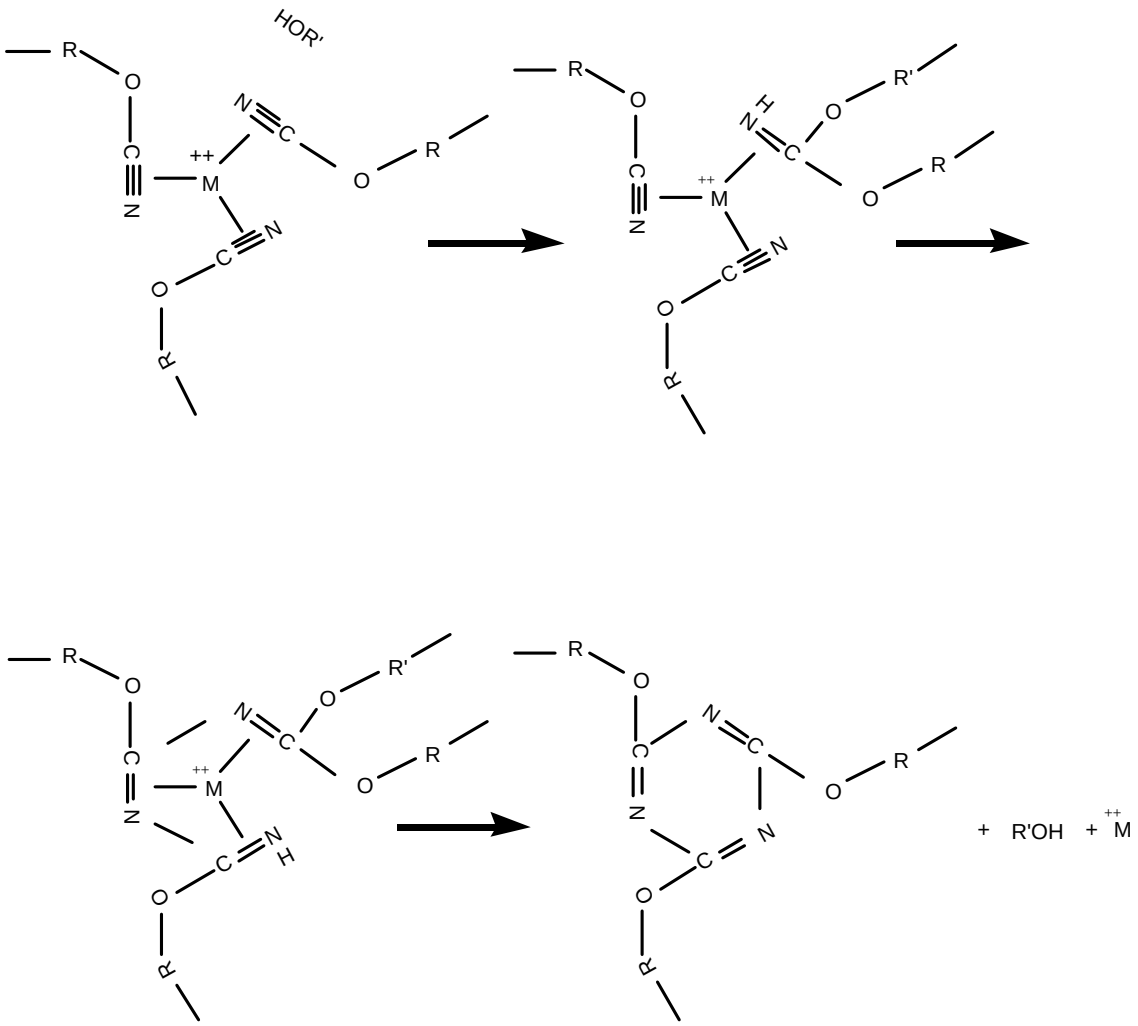

Scheme 3-2. Trimerization Catalyzed by Transition Metal Carboxylates and Active Hydrogens (nonyl phenol)

Scheme 3-2 is a representation of the mechanism believed to occur when transition metal catalysts are used to increase the reactivity of the cyclotrimerization reaction. As a result of the addition of the catalyst, the reactivity of the cyanate ester increased by almost ten-fold. Therefore, it was important to quickly add the catalyst and cool the mixture to room temperature until experimentation. At room temperature, the monomer mixture forms a

crystalline structure, and in this solid form, the polymerization reaction is retarded enough to consider the material to be “fresh” for up to seven days. After this time, the material was discarded and a new master batch was prepared for experimental use.

The materials were cured in a forced air oven at a selected curing cycle as discussed below. Silicone rubber molds were used to make rectangular bars of approximately 1.5 inches X 0.25 inches X 0.125 inches dimension. The molds allowed for all of the bars to be relatively equal in dimension. Before material was added, the molds were treated with a Teflon release agent to insure easy removal of the bars. All of the bars, for a particular aging experiment, were cured simultaneously to ensure identical cure conditions.

Two separate cure cycles were selected to deliberately yield two different morphologies in the experiments containing toughening agents (see below). However, a similar treatment was performed on the neat resin to provide a standard for comparison. The two cure cycles, A and B, begin with the reaction blends held at 104 °C for one hour to equilibrate the monomer and mold temperatures. Then in cycle A, the material was cured for one hour in the temperature region of 150 °C - 160 °C, followed by a post cure of two hours at 250 °C. The post cure ensured a full cure of the material. In cycle B, the cure region was raised to 200 °C - 250 °C, and the reaction mixture maintained at this

temperature for one hour. The material was then treated with a post-cure at 250 °C for 2 hours.

3.2.3 Toughened Resin

Because of the inherent brittleness of the cured cyanate ester material, toughening of the material is needed for practical application. In this research, a phenolphthalein based polysulfone thermoplastic toughener was chosen for study because of its relatively low suppression of the thermoset T_g, and its interesting phase separation behavior which is dependent on the cure schedule.

The polysulfone thermoplastic was a hydroxy functionalized (polyarylene ether sulfone) (Scheme 3-2) synthesized by Srinivasan et. al.[2-1]

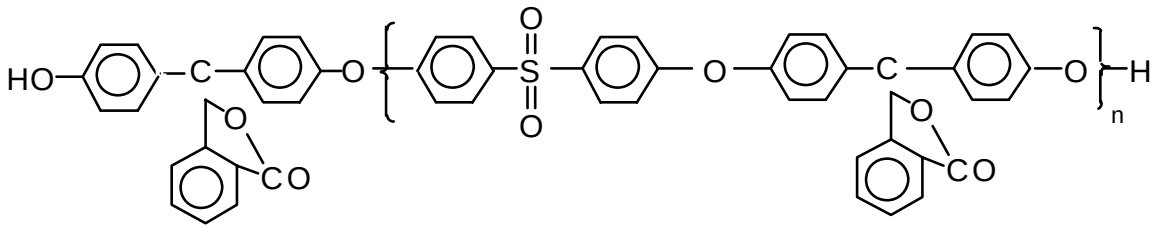

Scheme 3-3. Hydroxy Functionalized Poly(arylene ether sulfone)

The toughener was added at 25% by weight to the cyanate monomer at 100°C prior to the addition of catalysts. This addition was slow and with frequent stirring to insure full mixing of the materials (approximately 10% of toughener added per mixing cycle). Full mixing was determined by the disappearance of

cloudiness in the resin mixture. A vacuum (• -85 kPa) was applied to the mixture for 30 minutes to degas and remove any volatiles or entrapped air. While still at 100 °C, the material was poured into aluminum pans for later use. Again the seven day rule was applied to the room temperature mixture to insure sample "freshness". With the thermoplastic toughener added, a visible phase separation of the materials was observed as the system cooled. It was important to stir the mixture upon reheating to insure dispersion of the toughener and catalyst throughout the mixture.

Depending on the cure schedule applied to the 25% thermoplastic toughened materials, two distinctly different morphologies were observed (Figure 3-1). One aspect of this research was to determine if the observed morphology variation affected the aging properties of the cyanate materials, and if so, to what extent. As a result, two separate cure cycles were performed to yield these different morphologies. To this end, the material was first held at 104 °C for one hour to equilibrate material and mold temperatures. Then, to develop small spherical morphologies similar to that shown in Figure 3-1a, the material was cured for one hour in the temperature region of

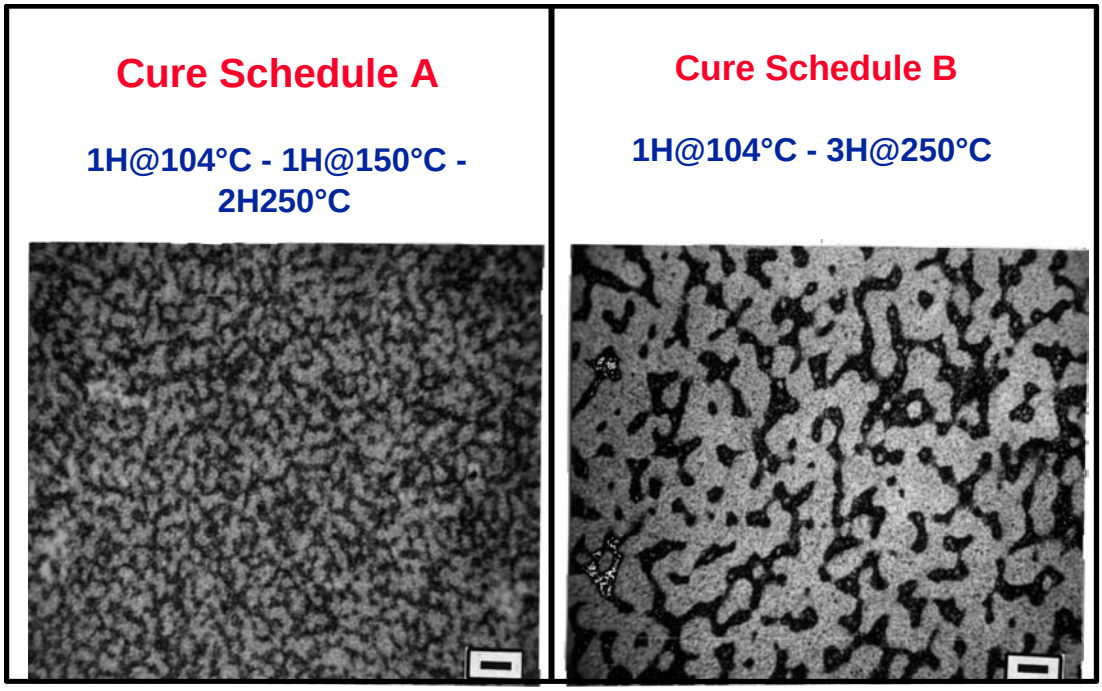

Figure 3-1. Scanning electron microscopy (SEM) comparison of two morpholgies controlled by cure cycle.
a) low temperature cure.
b) high temperature cure.

150 °C - 160 °C. To obtain the co-continuous type morphology (Figure 3-1b), the material was cured for one hour in the region of 200 °C - 250 °C. All of the materials were treated with a post-cure of 250°C for 2 hours to ensure complete conversion of the raw materials to representative morphologies.

3.3 Aging Profiles

For all aging experiments, samples were wrapped in aluminum foil, marked for identification, and annealed. The annealing process consisted of heating the material to 300 °C in a nitrogen atmosphere (approximately 40 °C above the T_g of the material), holding the material at that temperature for 20 minutes to erase any previous thermal history, and then immersing the material in liquid nitrogen as a quench cooling step. To obtain a nitrogen atmosphere in a forced air oven, a two liter Erlenmeyer flask was placed in the oven with the samples inside. Copper tubing was attached to the house nitrogen and channeled into the flask. It was extended to the bottom of the flask to ensure the exclusion of air in the flask. A second hole in the flask stopper was left open to allow a constant nitrogen sweep. The nitrogen was maintained at a relatively high flow rate of approximately 100 cc/min. The annealing process was performed to ensure that all samples received identical thermal history before aging, and quenching in liquid nitrogen allowed for trapping the maximum amount of free volume in the materials. Once the material was cooled, it was placed into an oven at the pre-determined aging temperature and atmosphere until it was ready for

examination. The aging times were recorded for each sample and ranged from 1 to 100 days.

A total of eight separate aging experiments was performed to determine behavioral variations as a result of aging temperature, aging atmosphere and material cure cycle (morphology variations). The first experiment consisted of quenching and annealing cured samples in an attempt to determine the maximum amount of observable physical property changes. Cured samples were placed in a forced air oven in an air atmosphere and heated to 300°C for annealing. The samples were held at temperature for twenty minutes to equalize the thermal histories of the samples. After annealing, samples were cooled at different rates before mechanical testing. The rates varied from a quench cool in liquid nitrogen to cooling rates of 5°C/min and 0.1°C/min to obtain "quenched", "intermediate," and "annealed" samples respectively.

The next two aging experiments were performed at 260°C, a temperature slightly below the T_g of the cyanate ester resin. The experiments differed by changing the aging atmosphere. Samples were aged in nitrogen and in air to assist in separating oxidative degradation from the physical aging process. The samples were heated to 300°C as above to equalize thermal histories of the samples, and subsequently all samples were quenched in liquid nitrogen to trap the maximum amount of free volume prior to the aging process. One set of samples was placed in nitrogen and the other left exposed to normal atmospheric conditions. A set of each sample type was removed at given time intervals (5, 10, 20, and 50

days). They were then prepared for mechanical study by cutting to size for placement in the appropriate instrument and sanding lightly to even the material thickness.

The last five aging studies were performed at 177°C. One study consisted of the neat resin aged in a nitrogen atmosphere. Two of the studies consisted of the neat resin aged in air and differentiated by the cure cycle of the resin (cure A&B discussed earlier). The last two studies incorporated the 25% thermoplastic toughener into the cyanate resin, and incorporated the morphology differences of the cured material due to the cure cycle selection.

3.4 Instrumentation

3.4.1 Mechanical Tests

A Polymer Laboratories Dynamic Mechanical Thermal Analyzer (DMTA) was used to collect the mechanical data for this experiment. In all instances, a small frame for the instrument and small ribbed clamps (B type) were used

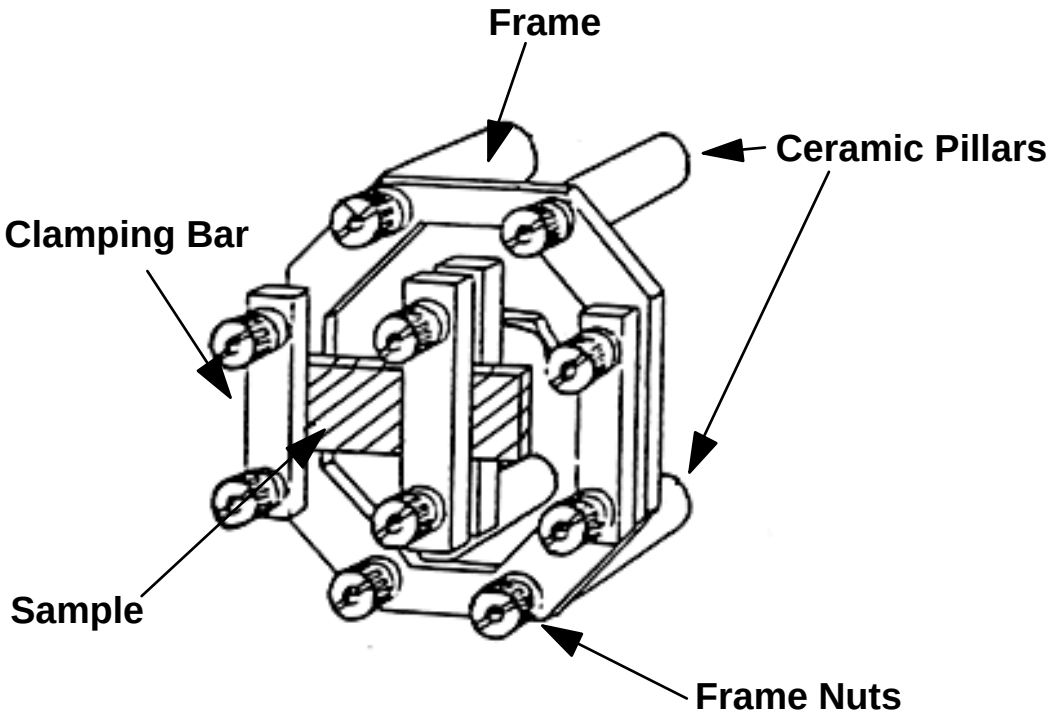

Figure 3-2. Schematic representation of single cantilever bending mode DMTA

(Figure 3-2). The samples were mounted in the single cantilever mode with a strain setting that resulted in a peak to peak displacement of 45 •m. This displacement was well within the linear viscoelastic region of the material as determined by a strain sweep of a test sample. A torque of 40 N/cm^2 was applied to the clamp nuts to secure the sample being tested. For the collection of master curve data, the instrument was run in a "step-isothermal" mode. In this mode, the instrument heated the material to a selected temperature, equilibrated the sample at that temperature, ran a sweep of 10 frequencies ranging from 0.03 Hz to 30 Hz, and then heated the sample to the next temperature. The "step-isothermal" conditions were 4°C intervals from 200 °C to 300 °C. Figure 3-3 is a representation of the raw data collected for the development of the master curves.

To determine material behavior over a temperature range, and to measure the T_g of a sample, a temperature sweep of the sample was required. In this mode, the instrument was run in the range of -150 °C to 300 °C at a heating rate of 5 °C/min. Storage modulus, loss modulus and tangent • curves were monitored over three decades of frequency (0.1 Hz, 1 Hz, and 10 Hz). The maximum of the tan • peak was used as the measurement of T_g. These experimental conditions also provided the information necessary to calculate activation energies for the measured transitions, if desired.

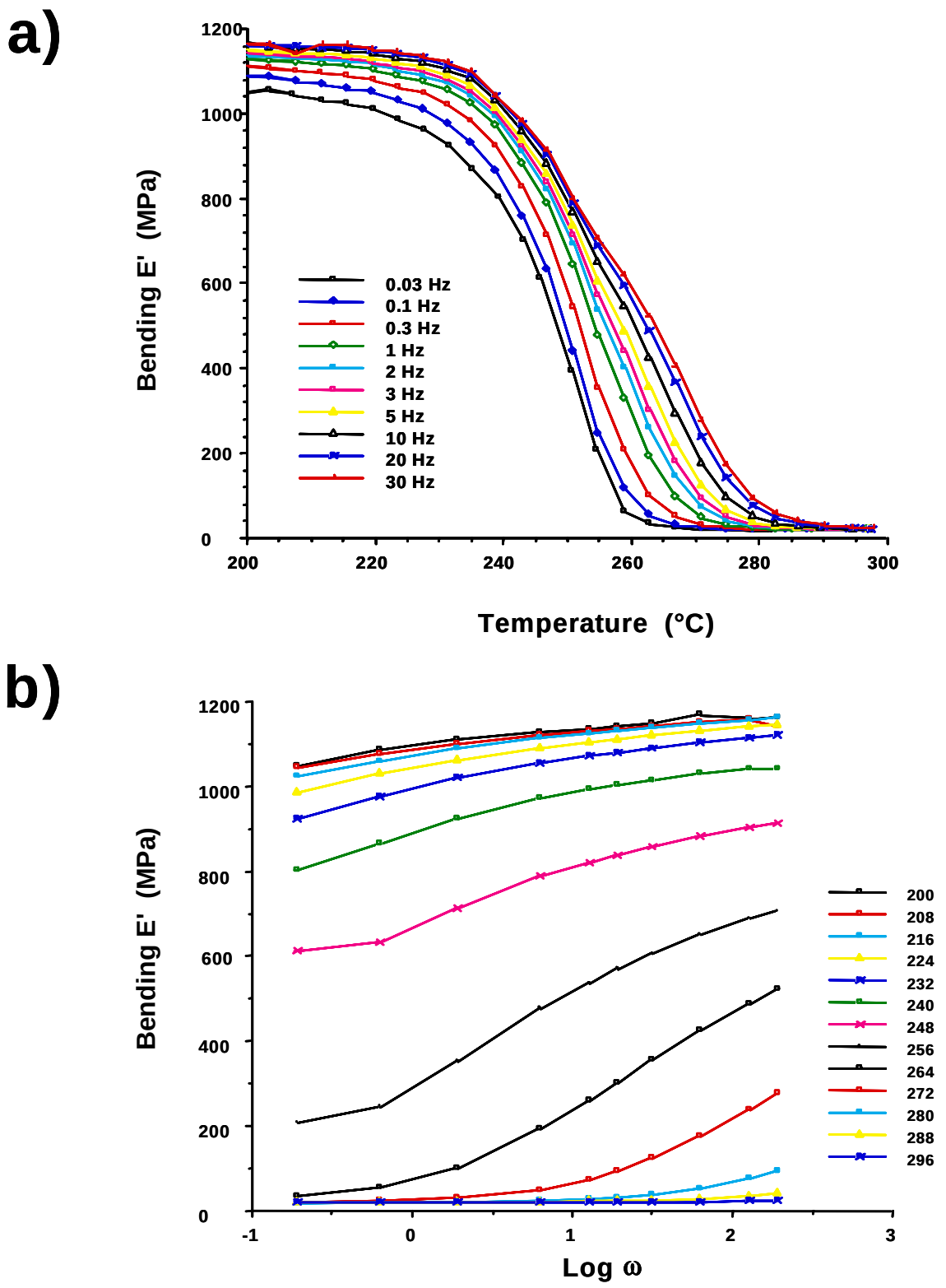

Figure 3-3. Typical Raw data collected for master curve development. (5 days aged @ 177°C in Air)
a.) Storage modulus, E' vs. temperature
b.) Storage modulus, E' vs. frequency

3.4.2 Thermal Gravimetric Analysis (TGA)

A DuPont 951 Thermogravimetric Analyzer was utilized to examine the degradation properties of the aged materials. Samples were heated to 900°C at 10°C/min. By the time the material reached the maximum temperature, material degradation was complete. When run in an air atmosphere, total degradation was determined by totally oxidizing the sample into volatile gases (final sample weight equaling zero milligrams). A bimodal decomposition was observed when the sample was degraded in air. This was determined by the shape of the thermal curve. During bimodal decomposition, the sample is thermally degraded to a degree, and then atmospheric oxygen reacts into the matrix yielding a re-crosslinking of molecules. This is demonstrated by a plateau region in the thermal curve. Continued heat and oxygen overcome the crosslinks and the material is further degraded into organic gases. When nitrogen was used as the atmosphere, the sample reached a relative equilibrium state in which the absence of oxygen retarded further degradation. The data from these scans were transferred to a Microsoft® Excel spreadsheet for processing and correlation.

The TGA was also employed to examine the degree of degradation and to examine the degradation kinetics of the materials. Again for thermal sweep comparisons, a heating rate of 10 °C/min was applied from room temperature to 900 °C in both air and nitrogen atmospheres. When degraded in an oxygen

atmosphere, a bimodal decomposition occurred. Measurements of temperature (·°C) and weight percent of remaining material were taken at the "plateau" onset and compared as a function of aging time. For the kinetic studies, four separate heating rates (5, 10, 15, and 20 °C/min) were employed. From these curves, the iso-conversion method of determining degradation kinetics was performed and the resultant data were examined for comparison purposes. Finally, isothermal (isotracking) measurements were also performed to determine material behavior over time. As part of the instrument software, an isothermal run holds the heater temperature constant, whereas, an isotracking run holds the sample temperature constant. For these experiments, samples were heated to 300 °C and isotracked for 24 hours.

3.4.3 Modulated Differential Scanning Calorimetry (MDSC)

A TA Instruments 2920 Modulated Differential Scanning Calorimeter (MDSC) was used as an alternate source to collect and compare T_g data of the aged cyanate ester samples. The instrument was run in the modulated mode with a specifically designed method. The method consisted of a modulation amplitude of 2°C and a modulation frequency of 60 seconds. The samples were subjected to a 4°C/min ramp from 150°C to 350°C. T_g was observed as a step transition in heat flow with respect to temperature. The inflection point (the point on the curve with the steepest slope) was measured as the T_g of the sample. In the cases where the T_g was not observable over the standard temperature range, the range

was lowered to a start temperature of 50°C. The modulated data were evaluated using TA Instruments Universal Analysis package. The data was also exported to a Microsoft® Excel spreadsheet for further processing, correlation, and presentation.

3.5 Summary of Experimental Data

Below is a summary of the experimental data collected for the aging studies discussed in the next two chapters.

Table 3-1 Quench / Annealing Study

Material: Neat Cyanate Ester Resin (AroCy® B-10) with co-catalysts (250 ppm $Al(acac)_3$ and 2 phr Nonyl Phenol)

Cure: 1 hour @ 104°C, 1 Hour @ 150°C, 2 Hours @ 250°C

Thermal Pre-Treatment: 300°C for 30 minutes in air

	T_g (°C) (by DMA)	Initial Modulus, E', (10^8 Dyn/cm^2) @ 180°C, 1 Hz
Quenched (Submerged into liquid nitrogen)	277	7.33
Intermediate (Cooled @ 5°C / min)	266	8.7
Annealed (Cooled @ 0.1°C / min	257	8.4

Table 3-2 260°C Aging Study

Material: Neat Cyanate Ester Resin (AroCy® B-10) with co-catalysts (250 ppm $Al(acac)_3$ and 2 phr Nonyl Phenol)

Cure: 1 hour @ 104°C, 1 Hour @ 150°C, 2 Hours @ 250°C

Thermal Pre-Treatment: 300°C for 30 minutes in nitrogen, then quench cooled in liquid nitrogen

Aging Time @ 260°C	T_g (°C) by DMA	T_g (°C) by MDSC	Initial Modulus, E', (10^8 Dyn/cm^2) @ 180°C, 1 Hz	TGA Knee Onset Temp. (°C)	Weight %
Nitrogen Atmosphere					
5 Days	275	278	7.9	431	59
10 Days	282	280	8.4	431	62
20 Days	283	265	10.7	436	61
50 Days	287	285	11.5	433	62
Air Atmosphere					
5 Days	N/A	Unable to detect	N/A	430	57
10 Days	N/A	Unable to detect	N/A	410	66
20 Days	N/A	Unable to detect	N/A	395	90
50 Days	N/A	Unable to detect	N/A	120	96

Table 3-3 177°C Aging Study

Material:	Neat Cyanate Ester Resin (AroCy® B-10) with co-catalysts catalysts (250 ppm $Al(acac)_3$ and 2 phr Nonyl Phenol) & 25% thermoplastic toughened resin (phenolphthalein based hydroxy functionalized poly(arylene ether sulfone, M_N = 15,000 g/mol) with co-catalysts catalysts (250 ppm $Al(acac)_3$ and 2 phr Nonyl Phenol).	
Cure:	Cure A	1 Hour @ 104°C, 1 Hour @ 150°C, 2 Hours @ 250°C
	Cure B	1 Hour @ 104°C, 3 Hours @ 250°C
Thermal Pre-Treatment:	300°C for 30 minutes in nitrogen, then quench cooled in liquid nitrogendan	

	Aging Time @ 177°C	Tg (°C) by DMA	Tg (°C) by MDSC	Initial Modulus. E', (10^8 Dyn/cm^2) @ 180°C, 1 Hz
Neat Resin Cure A				
	5 Days	272	263	10.5
	10 Days	270	259	10.4
	50 Days	255	242	8.1
	100 Days	228	220	Unable to Detect
Cure B				
	5 Days	268	253	10.8
	10 Days	266	252	12.8
	50 Days	254	226	10.5
	100 Days	244	218	10
25% Thermoplastic Toughened Cure A				
	5 Days	272	250	11
	10 Days	265	249	9
	50 Days	258	234	7.1
	100 Days	243	221	10.3
Cure B				
	5 Days	264	266	11
	10 Days	264	248	9.9
	50 Days	247	243	9.4
	100 Days	242	233	8.5

This chapter captures the experimental details applied to the chemical and physical evaluation of cyanate ester networks. As will be seen in the next chapter, this approach allowed the separation of the chemical and physical aging components related to environmental cyanate ester resin degradation. It also allowed for the elucidation of the impact of aging on the polymer material properties.

4.0 Results and Discussion

4.1 Introduction

The overall theme of this research was to examine the effects of physical aging and chemical degradation on a model system, while simultaneously evaluating the B-10 cyanate ester resin for applications at temperatures approaching the T_g of the resin. Below are the results of the research conducted and some discussion as to the material behavior observed.

One of the ways of evaluating a material for physical behavior at a specified temperature and over an expanded range of times is the development of a time-temperature master curve of the behavior. This process also allows an overview of material properties covering a wide range of temperatures. And it allows for material behavior predictions that are extrapolated to non-realistically long laboratory conditions, while obtaining the information from short time experiments. The research presented here utilized time-temperature master curve generation to evaluate the B-10 cyanate ester resin.

This chapter is broken down into several sections to better explain the research process. The first section discusses the generation and development of the master curves. The methods employed in obtaining the mechanical data and the comparison of shift factor plots to WLF theory are also covered.

Eight thermal aging studies were performed on the cyanate ester resin to map out its behavior over time, temperature and aging atmosphere. The first study (quench/anneal) was designed to determine the maximum amount of free volume the resin would trap on thermal cycling. This was done by varying cooling rates of the resin from above its glass transition temperature to room temperature (a temperature well below the T_g of the material).

Finally, comparisons are made at two different aging temperatures and atmospheres to examine the effects of physical aging as opposed to chemical degradation of the resins. One set of aging tests was performed at 260°C in air and in nitrogen. The temperature was chosen to be close to the glass transition temperature of the resin. The results yielded the maximum amount of aging (physical and chemical) over the shortest period of time. The second set of aging tests was performed at 177°C; and, this temperature was selected since it is a possible application temperature for the resin. Results discussed in this chapter cover the material behavior in nitrogen and air, and compare the effects of morphology variations in this thermoplastic toughened cross-linked system.

4.2 Master Curve Development

Physical and chemical aging in organic polymers clearly alters material properties. Over a given lifetime of a resin in service, there can be serious consequences of such changes. Therefore, the examination of physical and chemical aging was suggested to determine the extent of aging on the materials in this thesis. At question is the origin of the aging effect on the measurable properties of the material, and the significance of such changes when extrapolated to long times. As discussed in the literature review, the accepted method of investigating and quantifying the long-term properties of a polymer over a relatively short experimental time is through time-temperature-superposition, or TTSP. Although the application of TTSP to mechanical properties is relatively simple, the process can become increasingly complicated and tedious when an array of variables is active in the experiments. Presented below is an overview of the master curve development process used, followed by a discussion of the implications and relevance of the curves that were generated.

A step-isothermal mode of dynamic mechanical analysis was employed to perform this investigation and to supply the raw data for master curve development. Figure 4-1 illustrates an example of the curves obtained from a DMA step-isothermal experiment using the unmodified and cured cyanate ester (neat resin). Plotted is the dynamic storage modulus, E' (Pa) vs. log experimental frequency (ω) in Hz. The data were obtained in this manner to

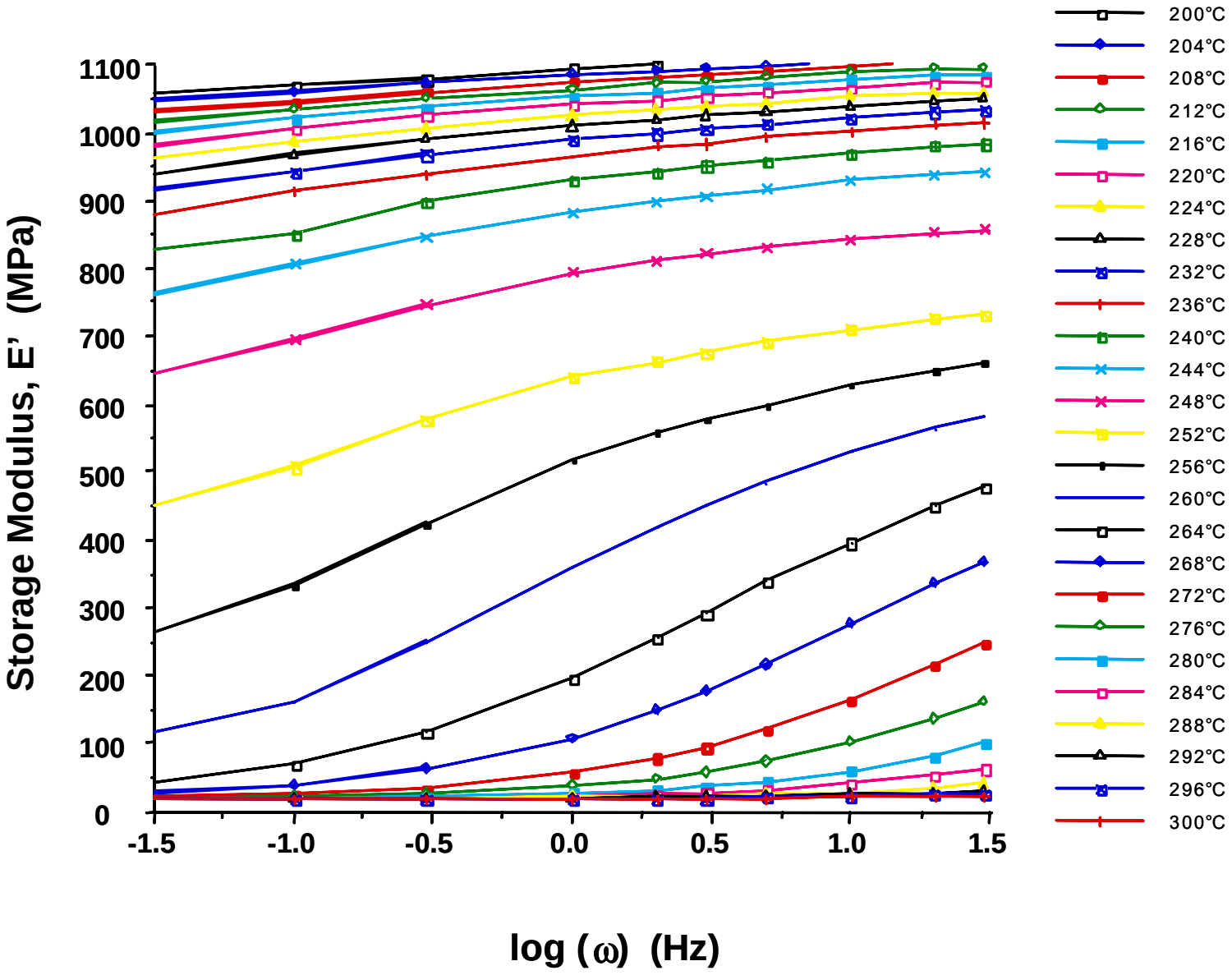

Figure 4-1. Set of isothermal curves developed by DMA in step-isothermal mode. Data collected from unmodified Cyanate ester resin aged for five days in an air atmosphere

develop a family of isothermal curves on a relatively short experimental time scale (~ 8hours). An important point is that in these accelerated experiments only 10% or less of the aging time was consumed. This was believed to prevent significant variation in the modulus response due to continued aging during the experimental temperature rise up to the aging temperature. Once the aging temperature was reached, continued aging was inevitable and meaningful information with respect to physical aging beyond this point in the experiment is severely limited.

The results obtained from these experiments, typical of those in Figure 4-1, show a significantly altered modulus response depending on the temperature of the measurement. The symmetry observed in this family of isothermal curves allowed for horizontal shifting (and some slight vertical shifting for continuity) of the curves with respect to a chosen reference curve. The resultant master curve (Figure 4-2) displayed a familiar s-shape, which is consistent with storage modulus behavior for a polymer of this type advancing through its glass transition. However, a significant difference was observed. The frequency axis of the displayed master curve (Figure 4-2) represents a five-decade increase over the experimental frequency sweep observed in Figure 4-1. The modulus behavior beyond the experimental frequency axis would not normally be detectable in a realistic experimental time frame. However, as explained below, this information is highly useful in predicting the long-term behavior of the material at the specified reference temperature.

a.)

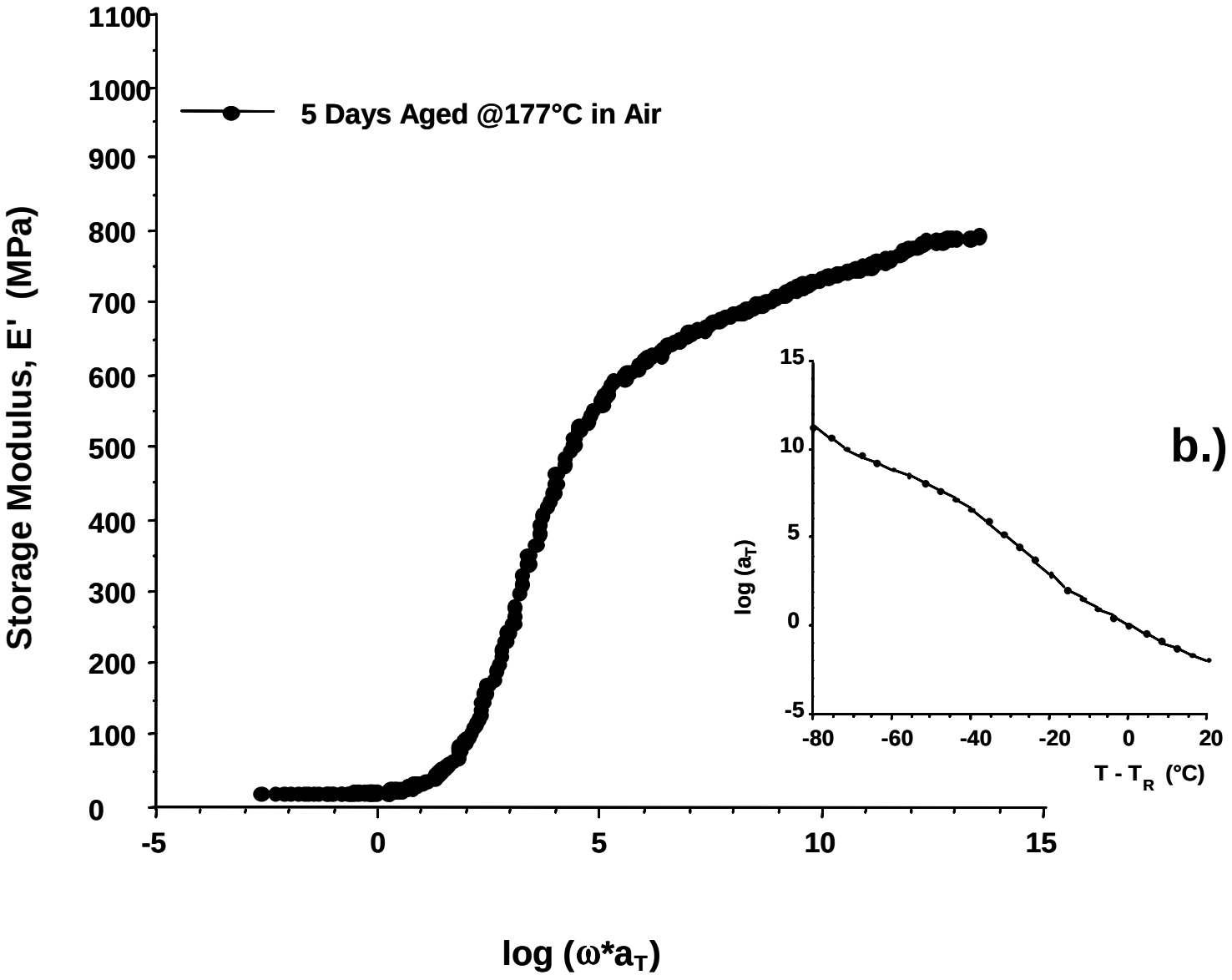

Figure 4-2. Master curve produced from time-temperature superpositioning.
a.) Master curve of storage modulus (E')
Reference temperature = 280°C
b.) Resultant shift factor plot

Accompanying the master curve in Figure 4-2 is a plot of the shift factor data. As an isothermal curve is shifted to produce superposition, the amount of shift is measured as the displacement on the frequency axis from the selected reference curve. [In this case, the reference temperature was 280°C, and was chosen as a temperature near but slightly above the T_g of the material where WLF behavior is observed.] The shift factor is plotted against the temperature of the isothermal curve, usually in a reduced form ($T-T_R$), and is called the shift factor plot. As was discussed in the literature review (Chapter 2, Page 44), the smoothness of the master curve, the continuous nature of the shift factor plot, and confirmation that the shift factor applies for other viscoelastic functions for the same polymer over the same temperature range (Figure 4-3), indicates that the superposition principle is valid as applied for this material.

Analysis of the above master curve information permits an interpretation of the dynamic response of neat cyanate ester resins over a specified time and temperature regime. Aging the material at a specified temperature, T_A, for varying amounts of time, t_e, in a specified atmosphere, and then applying the superposition principle to each set of resulting isothermal master curves, produces a family of time-temperature master curves. Figure 4-4 displays the storage modulus results when the neat cyanate ester resin was aged

4-3a.)

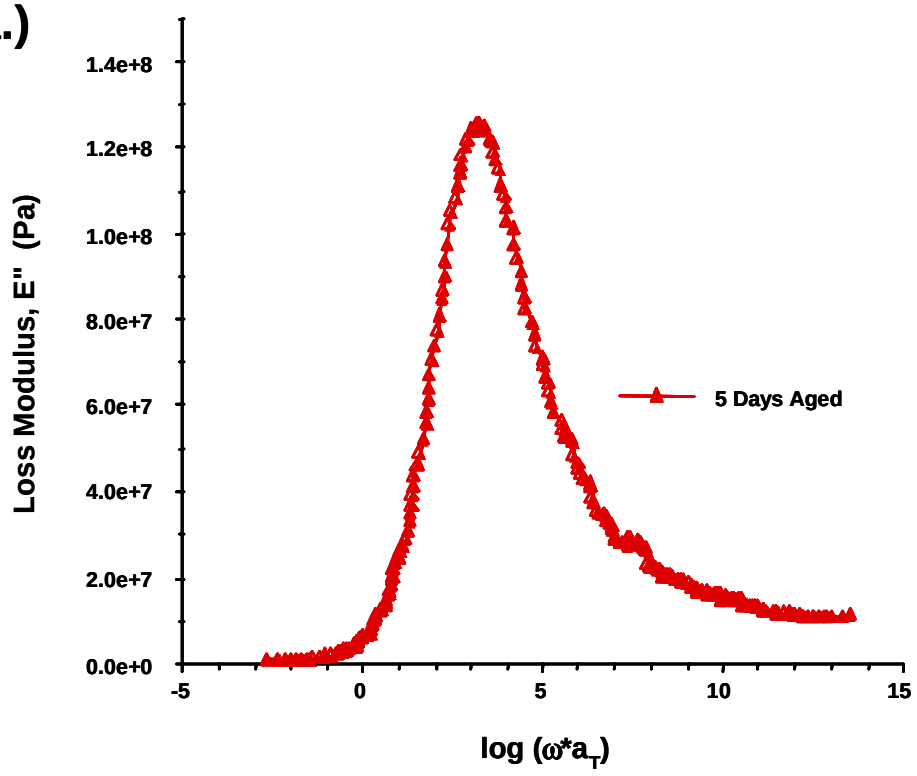

4-3b.)

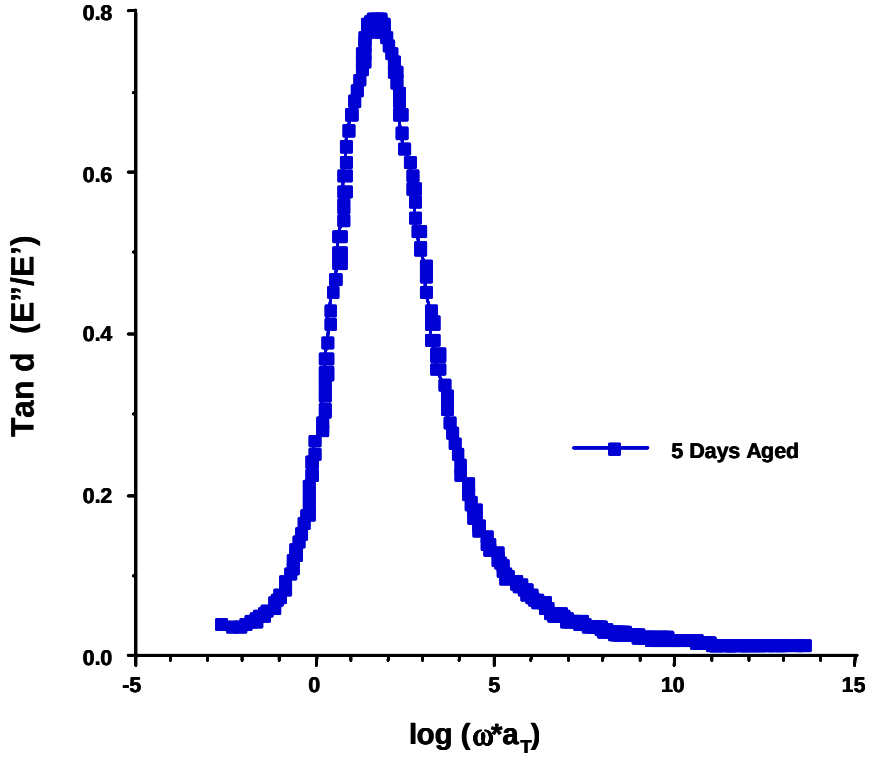

Figure 4-3. Other viscoelastic property master curves generated using the same shift factors, a_T
a.) Master curve of loss modulus (E")
b.) Master curve of tan δ (E"/E')

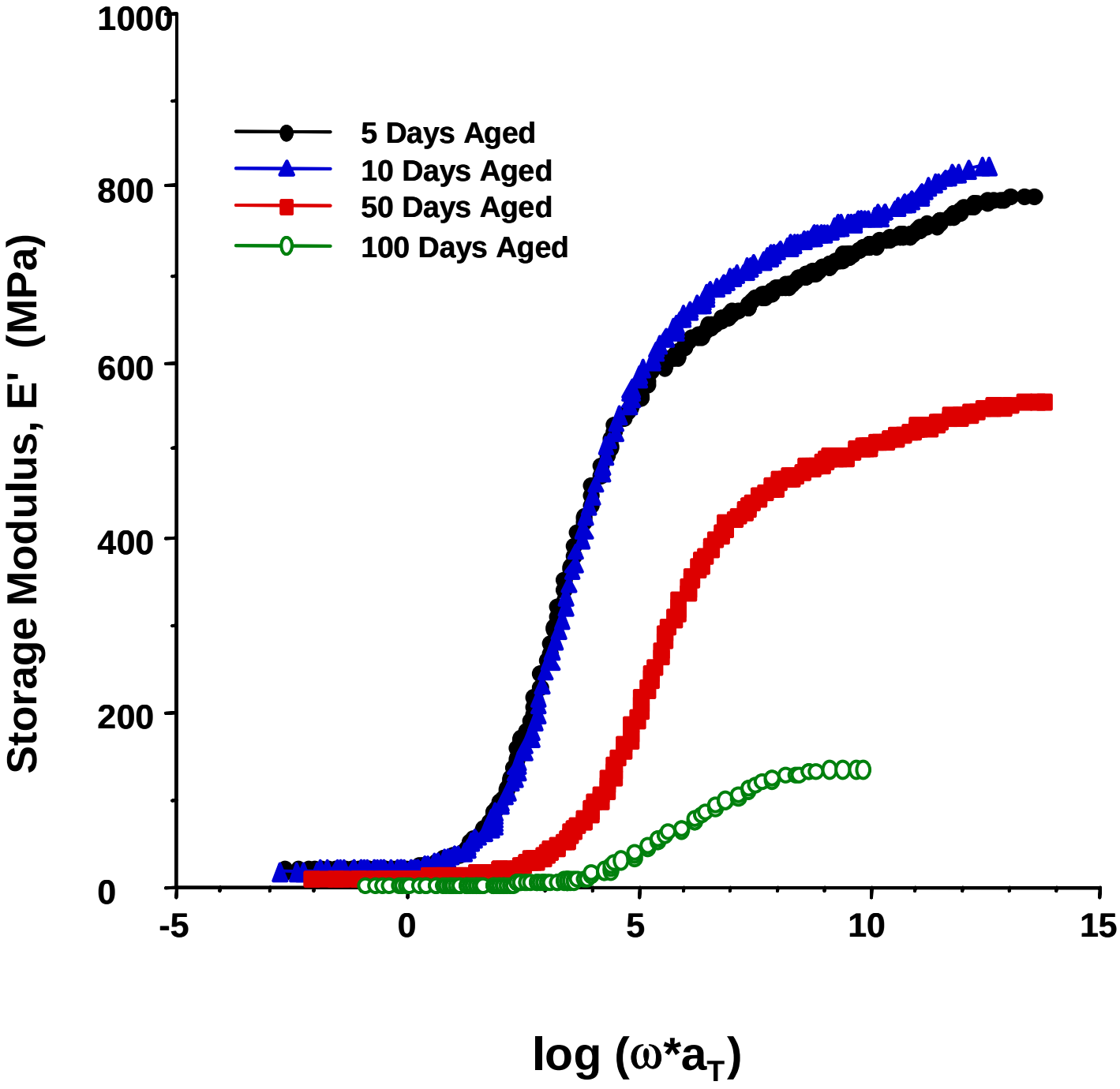

Figure 4-4. Family of master curves developed for neat cyanate ester resins at 177°C. The samples were aged in an air atmosphere for the times shown.

in an air atmosphere at 177°C. The curves displayed represent five, ten, fifty and one hundred days aging. In this case, the experimental time (8 hours) was substantially less than 10% of the aging time, supporting the assumptions for analysis. Therefore, the resultant shifts in the curves may be attributed to a material aging process and not to experimental artifacts (see section 4.3.1c for detailed explanations of material behavior).

A family of shift factor plots was also generated for the samples with varying aging histories (Figure 4-5). The behavior observed in these shift factor data can be compared to the theoretical prediction of WLF behavior for this polymer, as represented by the "calculated WLF line" in Figure 4-5.

4.3 Aging Analyses

4.3.1 Quench/Annealing Study

Screening studies were performed to determine the amount of measurable change in mechanical properties due to physical aging. This was accomplished by developing a “quench/annealing” process. In this study, each sample was rapidly heated (>20°C/min) to 300°C (an arbitrary temperature above the cyanate ester resin T_g) and held at temperature for 20 minutes in an air atmosphere. This process erased the thermal history residing in the

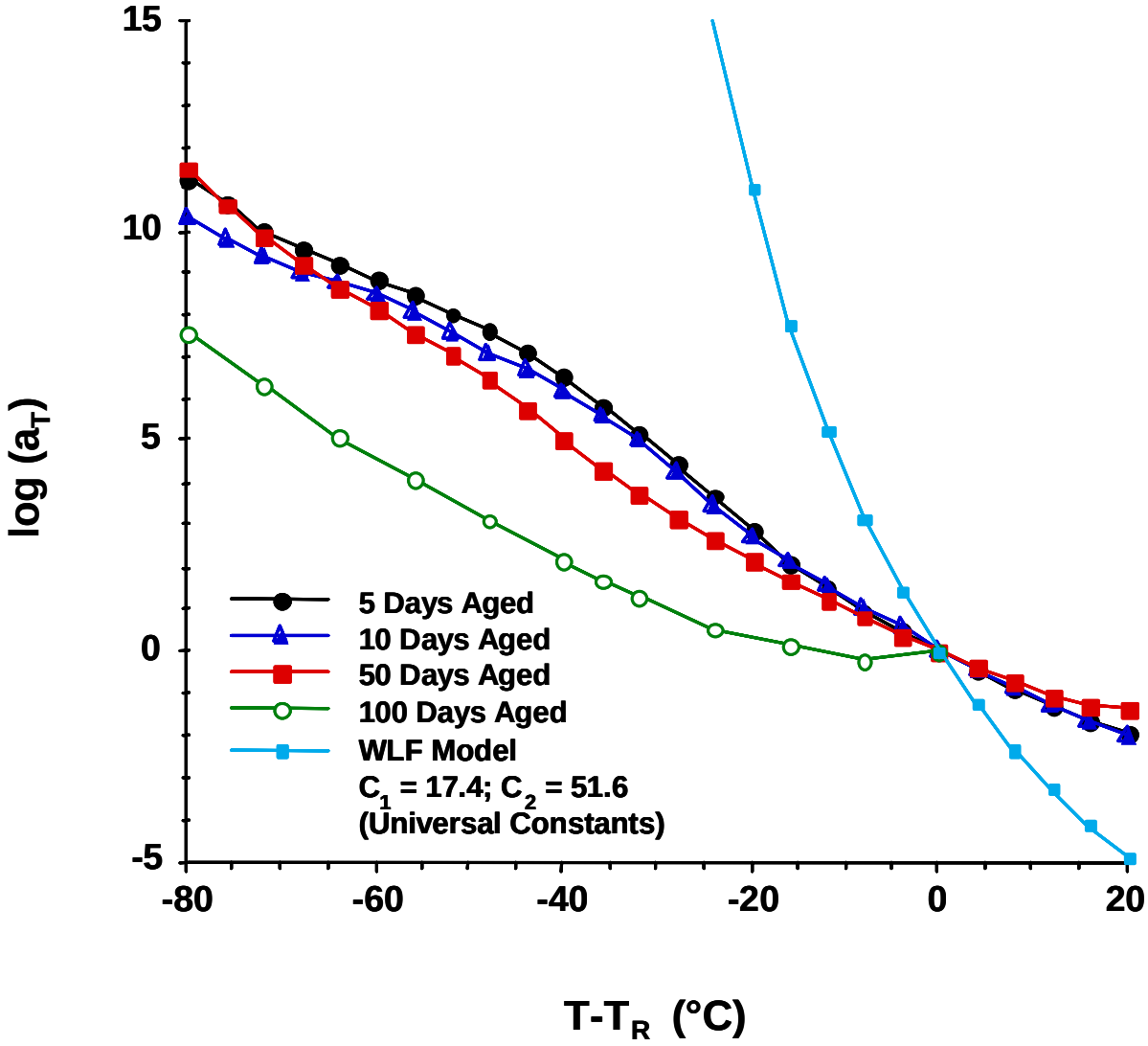

Figure 4-5. Shift factor plot data against reduced temperature. Data corresponds to master curves in Figure 4-4. WLF model calculated using universal constants.

samples and established a baseline for further study. Once the thermal history was erased, one set of samples was immediately removed from the 300°C atmosphere and quenched in liquid nitrogen. This process was employed to insure that the free volume trapped in the network was maximized. Other sets of samples were cooled at varying rates for subsequent analysis. The set cooled at the slowest rate (0.1°C/min) was designated as "annealed" since the slow cooling is anticipated to produce the greatest amount of material densification. One would expect a subsequent comparison of master curves for the quenched and annealed samples to yield an indication of the greatest range of shift in the mechanical properties associated with physical aging. This shift would be made manifest as an increase in initial modulus and an increase in material T_g with increasing densification. Unexpectedly, this was not observed (Figure 4-6). Figure 4-6 is a representation of the master curves of storage modulus (E') and Figure 4-7 is a representation of the tan δ curves for the quenched and annealed materials. The x-axes of the curves in Figure 4-6 and Figure 4-7 are the logarithm of experimental frequency multiplied by the amount of horizontal shift required to overlay the isothermal curves. Also, displayed in Figure 4-8, is the shift factor plot for these master curves. Figure 4-6 shows two, seemingly contrasting characteristics. First, by comparing the "unrelaxed" region of the master curves, the region below the T_g (in this case the region above 10^6 Hz), the expected quench verses annealed behavior is observed. The annealed sample displays a higher initial modulus in the glassy state indicating a denser, more compact, and stiffer material.

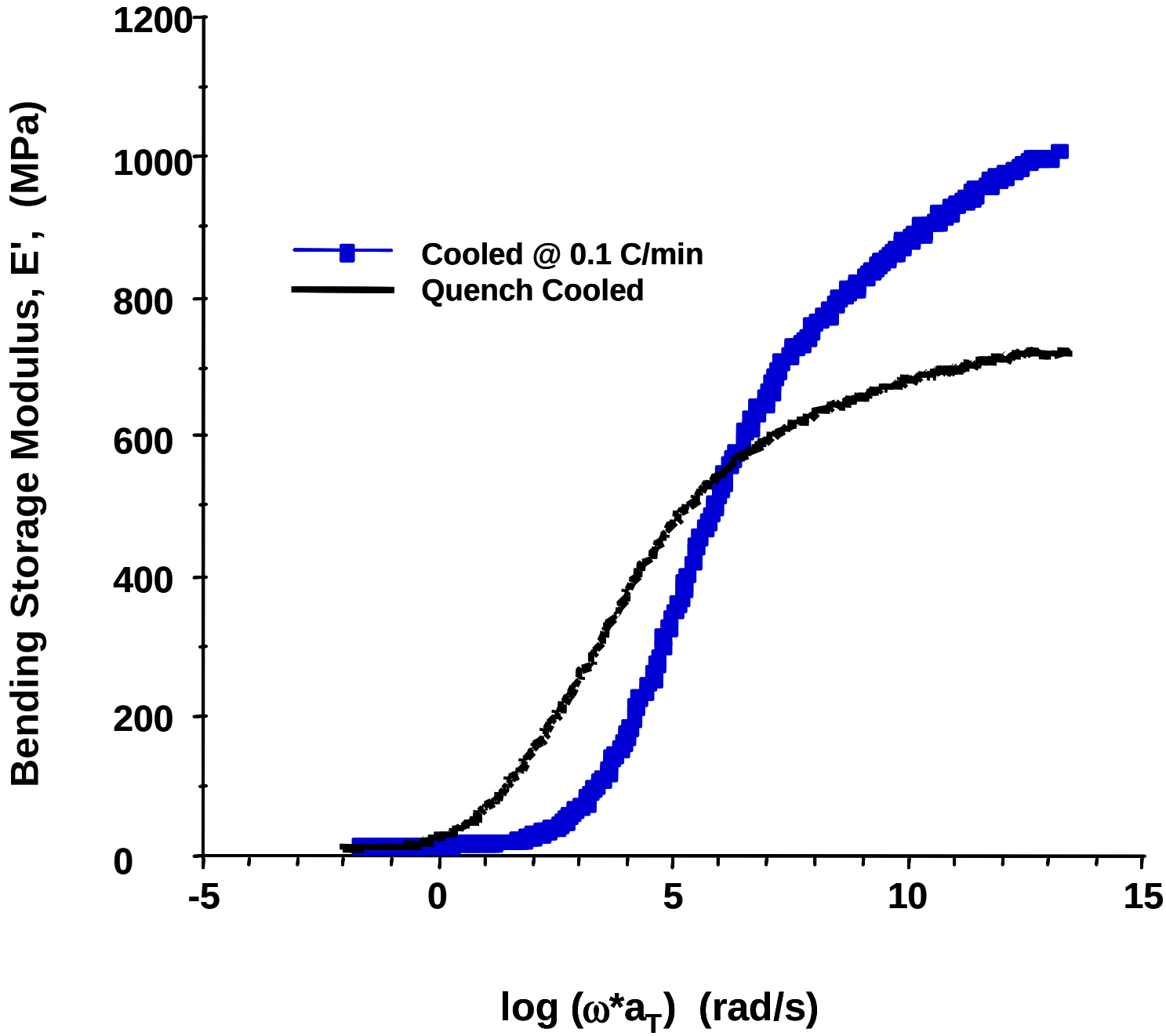

Figure 4-6. Bending storage modulus master curves of neat cyanate ester resins. A comparison is made of quench cooled verses annealed (slow cooled) samples. Samples were prepared in an air atmosphere; mechanical testing was performed under nitrogen.

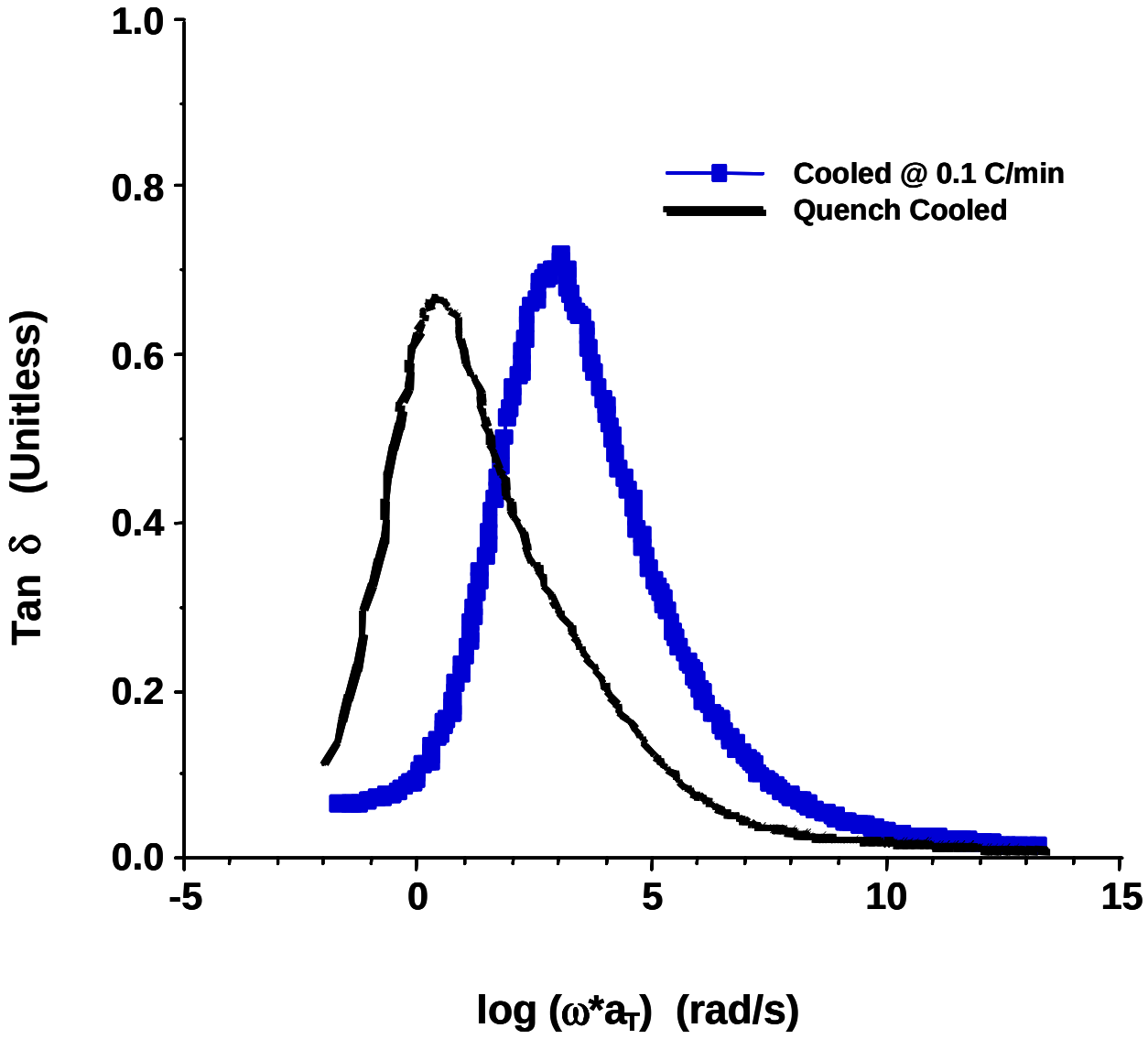

Figure 4-7. Bending tan• δ• master curves of neat cyanate ester resins. A comparison is made of quench cooled verses annealed (slow cooled) samples. Samples were prepared in an air atmosphere; mechanical testing was performed under nitrogen.

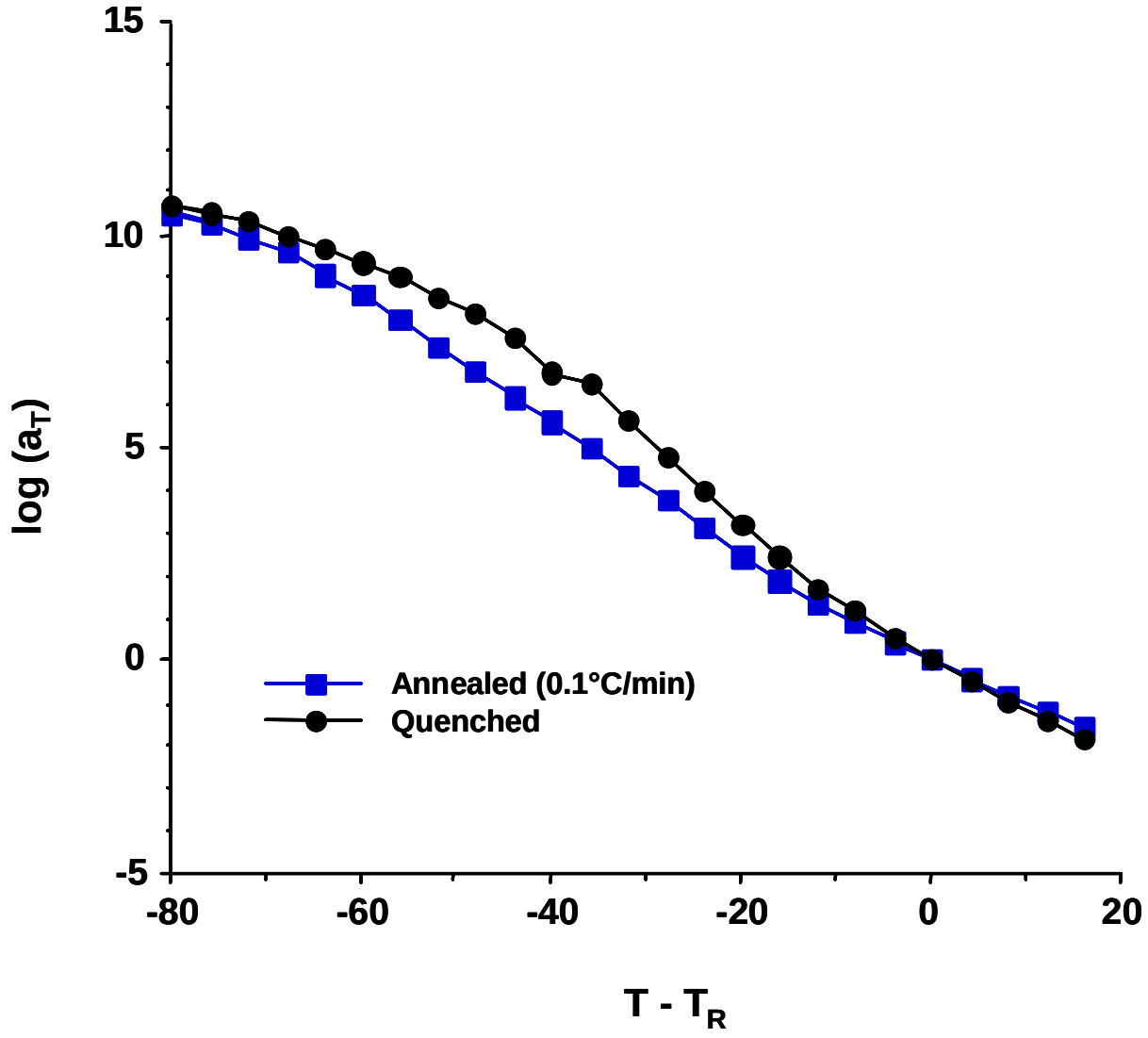

Figure 4-8. Shift factor plot generated corresponding to the master curves in Figure 4-6 and Figure 4-7.

However, a crossover in material behavior occurs toward the lower frequency side and the quenched sample appears to exhibit longer relaxation times (relaxations occurring at lower frequency). This behavior is contrary to the expected behavior assuming only reversible (physical) aging as the mechanism affecting the master curves. In theory, a more dense material would require more energy to produce the free volume sufficient to induce chain movement sufficient for a transition to occur. In this experiment, the increase in thermal energy is linear (a constant heating rate applied to the sample). The expected behavior would be a longer time required for the more dense material to relax. In fact, the opposite was observed.

Insight to this puzzling behavior comes from analyzing the data as a function of temperature (Figure 4-9). Figure 4-9a represents the E' behavior of the material as a function of temperature. Again, a crossover phenomenon is observed. Specifically, at temperatures below the T_g, the annealed sample displays a higher modulus (expected for a more dense material) yet it required less thermal energy (short relaxation times) to reach its glass transition on heating. This is clarified in Figure 4-9b, where the T_g of the annealed sample is considerably lower than that of the quenched sample as indicated by the change in the tan δ peak maximum. This crossover phenomenon suggests that competing mechanisms are occurring. Rationally, these competing mechanisms are likely to be physical and chemical aging. The physical aging process (loss of trapped free volume) is measurable in the region below the T_g.

4-9A

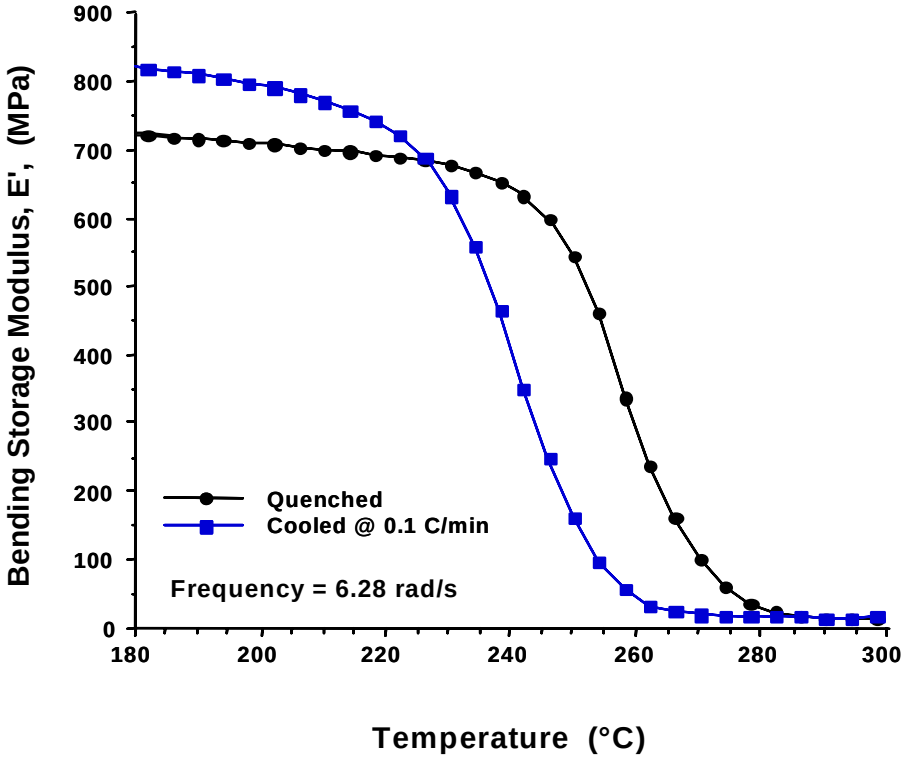

4-9B

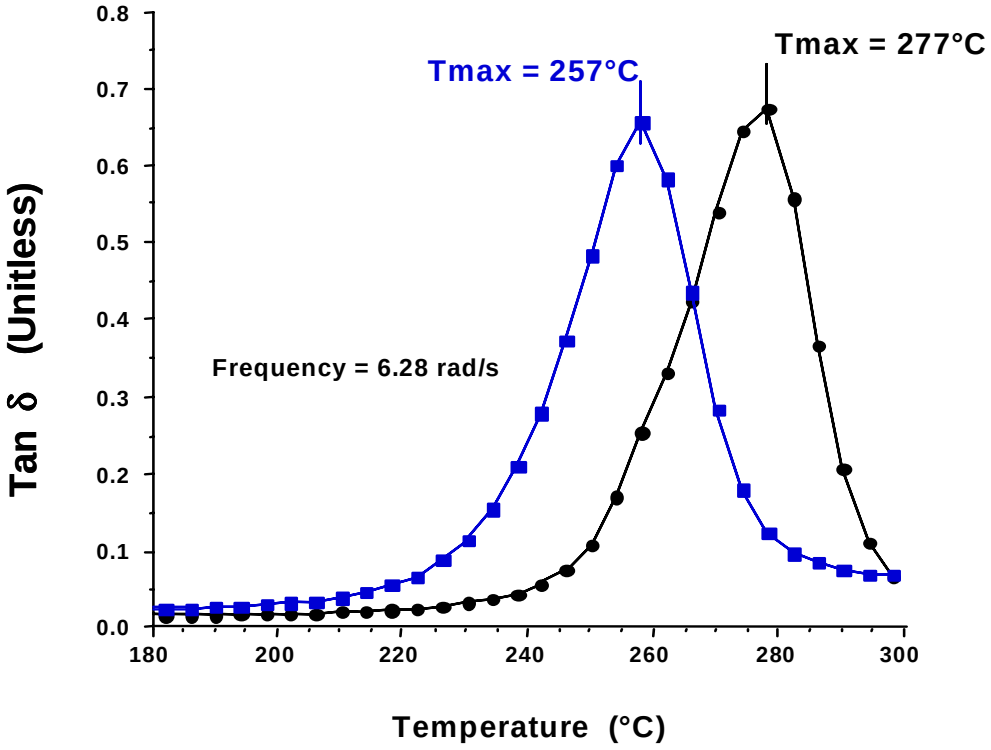

Figure 4-9. Mechanical data displayed as a function of temperature for the quenched and annealed samples. Samples were prepared in an air atmosphere; mechanical testing was performed under nitrogen.

a.) Storage modulus data

b.) Tan δ data

However, in the cases of the step-isothermal experiments, there was suitable time for the material to physically age as the T_g was approached during the experiment. This suggests that the measured T_g of the quenched sample was actually the maximum obtainable T_g for this material. To observe a lower T_g due to trapped free volume would require a more rapid heating rate through the T_g to prevent the onset of physical aging during the experiment. The second of the proposed competing mechanisms is chemical degradation resulting from the high temperature exposure. For proper annealing to occur, the sample was cooled from 300°C to room temperature at 0.1 °C/min. This slow heating rate subjected the samples to high temperatures and an oxidative atmosphere for almost two days. This harsh environment is expected to cause chemical changes and result in the lower T_g. At temperatures below the T_g, the effects of densification are clearly observed. However, as a sample was heated to its T_g, the chemical degradation (which leads to an increase in low molecular weight species and chain ends) manifested itself as a decrease in the T_g.

Supporting evidence that degradation of the annealed sample caused the above behavior was obtained by comparing the above results with a sample that was cooled at 5°C/min. These results are displayed in Figure 4-10, where the 5°C/min cooling cycle is designated as an "intermediate" rate. Several confirming observations are made from this data. First, at temperatures below the T_g, the intermediate sample had the highest initial storage modulus. This indicates that cooling at

4-10a.)

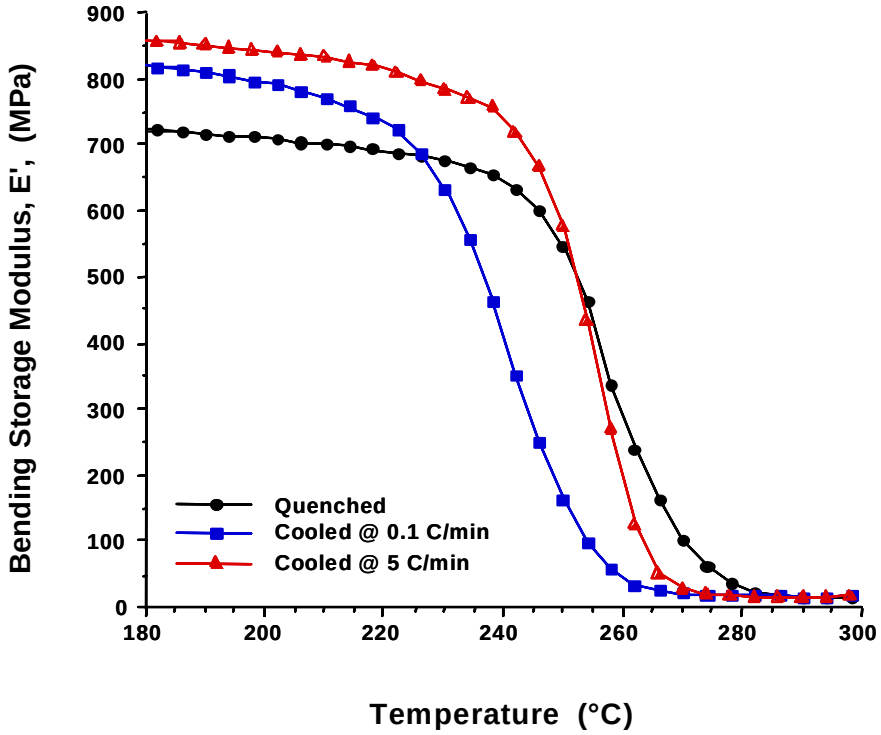

4-10b.)

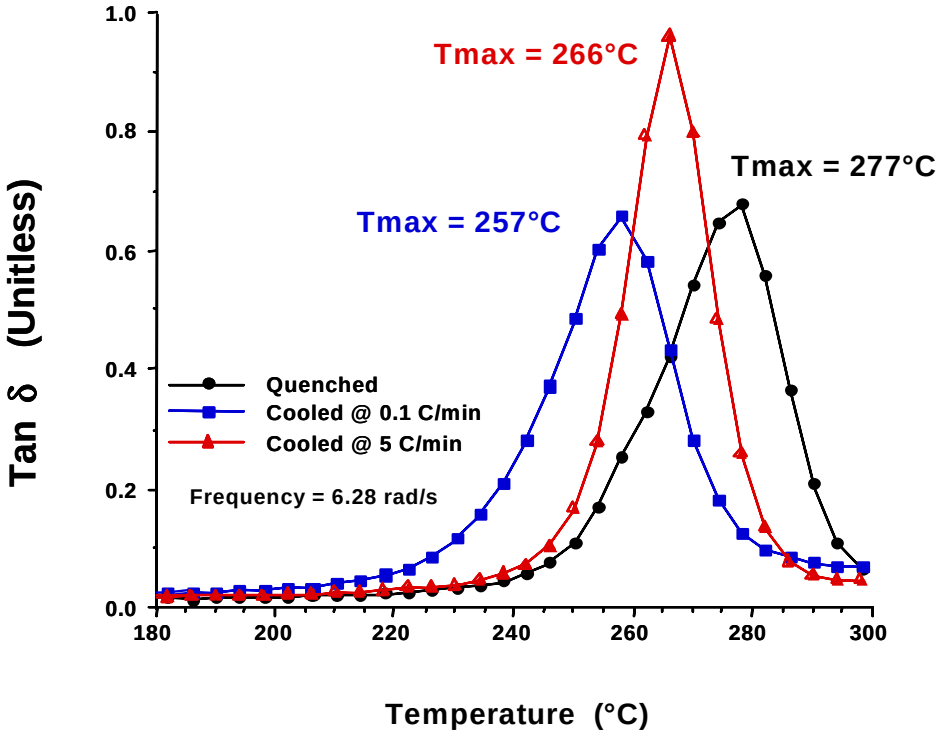

Figure 4-10. Mechanical data displayed as a function of temperature for the quenched, intermediate and annealed samples. Samples were prepared in an air atmosphere; mechanical testing was performed under nitrogen.

a.) Storage modulus data

b.) Tan δ data

5°C/min is relatively slow compared to the quench cooling, and resulted in a more dense sample. The modulus was also higher than the annealed sample suggesting that the sample experienced far less change initiated by high temperature and atmosphere resulting in less chemical degradation. The second observation notes the higher temperature required for the initiation of the glass transition by intermediate cooling compared to the annealed sample. This indicates that the intermediate material experienced much less chemical degradation than the annealed sample. Next, by examining the peak maximum (T_g) in Figure 4-10b, the intermediate sample displays a higher T_g than for the annealed material. This finding supports the concept that less degradation is occurring. It is interesting however to note that some degradation did occur in the intermediate sample, and this resulted in a lower T_g compared to the quenched sample. Finally, the breadth of the tan δ peak for the intermediate sample is much narrower than for either the quenched or the annealed sample. This observation again confirms there is less free volume in the intermediate sample than in the other two. It also displays the sensitivity of the measurement process.

4.3.2 Aging in Nitrogen

4.3.2a 260°C Aging Study , Neat Resin

The information obtained from the “quench/anneal” study above (especially in the un-relaxed region of the mechanical data) substantiates the ability of these master curves to detect physical aging in the cyanate ester resins. The next step in the experimental process was to determine if physical aging alone could be isolated in a family of these time-temperature master curves. Tests were conducted to age a set of cyanate ester resin samples in a nitrogen atmosphere at 260°C, a temperature close to the observed glass transition temperature (~ 280°C) of the material. These conditions were selected to eliminate oxidative degradation pathways and to allow for analysis of the thermally stimulated aging processes. The results of these experiments are displayed in Figures 4-11, 4-12, and 4-13 which show the storage modulus master curves, the tan δ master curves and the shift factor plots for these samples, respectively. Displayed are the curves for five, ten, twenty and fifty days of aging. From examination of the storage modulus master curves (Figure 4-11), some anticipated trends are confirmed. The most significant observation is the increase in initial modulus with increasing aging time. This increase is evident in the high frequency region of the data, and suggests that a densification process is occurring during the thermal aging process. This densification causes the increase in initial stiffness, and is also observed as the increase in the slope of

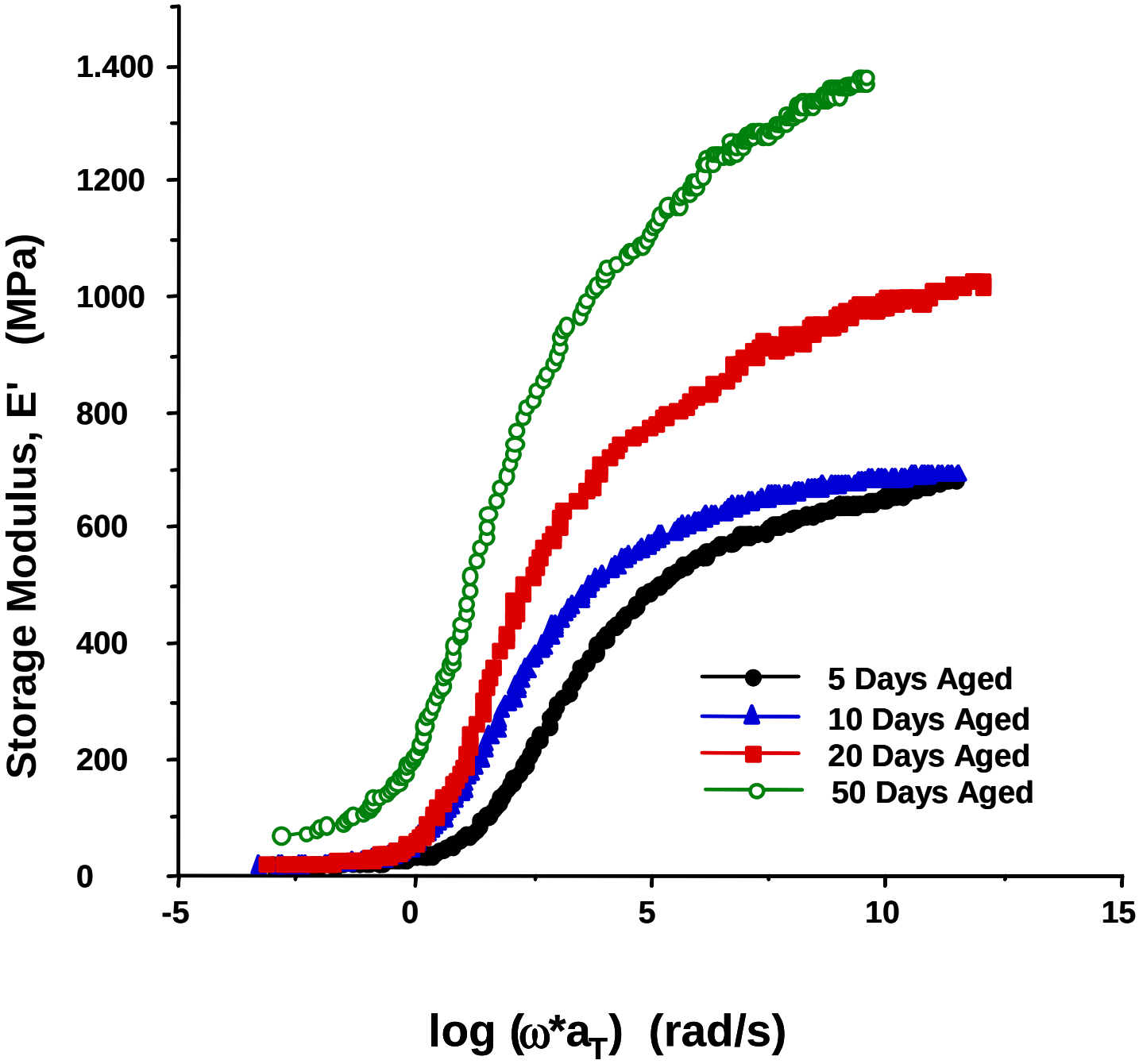

Figure 4-11. Bending storage modulus master curves of neat cyanate ester resins. A comparison of samples aged in nitrogen at 260°C for varying amounts of time.

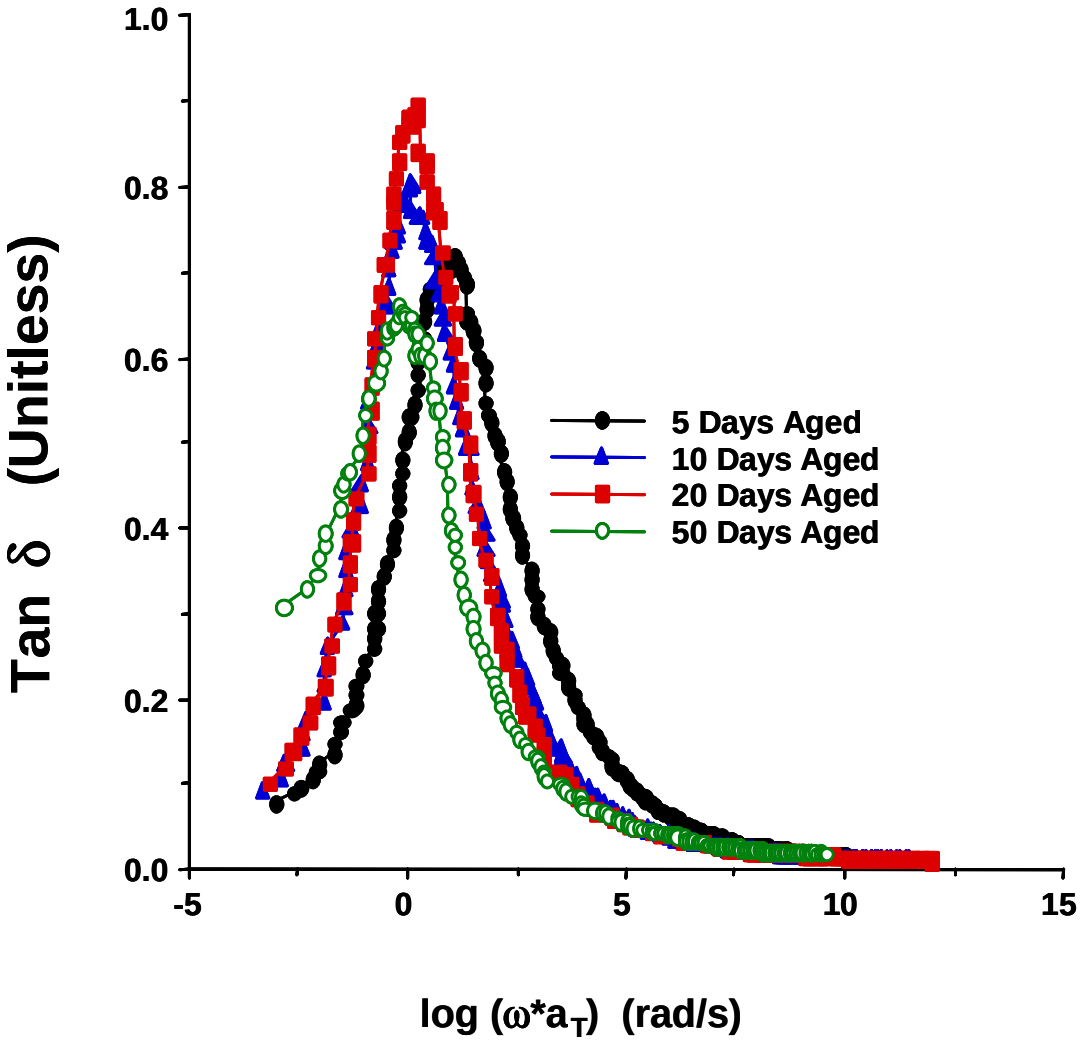

Figure 4-12. Bending tan •δ• master curves of neat cyanate ester resins. A comparison of samples aged in nitrogen at 260°C for varying amounts of time.

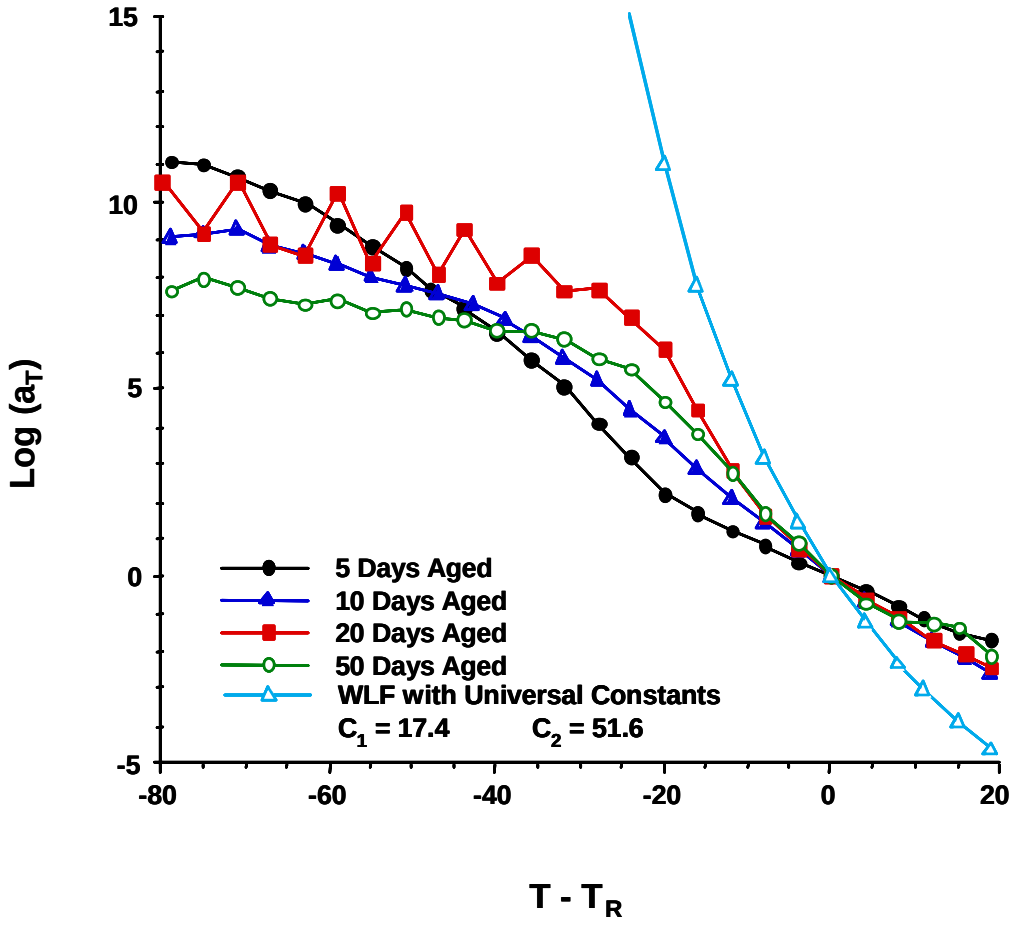

Figure 4-13. Shift factor plot generated corresponding to the master curves in Figure 4-11 and Figure 4-12.

the modulus curve during the maximum change in the modulus property. This change in slope, along with the shifting of the curves to lower frequency (longer time), suggests an apparent increase in the T_g of the material. This increase in T_g was supported by the tan δ master curves shown in Figure 4-12. Although slight, a shift in the maximum of the tan δ peak toward lower experimental frequency was detected and can be correlated with longer relaxation times.

To better illustrate the changes in the material as a function of aging time, the mechanical test data were reorganized and the isochronal data corresponding to a single frequency (1 Hz) was plotted as a function of temperature. This analysis method is perhaps more intuitive for interpretations and is displayed in Figure 4-14. Figure 4-14a (the storage modulus plot) demonstrates the increase in initial modulus with increasing aging time, and the steeper slope during the transition agrees with an initially increased material densification associated with physical aging. Also observed, is the advancing of the "knee" in the curves to higher temperatures. This represents an increase in the T_g of the material. Figure 4-14b contains the companion plot of the tan δ clearly showing the T_g increase. This is demonstrated as the shift in the tan δ peak maximum to higher temperatures with increasing aging time.

A visual examination (Figure 4-15) of samples aged at 260°C in nitrogen and in air suggests the introduction of oxygen into the aging atmosphere greatly affects the material's appearance. Figure 4-15a displays the set of samples aged in

4-14a.)

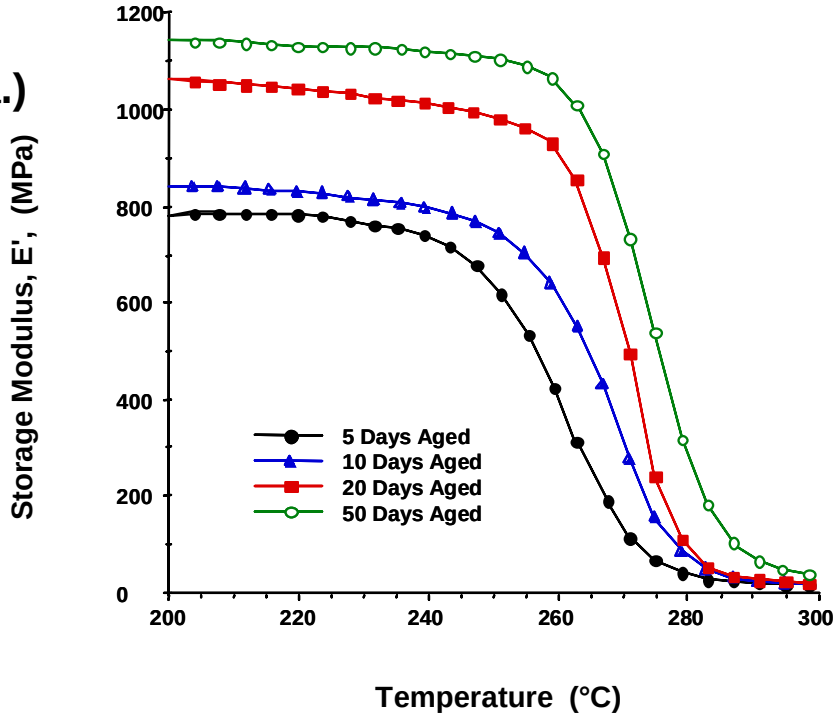

4-14b.)

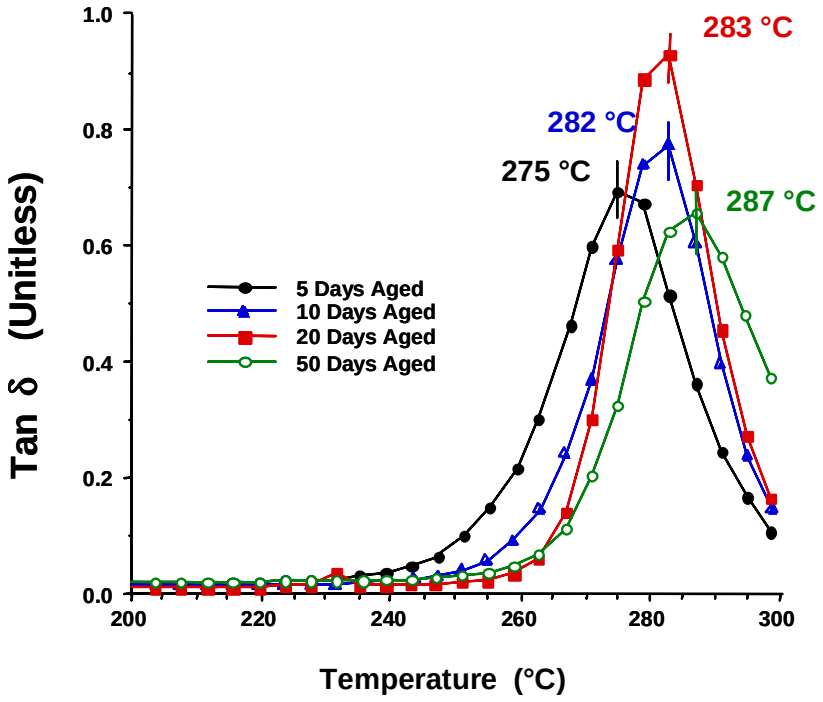

Figure 4-14. Mechanical data displayed as a function of temperature for neat cyanate ester resins aged in nitrogen at 260°C.
a.) Storage modulus data
b.) Tan δ data

4-15a.) Nitrogen Aged Samples

0 Days **5 Days** **10 Days** **20 Days** **50 Days**

4-15b.) Air Aged Samples

0 Days **5 Days** **10 Days** **20 Days** **50 Days**

Figure 4-15. Visual Examination of neat cyanate ester resins aged at 260°C. Photographs of actual samples are displayed
a.) Materials aged in a nitrogen atmosphere
b.) Materials aged in an air atmosphere

nitrogen. Some discoloration is observed after the polymer was exposed to the high temperature environment, but this slight discoloration does not have an associated negative component. For example, there is not a heavy impact on the physical behavior of the nitrogen-aged specimens as observed in the master curves above and in the TGA data discussed in the following section. In contrast, the samples aged in air (Figure 4-15b) display significant appearance changes including massive darkening, bloating and ultimately, disintegration. It is believed degradation occurs at the triazine linkage, and/or with volatile gases generated (ultimately NH_3 and CO_2). One of the physical effects of degradation is the decrease in the T_g of the material as a function of the network breakdown. As the T_g decreases to a temperature below the aging temperature, the volatile gases expand the material causing the cavitation effect. As degradation continues, enough network breakdown occurs and sufficient volatiles are produced to increase the pressure on the material to the point of explosion. The gases generated escape from the network at the expense of material dimensional integrity.

Thermal gravimetric analyses (TGA) were performed on both nitrogen and air aged samples in an attempt to observe the role of chemical degradation in the aging process. It was also important to determine what effect, if any, the processes associated with the discoloration of the nitrogen-aged samples had on the aging process. Figure 4-16 compares the TGA results of samples aged in nitrogen and in an air atmosphere. The TGA experiments were performed in

4-16a.)

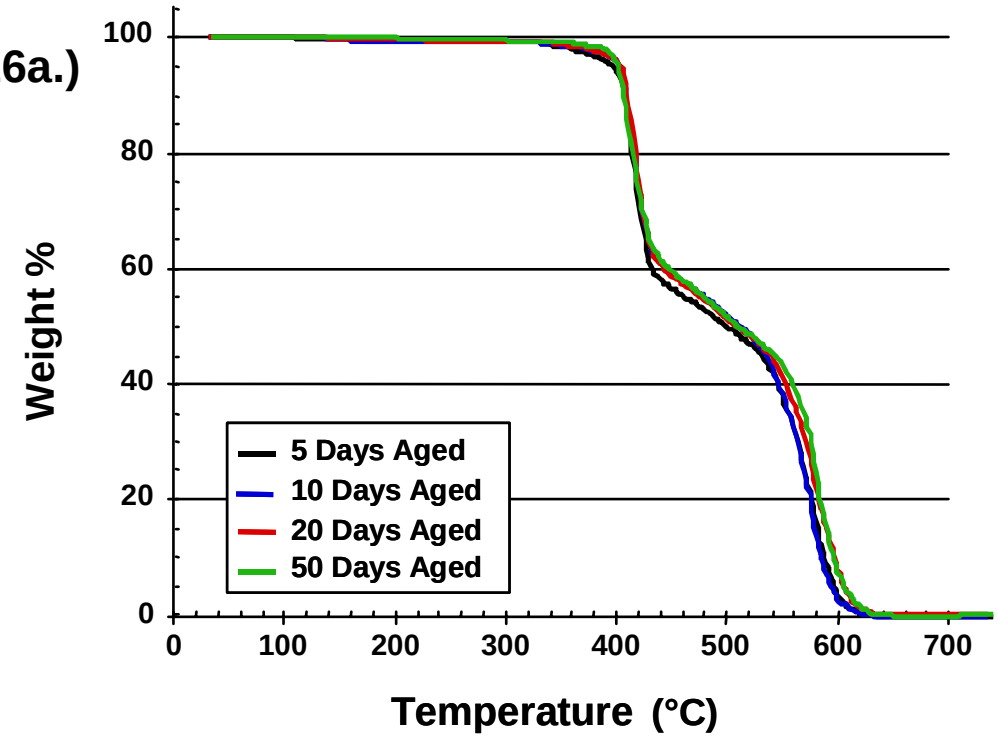

4-16b.)

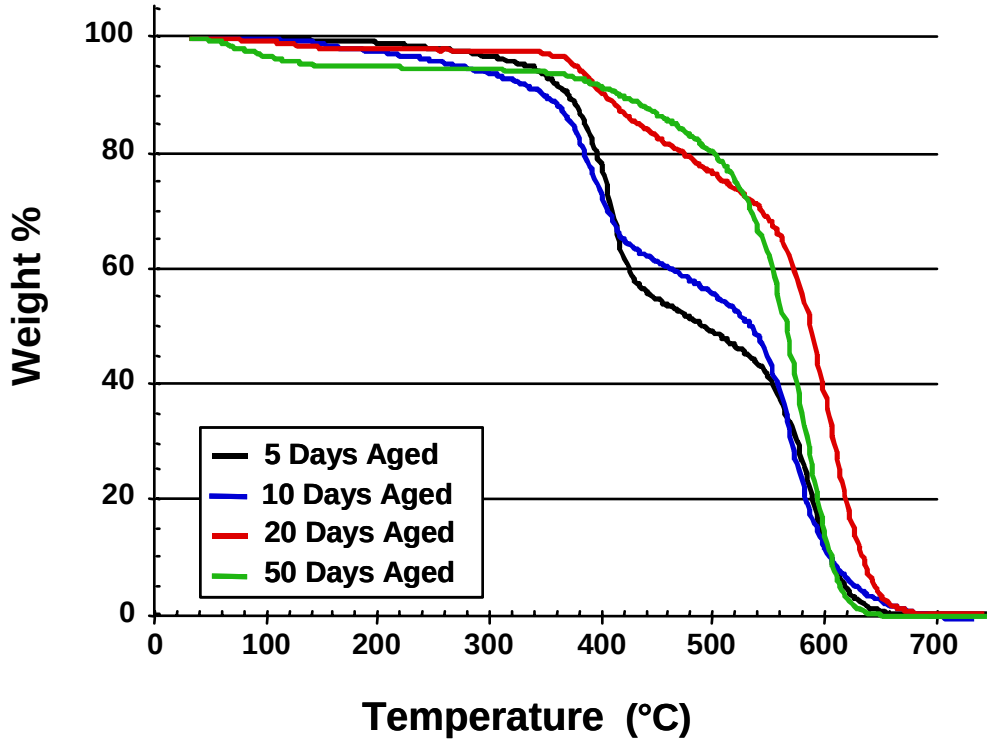

Figure 4-16. TGA comparison of neat cyanate ester resins aged at 260°C. Thermal sweeps performed in Air at 10°C/min.
a.) Nitrogen Aged Samples
b.) Air Aged Samples

an air atmosphere as well. The TGA results exhibited a bi-modal structure to the decomposition and the subsequent complete disintegration of the test sample. The same experiments were performed in a nitrogen atmosphere, and these results are displayed in Figure 4-17. A detailed analysis of this data will occur in a later section of these discussions, but important for this argument is the apparent lack of chemical degradation in the nitrogen-aged samples. The TGA data confirm that the mechanical data discussed above has been affected by physical aging and not by chemical degradation.

4.3.2b 177°C Aging Study

One of the proposed applications for the AroCy B-10 cyanate ester resins requires the material to retain its physical properties at temperatures up to and including 300°F (~ 177°C). Therefore, it is of interest to characterize the behavior of the material at that temperature in addition to clarifying thermoxidative mechanisms. Since the aging data above indicated the viability of evaluating physical aging via time-temperature master curves of samples aged in a nitrogen atmosphere, the first set of experiments aged at the lower temperature was also performed in nitrogen.

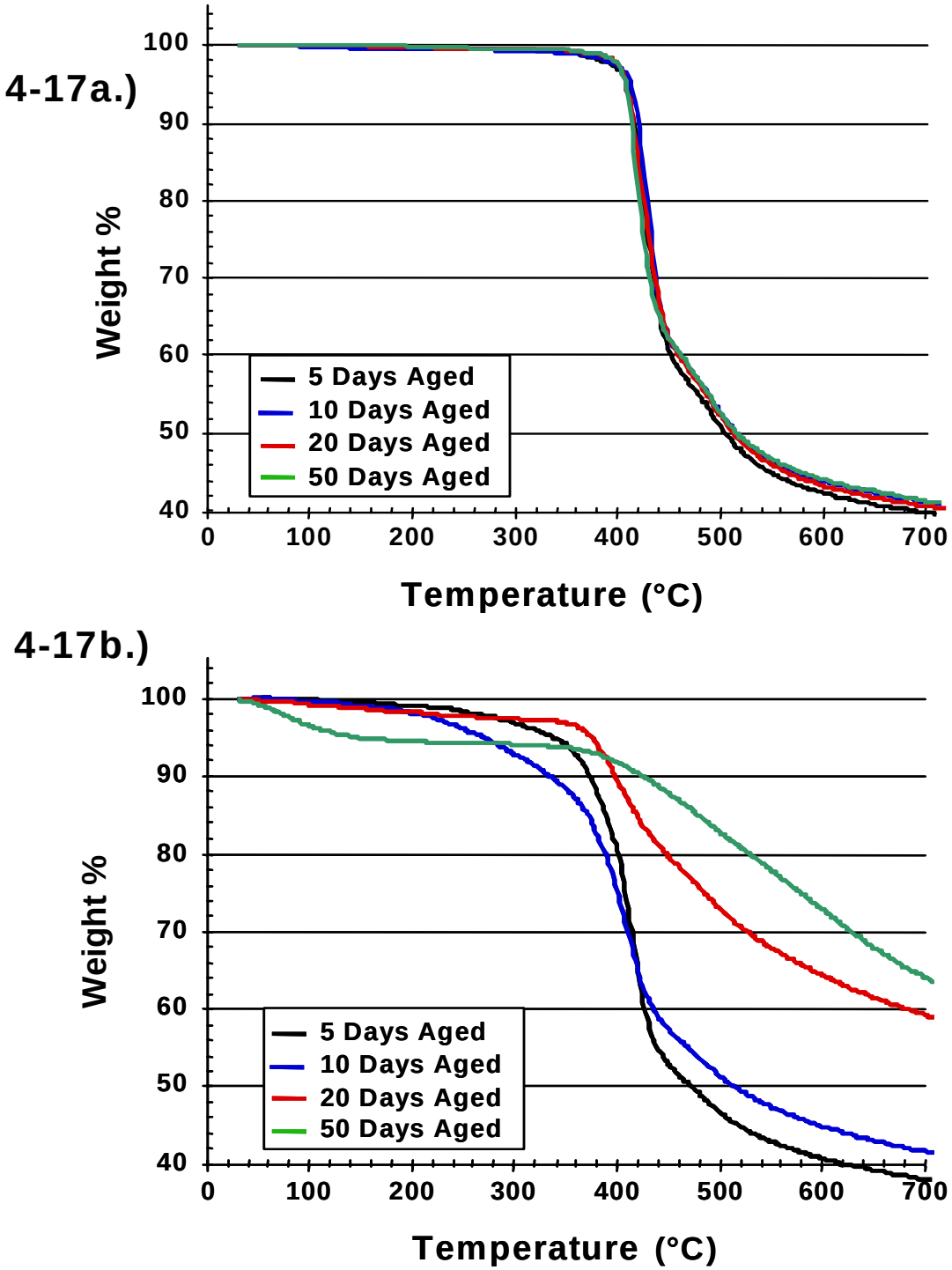

Figure 4-17. TGA comparison of neat cyanate ester resins aged at 260°C. Thermal sweeps performed in Nitrogen at 10°C/min.
a.) Nitrogen Aged Samples
b.) Air Aged Samples

Figures 4-18, 4-19, and 4-20 represent the storage modulus and tan δ master curves and the shift factor plots developed when the cyanate ester resins were aged in a nitrogen atmosphere for five, ten and fifty days at 177°C. Figure 4-21 contains the rearranged data and displays the thermal DMA behavior of the aged samples at a frequency of 1 Hz.

The first observation from these 177°C aging data is that the ten days aged sample has a different behavioral pattern from that of the other two aging times samples which bracket it on the time scale. A lower initial modulus was observed in the ten day aged sample, which is contradictory to the purely physical aging predictions. Also, on examination of the modulus of the ten day aged sample in Figure 4-21a, the slope in the s-shaped portion of the curve is much lower than the other two curves. This variation in slope was also observed as a higher temperature peak maximum in Figure 4-21b. No physical explanation is offered to describe this variation in behavior except to speculate that an error occurred during the sample preparation process causing the material to behave anomalously. With this anomalous curve removed, some generalized comparisons can be tentatively made. By examining the master curve data (Figure 4-22 and Figure 4-23) only minor differences between the five-day and fifty day-aged samples is observed. This indicates little to no physical aging occurred at 177°C. This was an expected outcome since the aging temperature was so much lower than the T_g of the resin. Figure 4-24 is a representation of the thermal sweep data at 1 Hz for these two differently aged

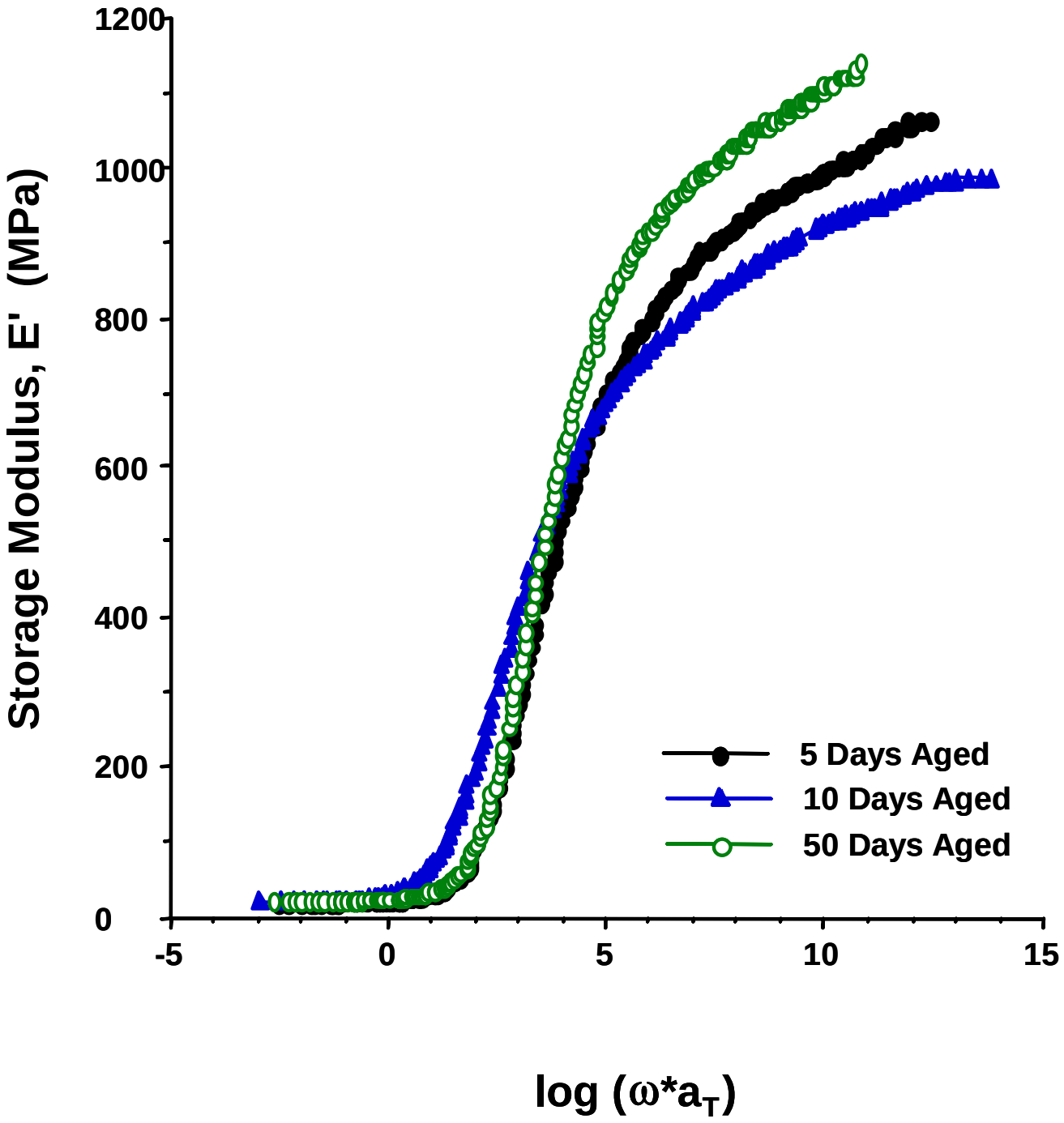

Figure 4-18. Storage modulus master curves for cyanate ester resin aged in a nitrogen atmosphere at 177°C for times shown.

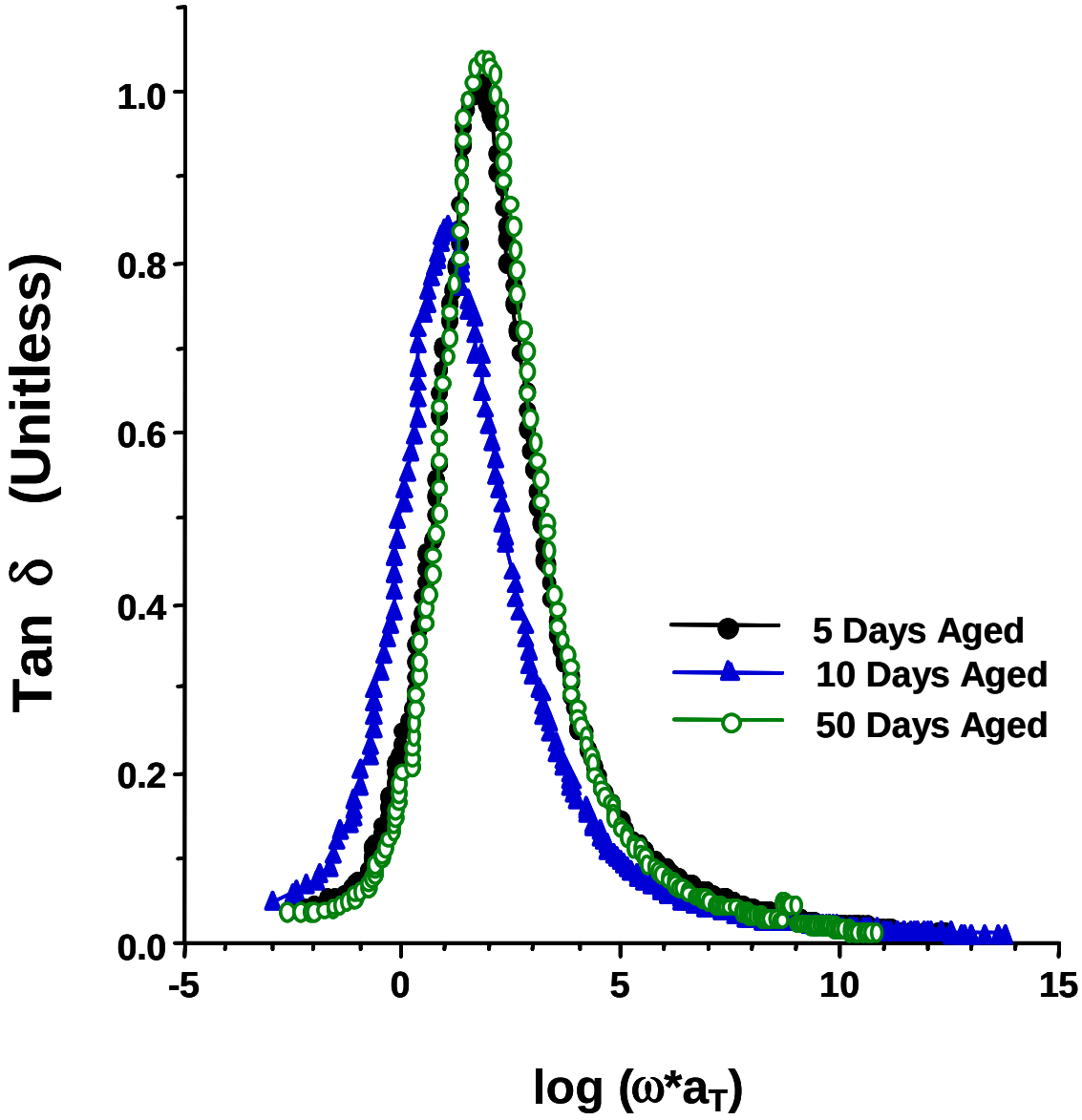

Figure 4-19. Tangent δ master curves for cyanate ester resins aged in a nitrogen atmosphere at 177°C for times shown.

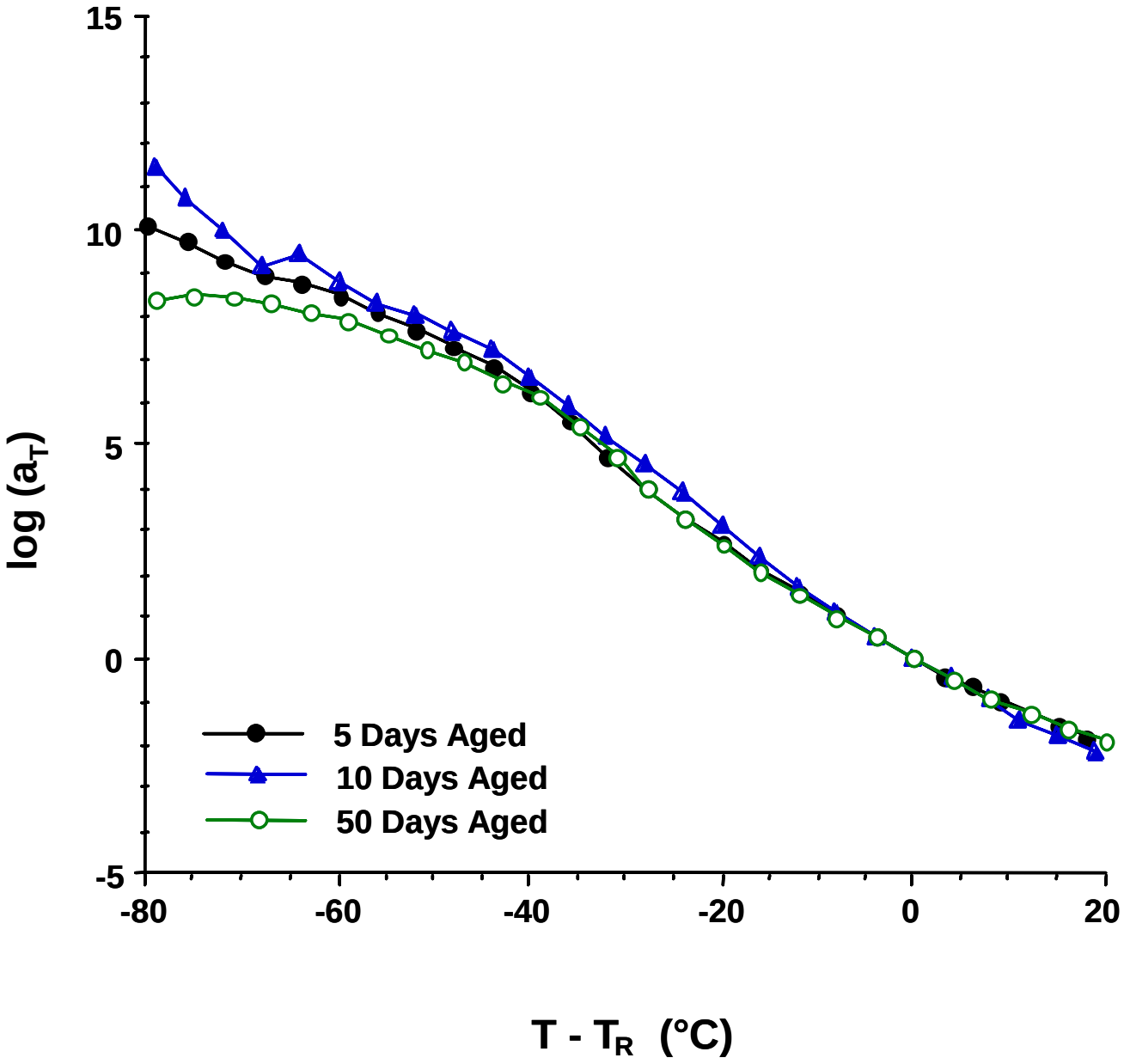

Figure 4-20. Shift factor plots for cyanate ester resins aged in a nitrogen atmosphere at 177°C for times shown.

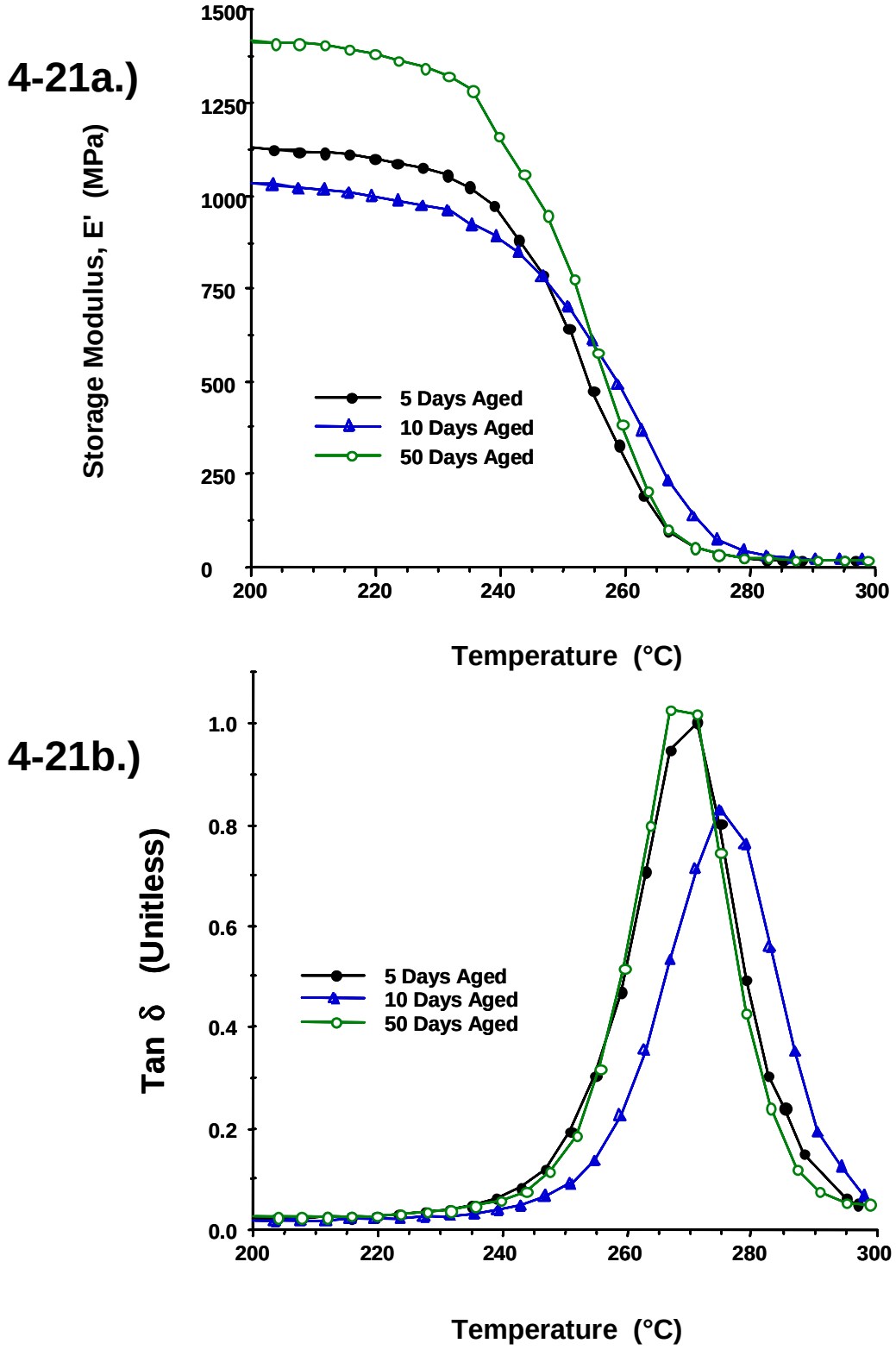

Figure 4-21. Rearranged data at a frequency of 1 Hz for examination on the temperature axis
a.) Storage Modulus, E'
b.) tan •δ

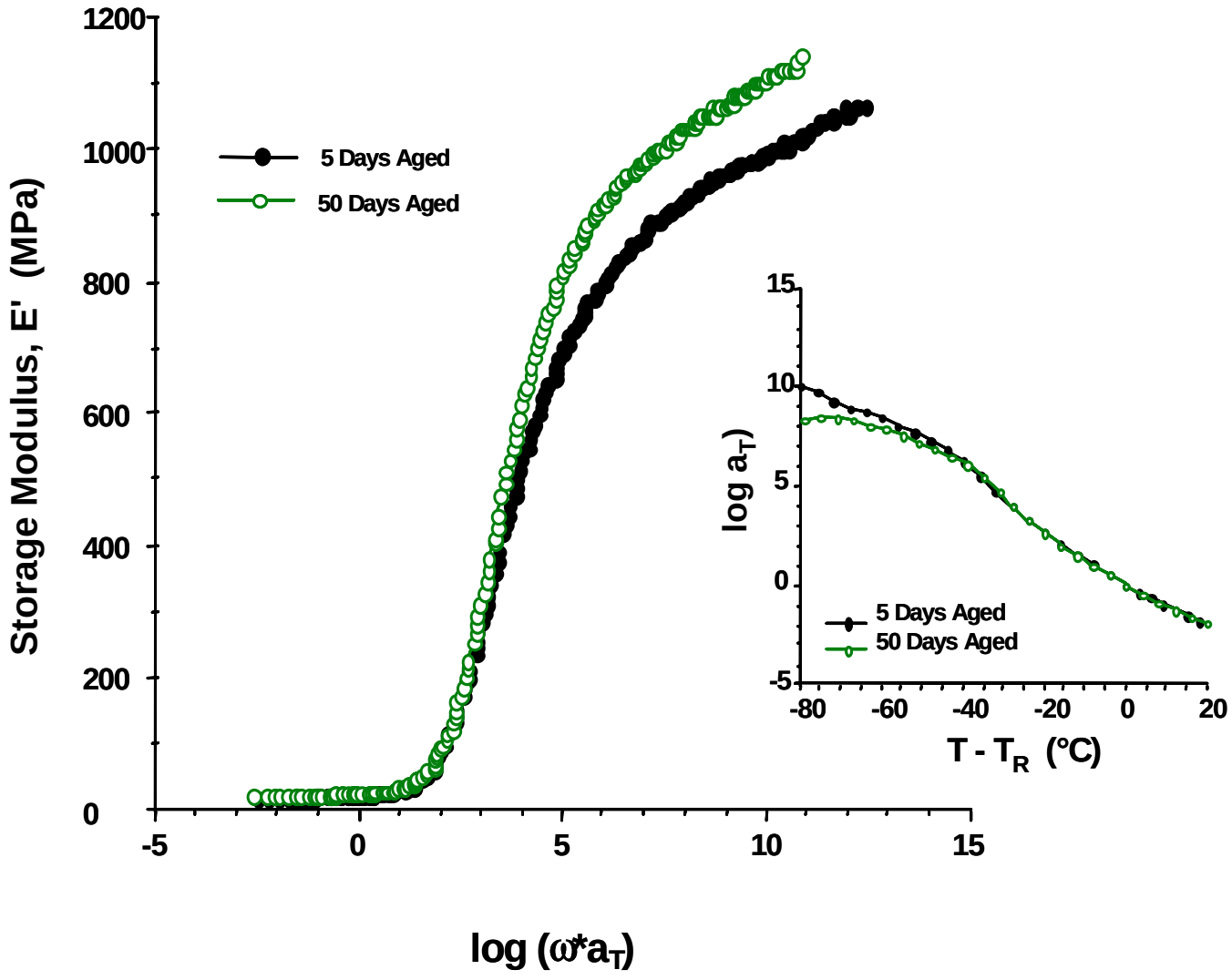

Figure 4-22. Storage modulus master curves and shift factor plots (less 10 days aged) for cyanate ester resin aged in a nitrogen atmosphere at 177°C for times shown.

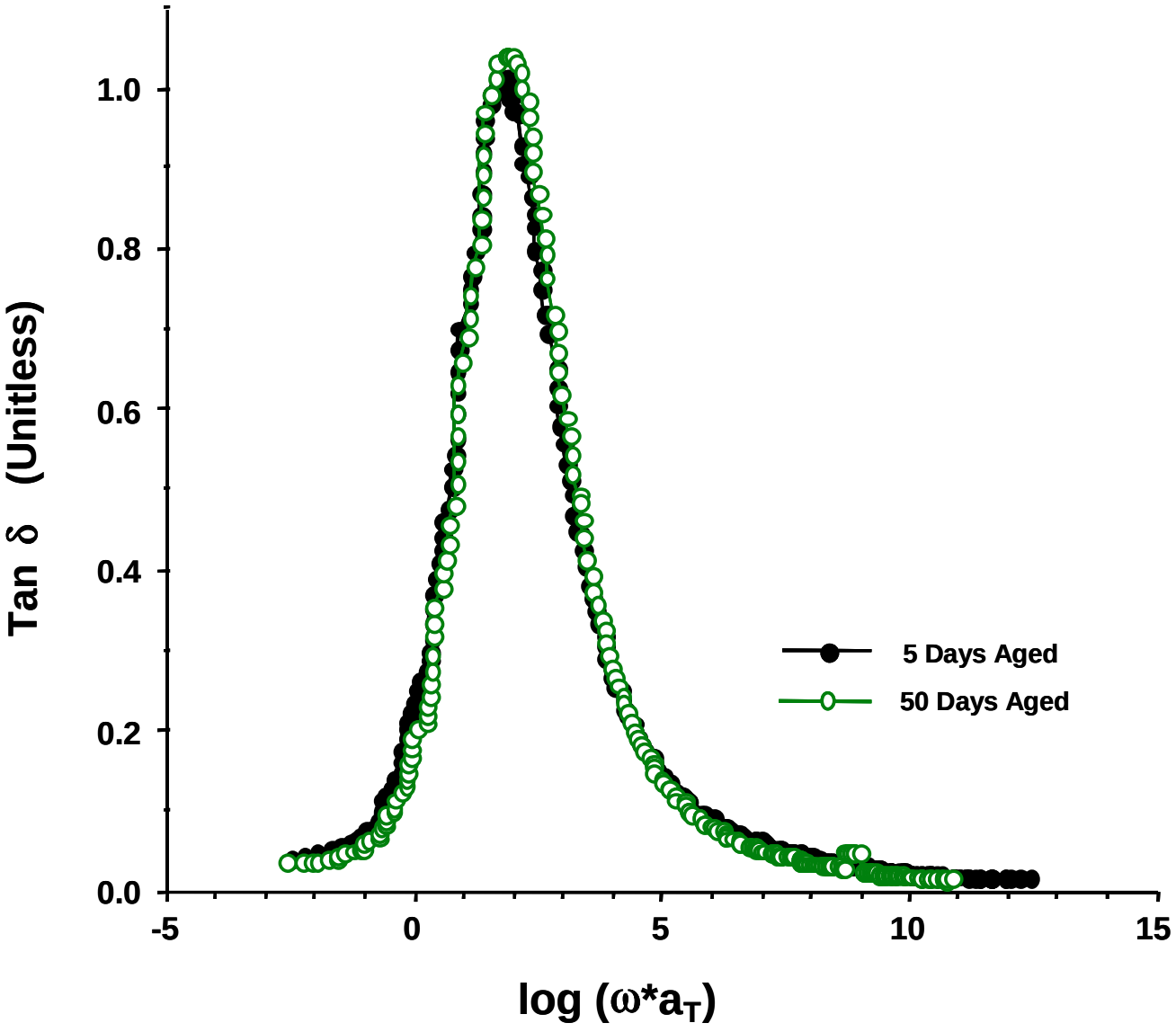

Figure 4-23. Tan δ master curves (less 10 days aged) for cyanate ester resin aged in a nitrogen atmosphere at 177°C for times shown.

4-24a.)

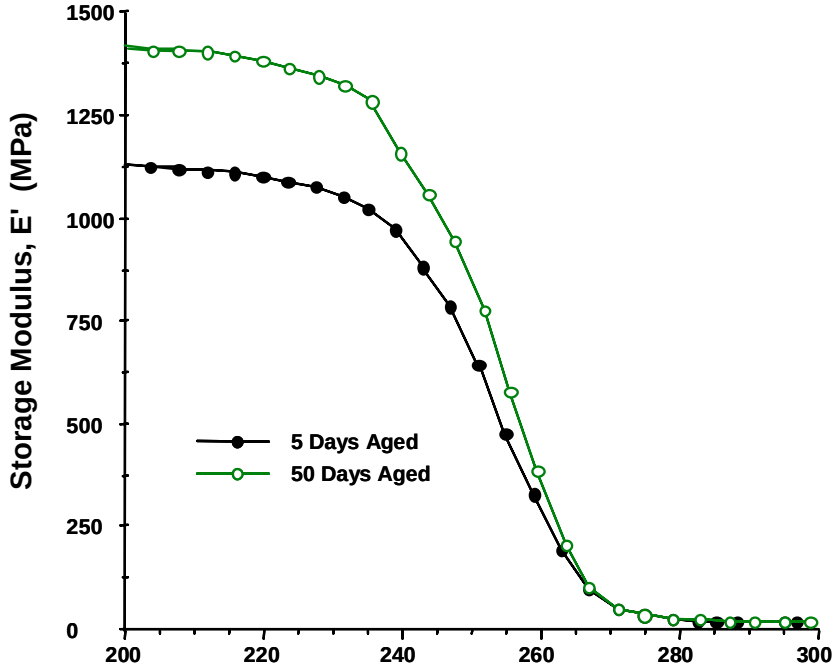

4-24b.)

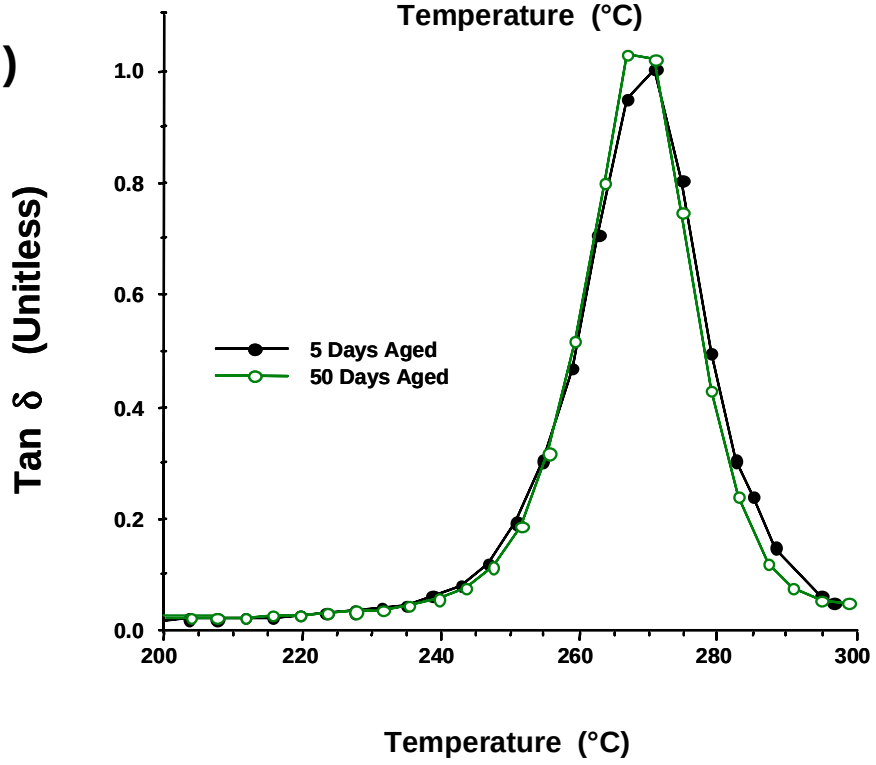

Figure 4-24. Continuous sweep thermal scans of 5 and 50 day aged samples at a frequency of 1 Hz.
a.) Storage Modulus, E'
b.) Tan δ

samples. These data indicate aging produces moderate differences in the low temperature portion of the storage modulus curves and in the subsequent transition zones encountered on heating. This point is not well illustrated by the matching tan δ data (Figure 4-24b) with only a slight increase in the peak maximum (T_g).

4.3.3 Aging in Air

4.3.3a 177°C Aging Study

4.3.3a.1 Neat Resin

In the last sections, it was reported that under the right conditions (temperature and atmosphere), the neat cyanate ester resin will physically age. It was also explained that under the right conditions, these polymers chemically degrade as well. A question that arises is "how does this system behave under typical application conditions with respect to the two mechanisms that have been observed?" Typical application conditions are such that the cyanate ester resins maintain their properties at temperatures up to and including 300°F (177°C) and in an oxygenated atmosphere. If chemical degradation occurs, it is important to know its impact on physical and mechanical properties. Simply stated, does this cyanate ester derived network's behavior change in an air atmosphere at high application temperatures, and, if so, to what extent?

Another interesting inquiry about the neat resin concerns the effect of cure conditions on the aging properties. Recalling the discussion in Chapter 3, Page 80, different morphologies were obtained in thermoplastic toughened blends of cyanate esters when the cure properties were varied. Specifically, a micro-phase-separated morphology was obtained when the material was cured at 150°C for one hour and then post-cured at 250°C for two hours. However, if similar samples were cured at 250°C for three hours, a co-continuous morphology was obtained. Of course, this variation in morphology indicated a blend of materials. However, it is important to understand the behavior of the neat resin under the same conditions for comparison purposes, and to note any possible changes in properties as a result of the cure process that is not related to the morphology differences.

In this study, two sets of samples were prepared for aging by curing using the two curing profiles discussed above. The sets were designated as "low temperature" and "high temperature" cured resins as appropriate. The samples were subjected to a 177°C, air atmosphere for five, ten, fifty and one hundred days immediately followed by the mechanical measurements. Figures 4-25 and Figure 4-26 illustrate the storage modulus and tan δ master curves for the set of

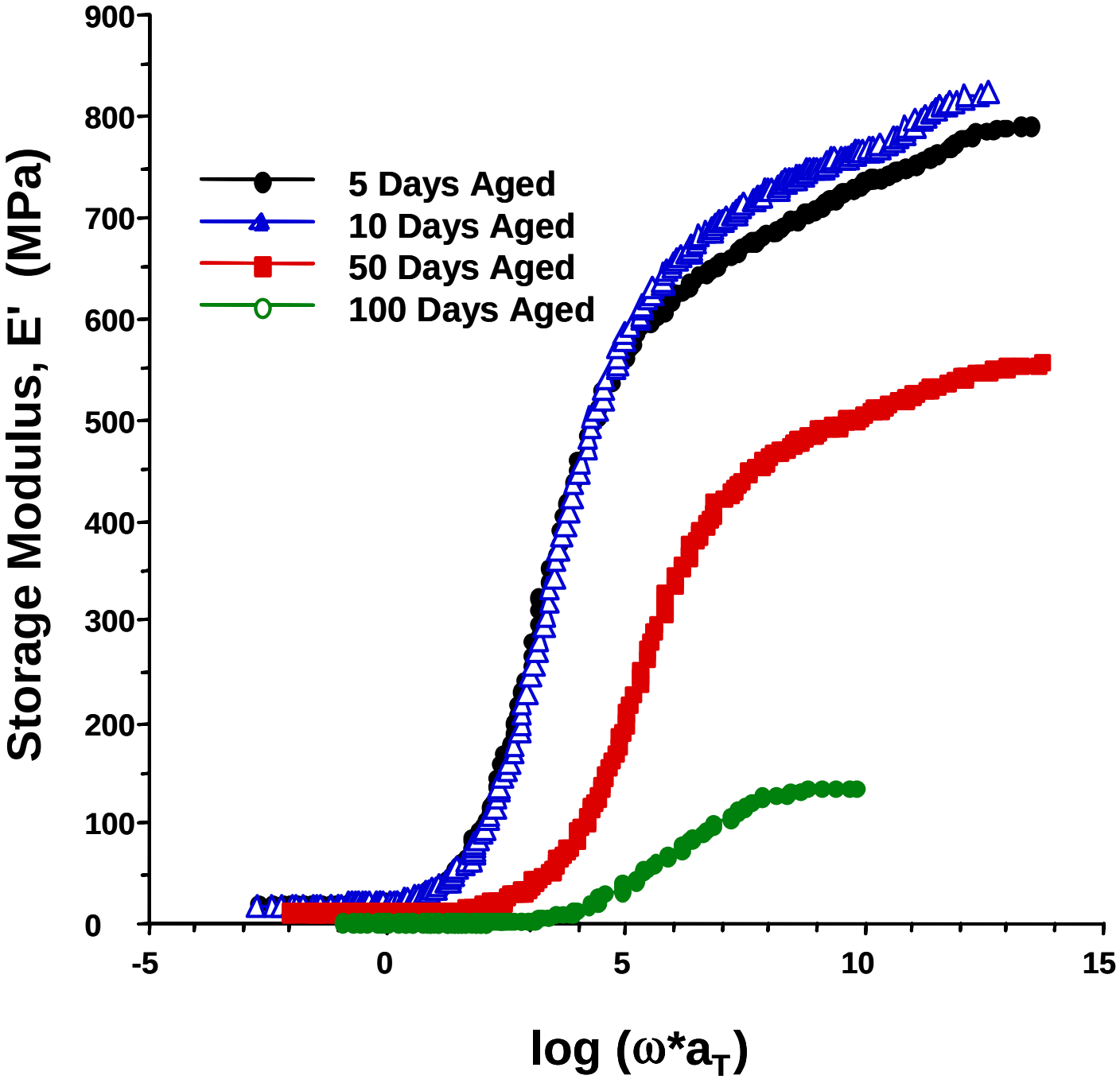

Figure 4-25. Storage modulus master curves for neat cyanate ester resin aged in an air atmosphere at 177°C for times shown. Cure schedule was one hour at 150°C and two hours at 250°C as a post-cure.

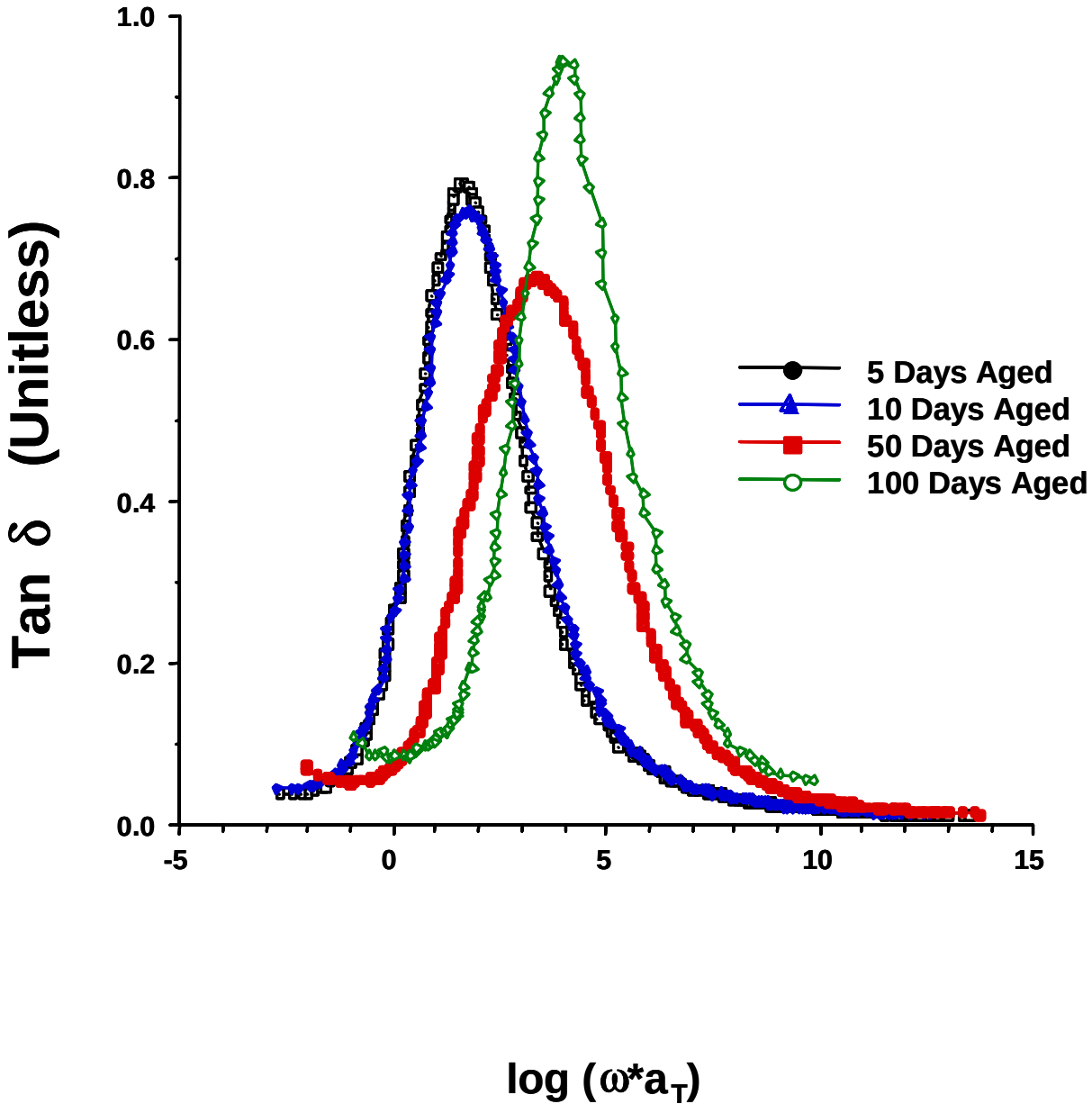

Figure 4-26. Tangent δ master curves for neat cyanate ester resins aged in an air atmosphere at 177°C for times shown. Cure schedule was one hour at 150°C and two hours at 250°C as a post-cure.

samples designated as the low temperature cured resins (150°C for one hour, 250°C for two hours). Figure 4-27 contains the family of shift factor plots resulting for these master curves from DMA experiments. The storage modulus data (Figure 4-25) are unusual in the magnitude of the change that is observed. Concentrating on the higher modulus region of the master curves (above seven decades of frequency), a trend toward a major decrease in the storage modulus was produced by the aging. This decrease is contradictory to the effects of physical aging, which would suggest an increase in that modulus, and implies chemical degradation is playing a significant role in varying the mechanical properties. Also, from the tan δ master curves, a shift in peak maximum to higher frequencies (corresponding to shorter relaxation times) is observed. This shift suggests a decrease in T_g has resulted, which again is contrary to typical physical aging behavior. This observation is reinforced when temperature profiles of the mechanical data are examined (Figure 4-28). One notes that a significant decrease in T_g with increased aging as indicated via the tan δ curves in Figure 4-28b. The storage modulus data also show the steady drop of T_g and of initial modulus as a result of aging in this environment.

Visual examination of the samples (Figure 4-29) supports the hypothesis that degradation is a major cause of concern for these cyanate esters in this type of temperature and atmosphere. A distinct darkening of the specimens occurred and, as seen in the mechanical data, a destructive effect

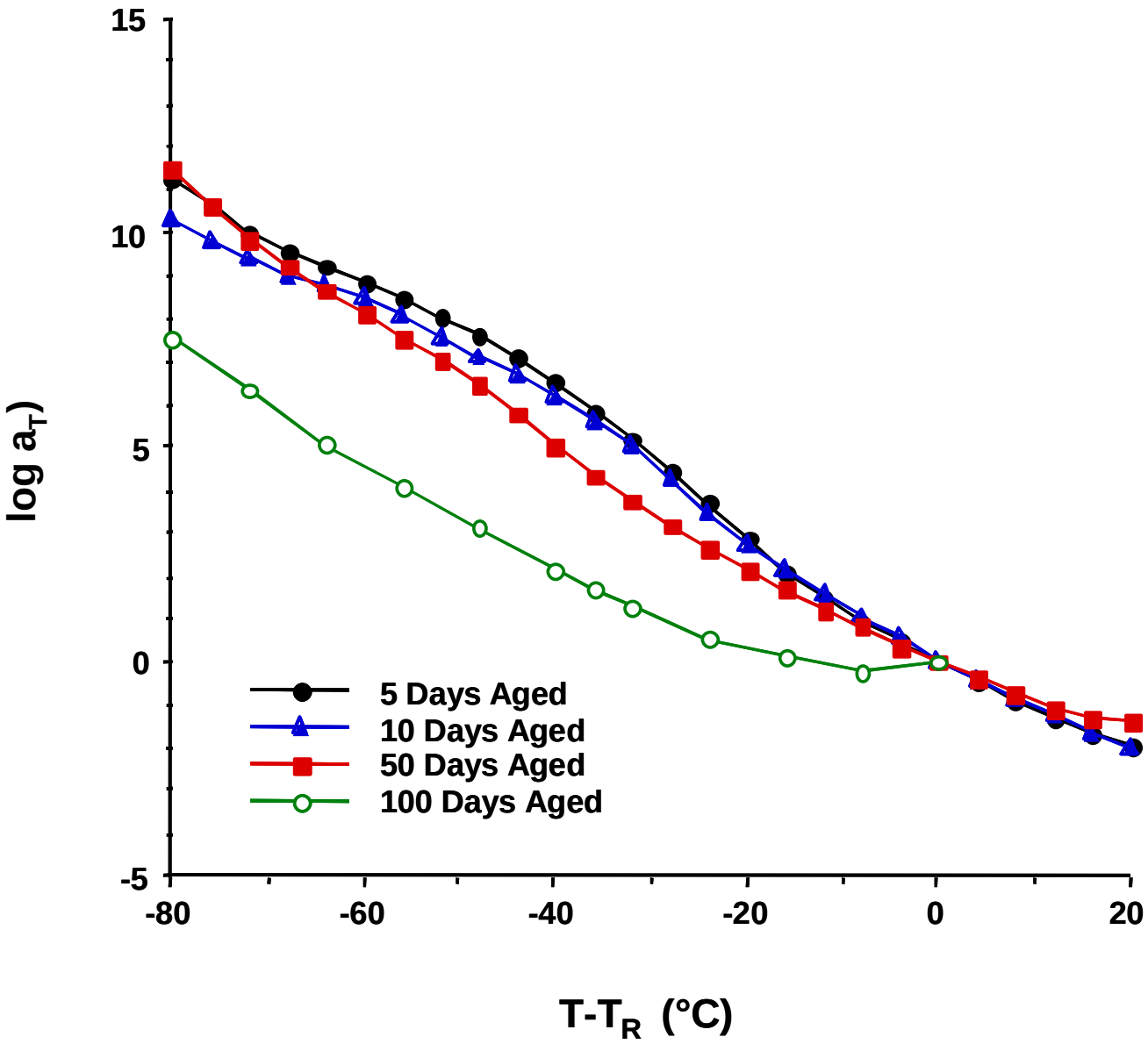

Figure 4-27. Shift factor plots for neat cyanate ester resins aged in an air atmosphere at 177°C for times shown. These plots correspond to the master curves displayed in Figure 4-25 and Figure 4-26.

4-28a)

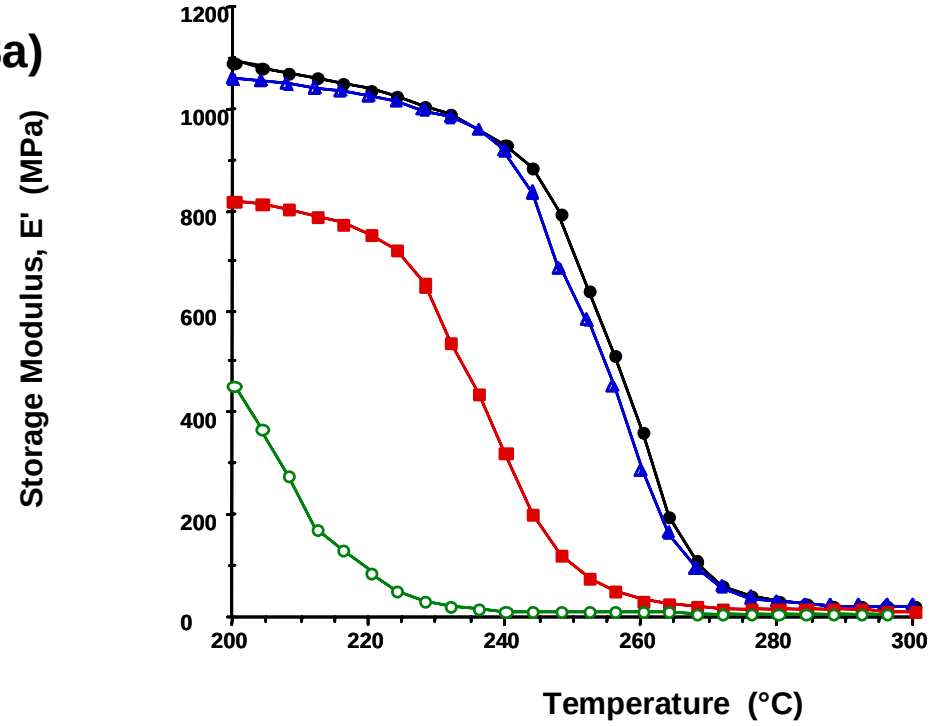

4-28b)

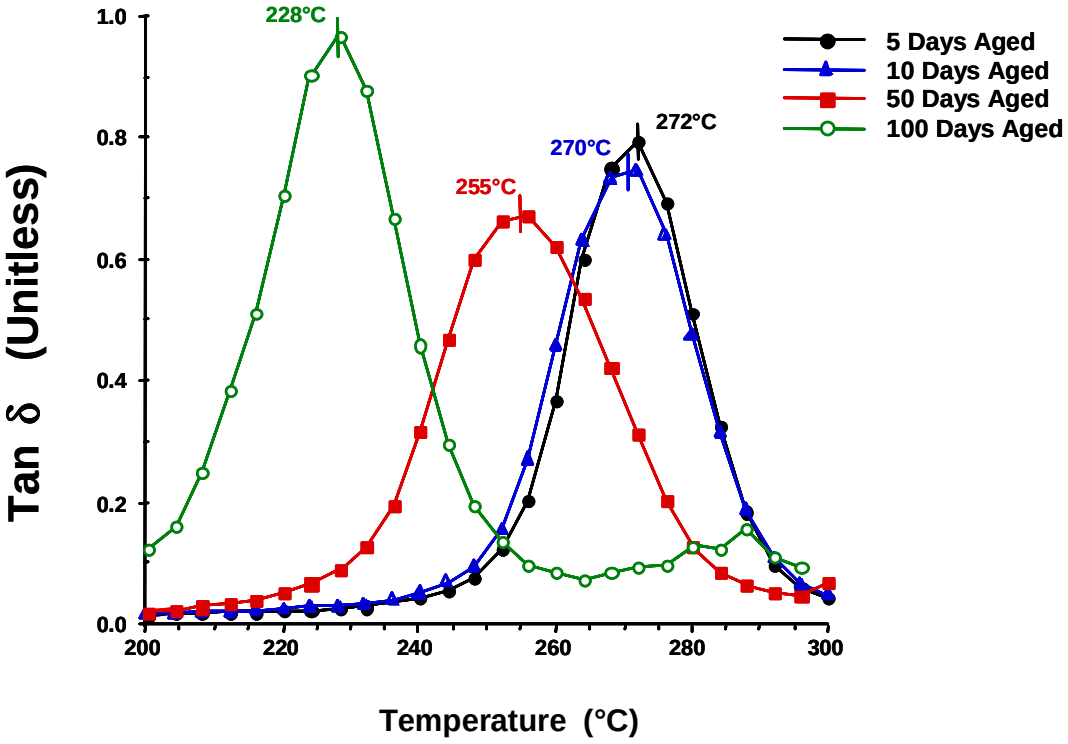

Figure 4-28. Rearranged data at a frequency of 1 Hz for examination on the temperature axis
a.) Storage Modulus, E'
b.) tan •δ

Neat Resin

4-29a) AGED IN AIR @ 177°C

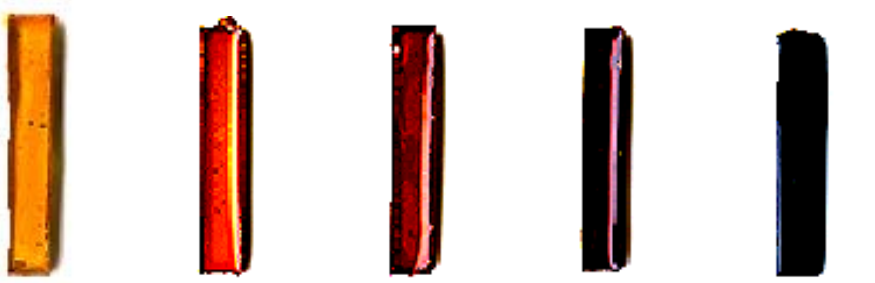

0 DAYS **5 DAYS** **10 DAYS** **50 DAYS** **100 DAYS**

4-29b) AGED IN NITROGEN @ 177°C

0 DAYS **5 DAYS** **10 DAYS** **50 DAYS**

Figure 4-29. Visual examination of neat cyanate ester resins after aging at 177°C for the displayed time in the corresponding atmosphere
a.) Air aged samples
b.) Nitrogen aged samples

on material properties occurred. Further evidence is needed to support the chemical breakdown and may be found in Figure 4-30. These modulated DSC scans of the aged samples (Figure 4-30) clearly show significant decreases in the T_g of the material with aging time. The magnitude of the decrease (~ 45°C) can only be associated with chemical degradation, an "irreversible" process.

The next set of figures (Figure 4-31, 4-32, 4-33) is the collection of storage modulus and tan δ master curves and their corresponding family of shift factor plots for the high temperature cured resins. This data indicate a slightly more stable behavior than the data obtained from the low temperature-cured sample. The inference drawn from these data is that the high temperature cure produced a more fully reacted material. This additional cure provided some resistance to degradation. Examination of the temperature profiles for these samples (Figure 4-34) shows that significant property changes did occur, but to a lesser extent. However, the modulated DSC scans (Figure 4-35) display similar lowering of the T_g behavior compared to the low temperature-cured material. This added information leads to the conclusion that apparent changes in these samples' properties caused by the difference in cure cycle are relatively insignificant.

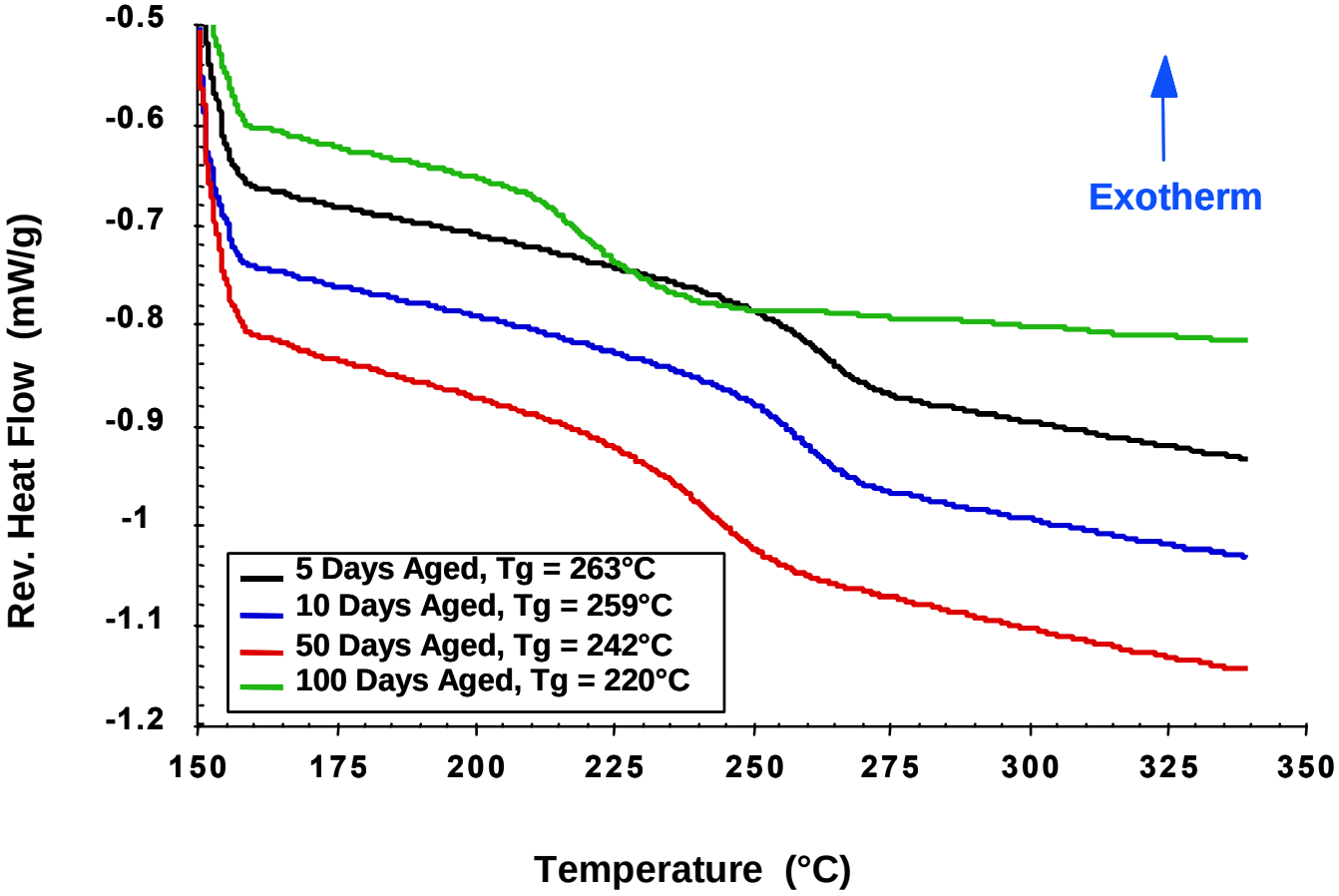

Figure 4-30. Modulated DSC scans of neat cyanate ester resin samples aged in an air atmosphere at 177°C for the times shown. Cure schedule was one hour at 150°C and two hours at 250°C as a post-cure. T_g was determined using the TA Universal Analysis Software. The midpoint of change in the reversible heat flow was used as the measured value.

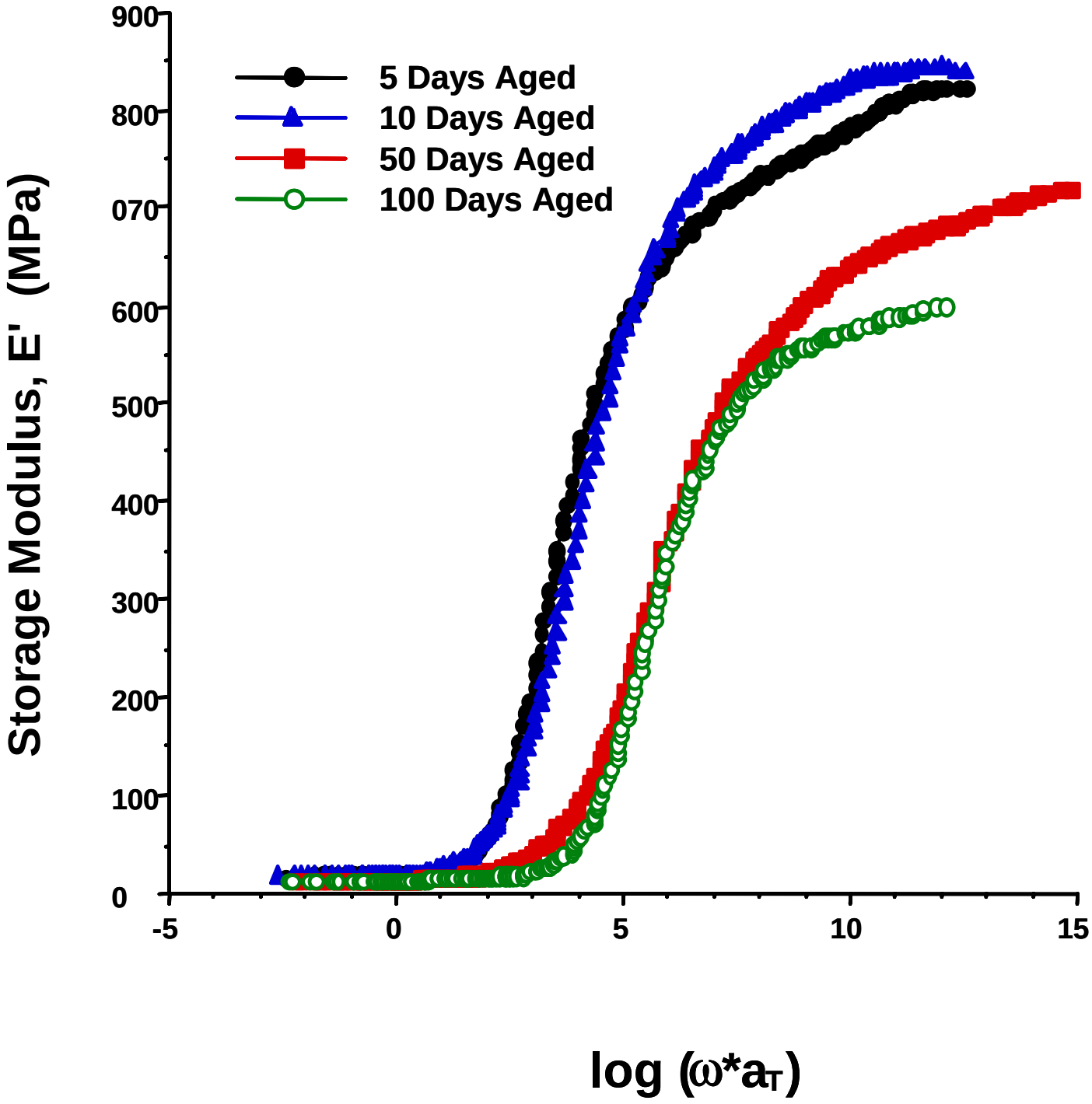

Figure 4-31. Storage modulus master curves for neat cyanate ester resin aged in an air atmosphere at 177°C for times shown. Cure schedule was three hours at 250°C.

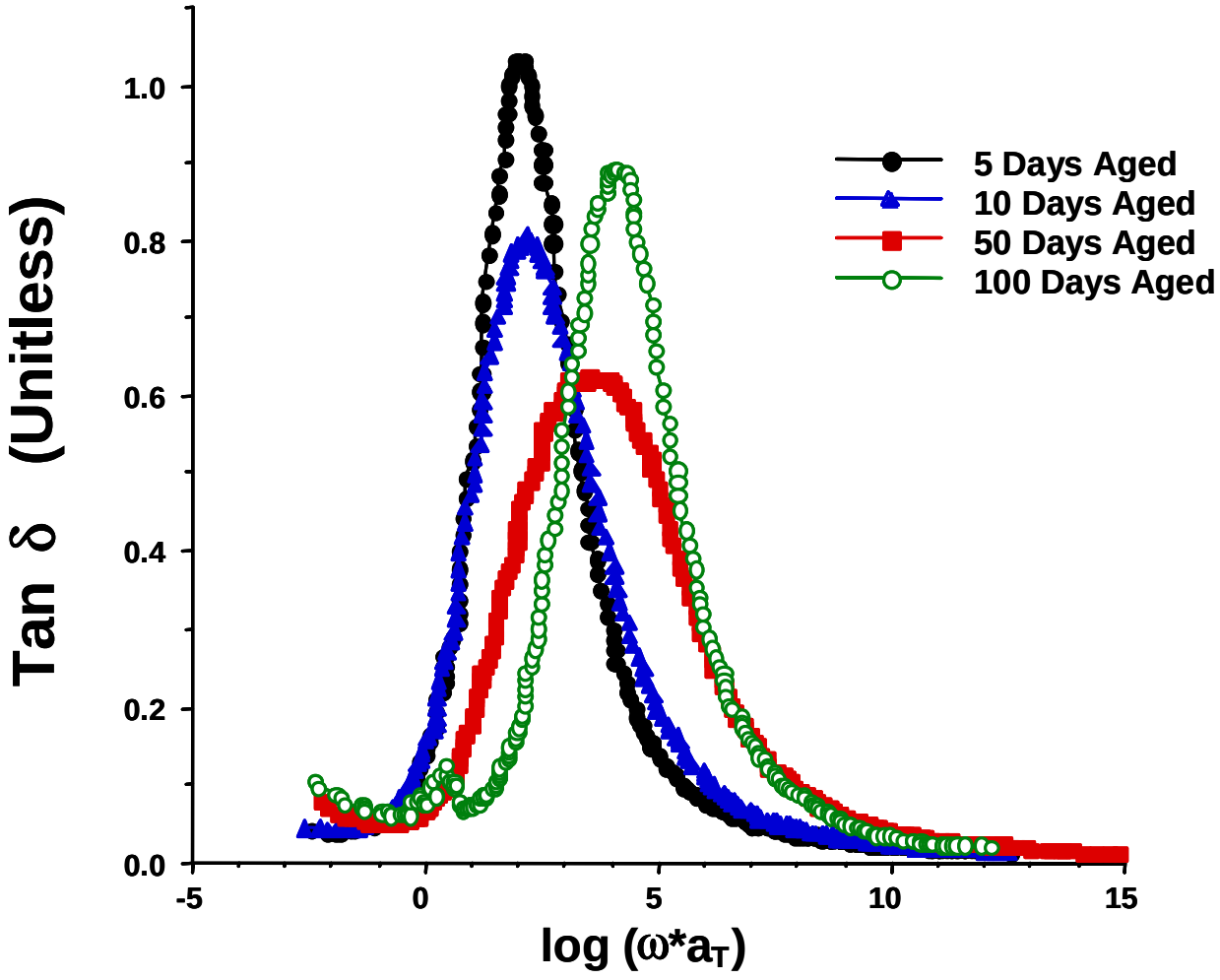

Figure 4-32. Tangent δ master curves for neat cyanate ester resins aged in an air atmosphere at 177°C for times shown. Cure schedule was three hours at 250°C.

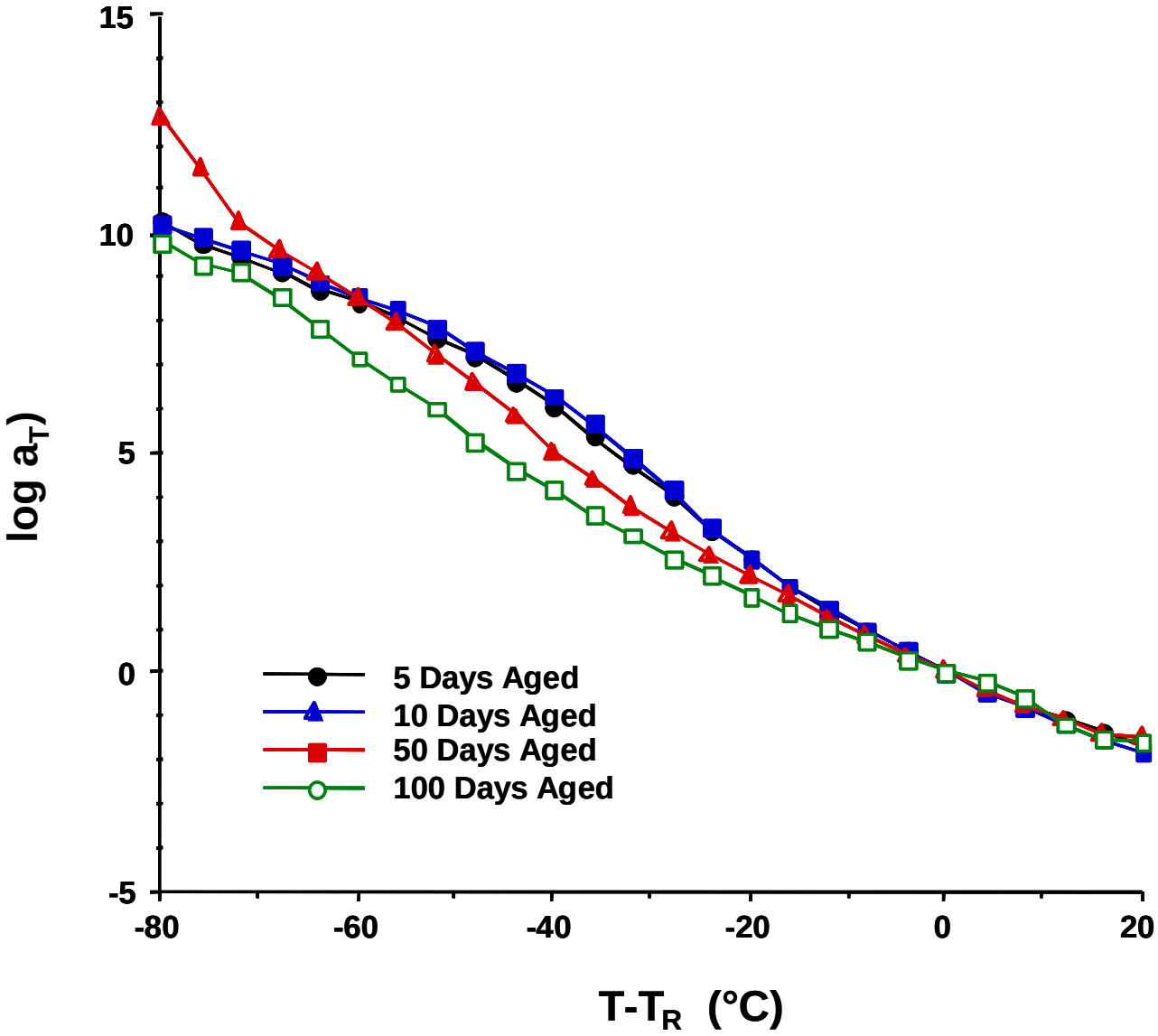

Figure 4-33. Shift factor plots for neat cyanate ester resins aged in an air atmosphere at 177°C for times shown. These plots correspond to the master curves displayed in Figure 4-30 and Figure 4-31.

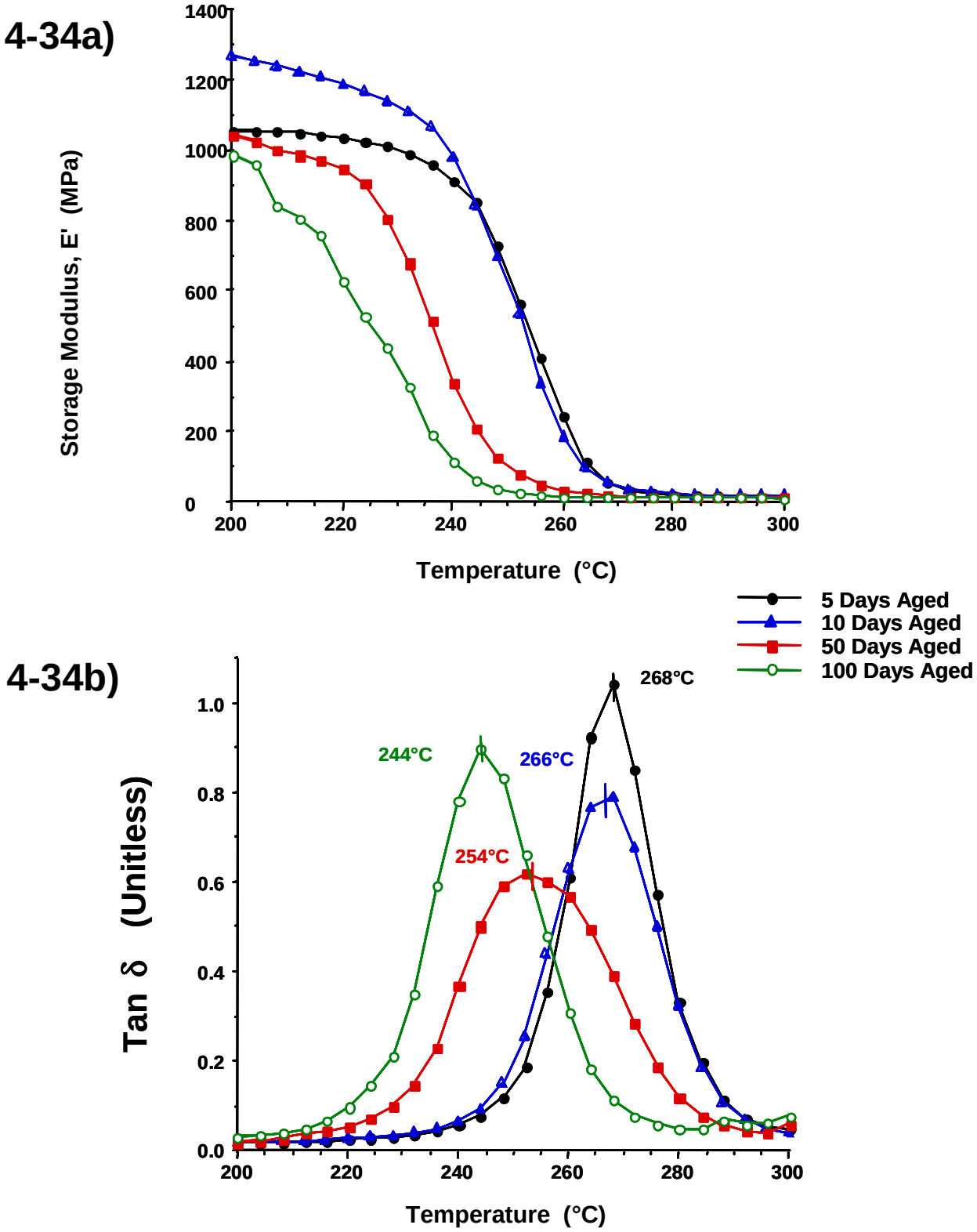

Figure 4-34. Rearranged data at a frequency of 1 Hz for examination on the temperature axis
a.) Storage Modulus, E'
b.) tan •δ

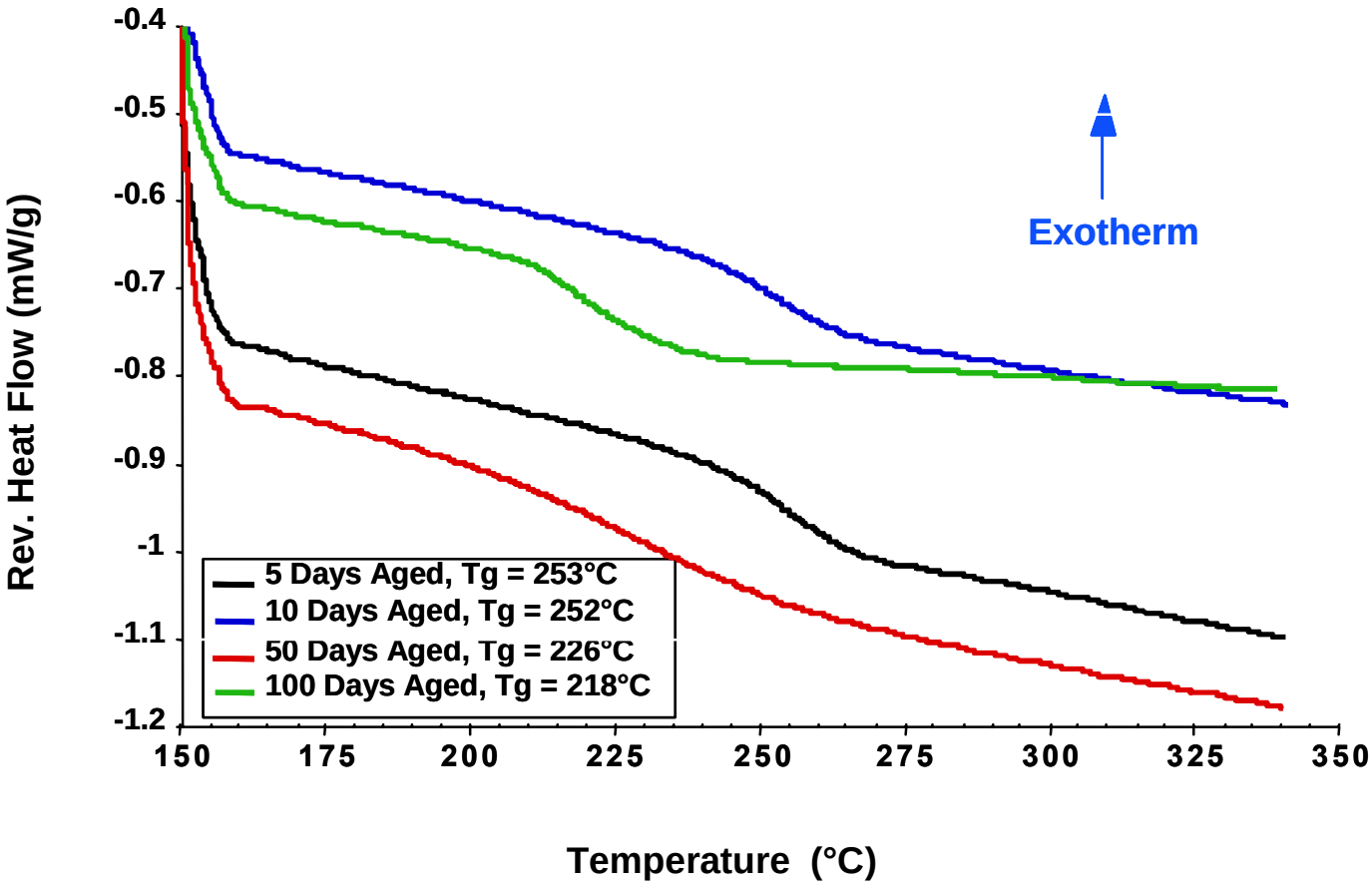

Figure 4-35. Modulated DSC scans of neat cyanate ester resin samples aged in an air atmosphere at 177°C for the times shown. Cure schedule was three hours at 250°C. T_g was determined using the TA Universal Analysis Software. The midpoint of change in the reversible heat flow was used as the measured value.

4.3.3a.2 Thermoplastic Toughened Resin

The data above have led to a conclusion that the neat cyanate ester resin is highly unstable at elevated temperatures when oxygen is present. The question then arises as to what effect, if any, a thermoplastic toughener might have on the cyanate ester system. Also of interest is the stability of the two-phase structure under degradation conditions

Figures 4-36 and 4-37 display the family of storage modulus and tan δ master curves generated from aging 25% thermoplastic toughened cyanate ester resins for varying amounts of time in an oxygen rich atmosphere. These samples represent the co-continuous phase domain as is displayed in Figure 3-1b. Figure 4-38 continues the family of shift factor plots generated from shifting these master curves. Figure 4-39 shows the dynamic mechanical results as a function of temperature for this family of toughened resins. These allow for a clearer understanding of the T_g behavior of the material over time at the aging temperature. Also, Figure 4-40 displays the modulated DSC scans of the aged samples. This determination of the material T_g was then compared to that of the DMA data displayed in Figure 4-39.

From examination of the master curves, one notes similar behavior to that observed with the neat resin in an air atmosphere at 177°C (Figures 4-25, 4-26,

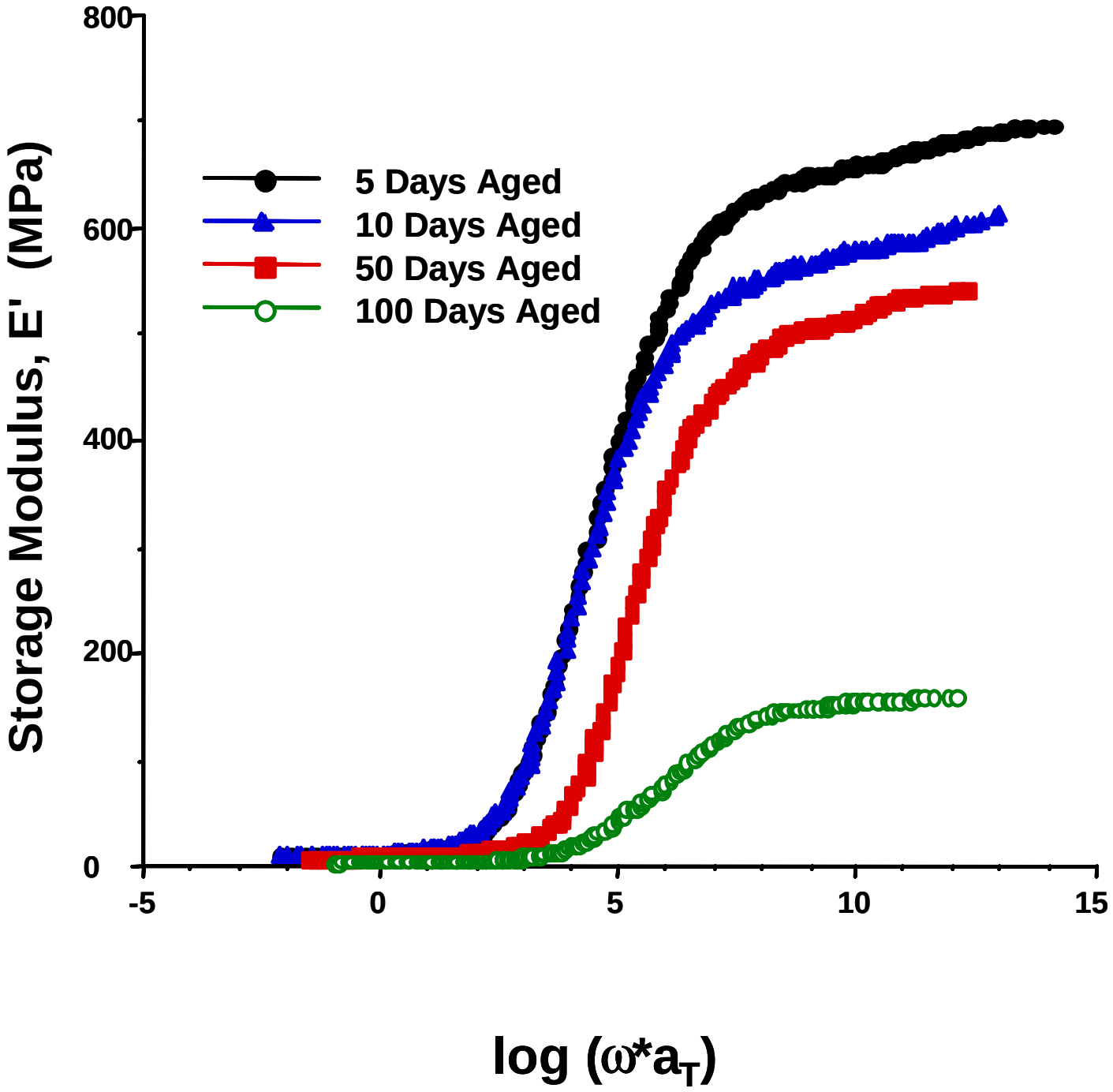

Figure 4-36. Storage modulus master curves for 25% thermoplastic toughened cyanate ester resins aged in an air atmosphere at 177°C for times shown. Cure schedule was three hours at 250°C.

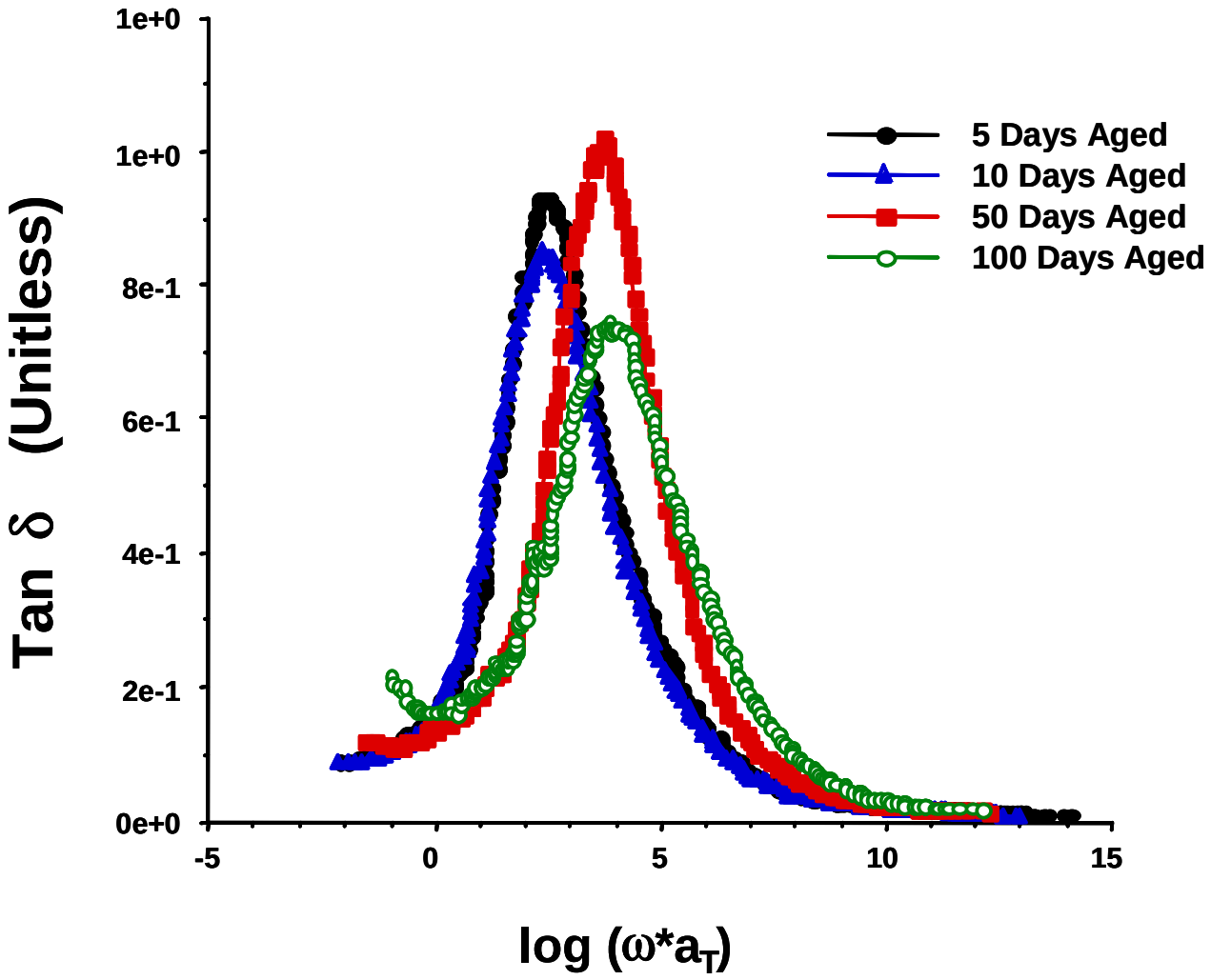

Figure 4-37. Tangent δ master curves for 25% thermoplastic toughened cyanate ester resins aged in an air atmosphere at 177°C for times shown. Cure schedule was three hours at 250°C.

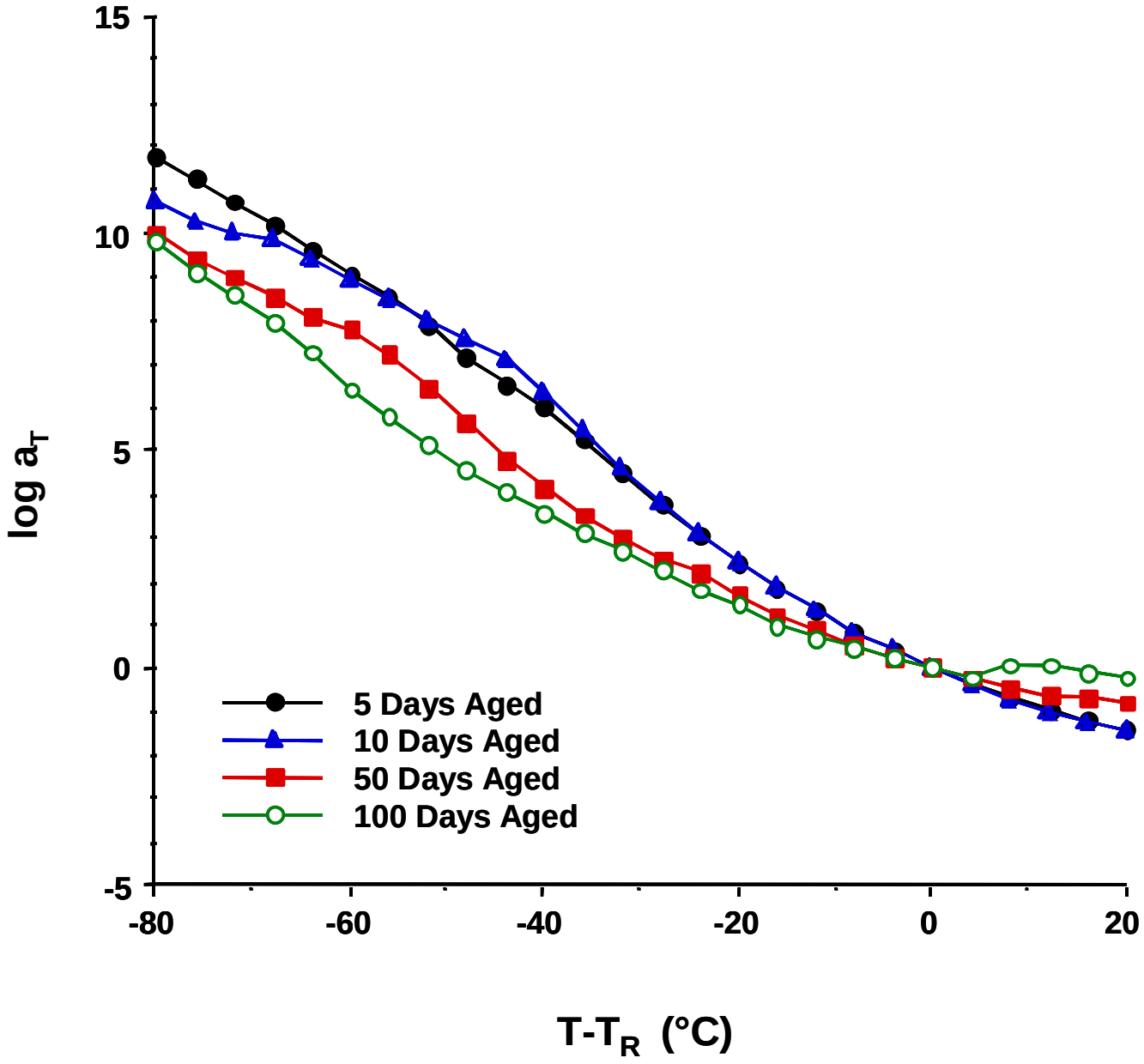

Figure 4-38. Shift factor plots for 25% thermoplastic toughened cyanate ester resins aged in an air atmosphere at 177°C for times shown. Plot corresponds to master curves displayed in Figure 4-36 and Figure 4-37.

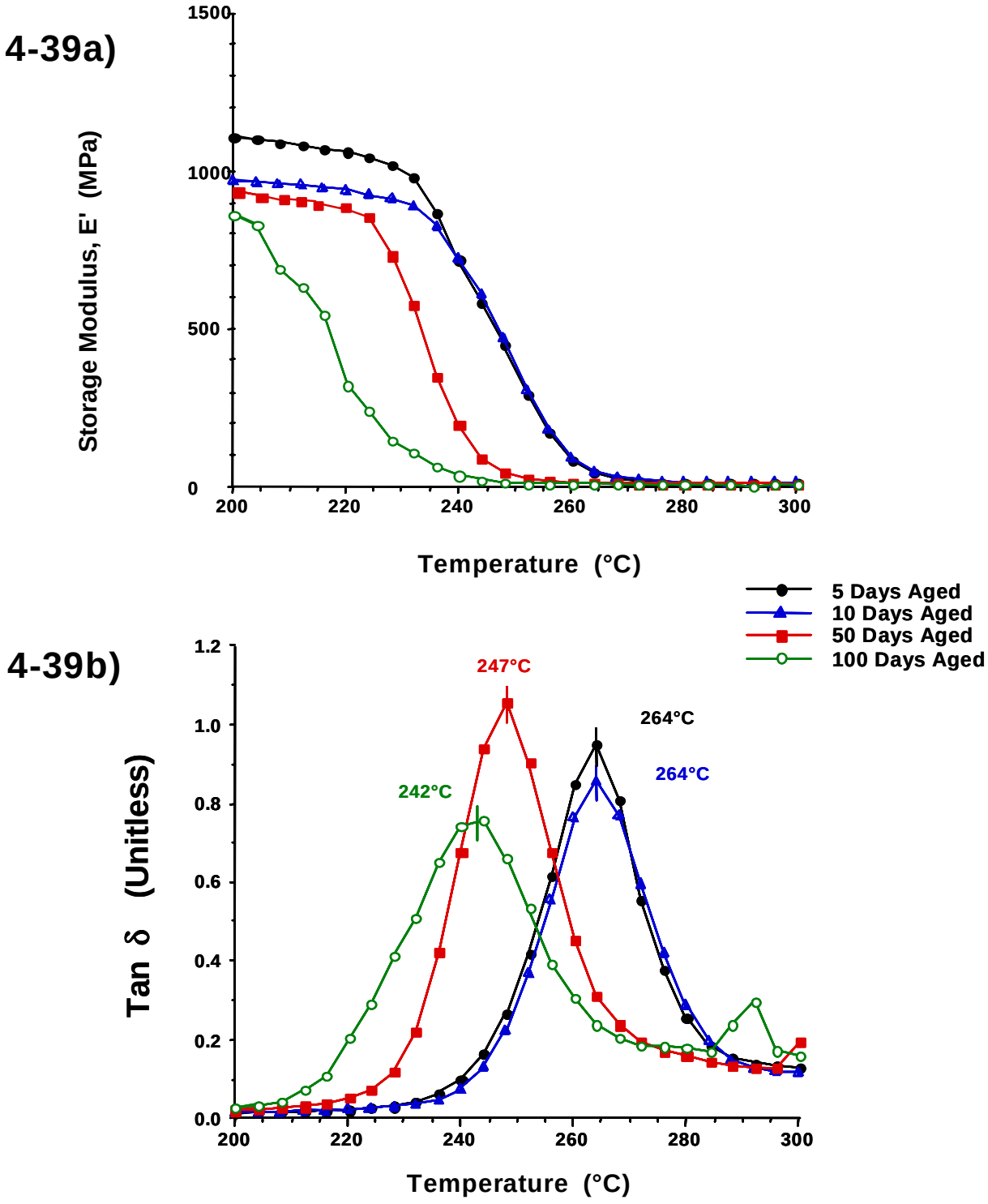

Figure 4-39. Rearranged data for 25% thermoplastic toughened cyanate ester resins aged in an air atmosphere at 177°C for times shown. Data at a frequency of 1 Hz is represented for examination on the temperature axis.

a.) Storage Modulus, E'

b.) tan •δ

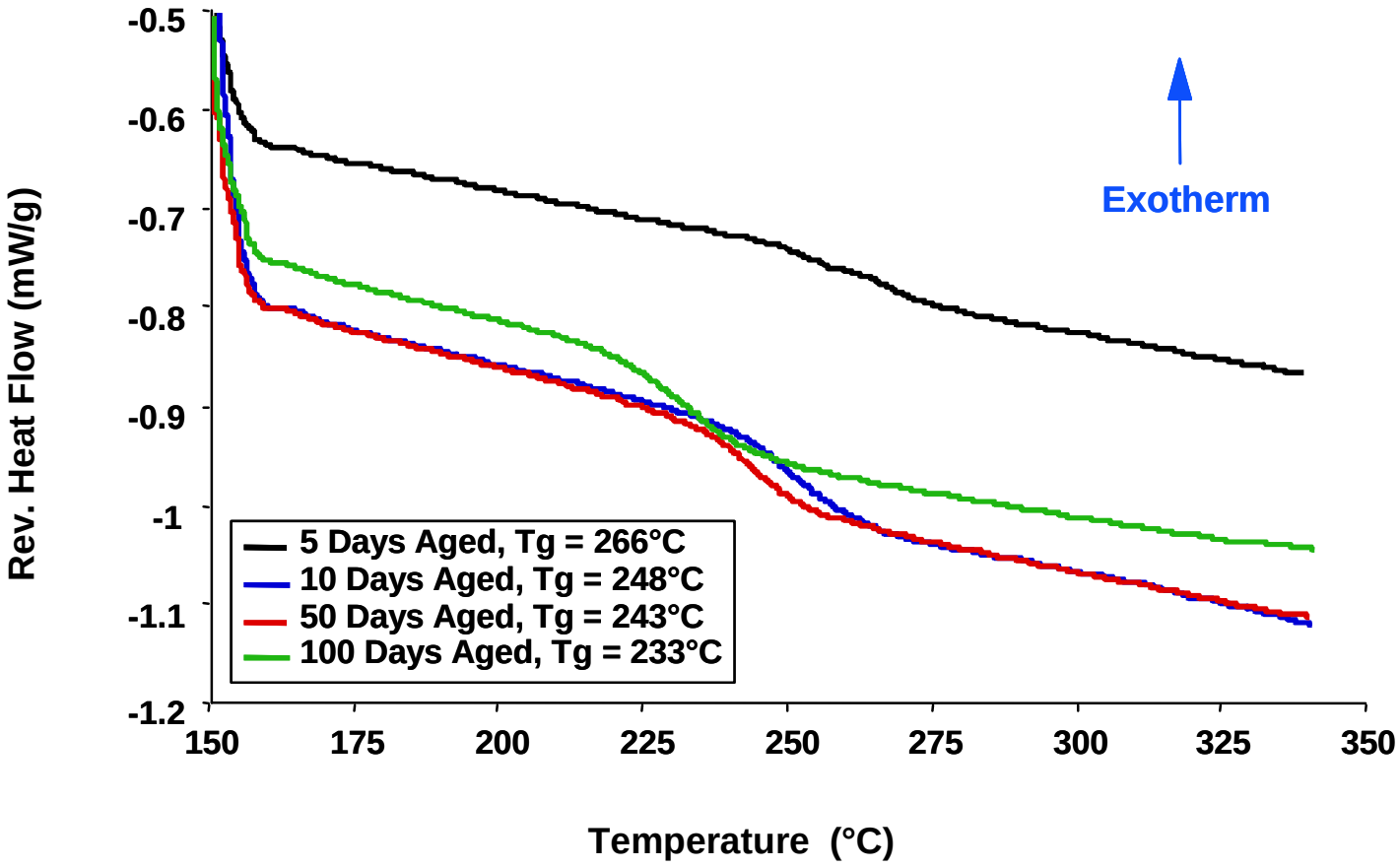

Figure 4-40. Modulated DSC scans of 25% thermoplastic toughened cyanate ester resin samples aged in an air atmosphere at 177°C for the times shown. Cure schedule was one hour at 150°C and two hours at 250°C as a post-cure. T_g was determined using the TA Universal Analysis Software. The midpoint of change in the reversible heat flow was used as the measured value.

4-31 and 4-32). This observation is strengthened by the fact that in a co-continuous material, any changes in the properties of one of the two materials will be reflected in the whole material as a consequence of the continuity of the phases. Therefore, the micro-phase separated samples of this thesis (Figure 3-1a) would be expected to behave differently on a global scale as the cyanate ester material breaks down. One concludes that at some point in the degradation process, the properties of the thermoplastic material would become the dominant behavior of the combined resin as the cyanate ester falls apart.

Figures 4-41 and 4-42 display the family of master curves of storage modulus and tan δ for the micro-phase-separated resins with low temperature cure. The pattern of longer aging producing lower high frequency modulii was reversed between fifty and a hundred days aged. It is postulated that cyanate ester is so thoroughly degraded at this point that the properties of the thermoplastic toughener begin to dominate the mechanical response. Also displayed is the family of shift factor plots for these resins (Figure 4-43). The smoothness of the curves is interesting. Time-temperature superposition requires a simple mechanism of change induced by temperature changes. The fact that two mechanisms are suggested by this research means the continuous nature of the solids obscures each mechanism's impact on the shift factors. Finally, the mechanical responses of these samples are shown as a function of temperature in Figure 4-44. Also, the modulated DSC scans used for determination of T_g behavior (Figure 4-45) appear. An interesting observation

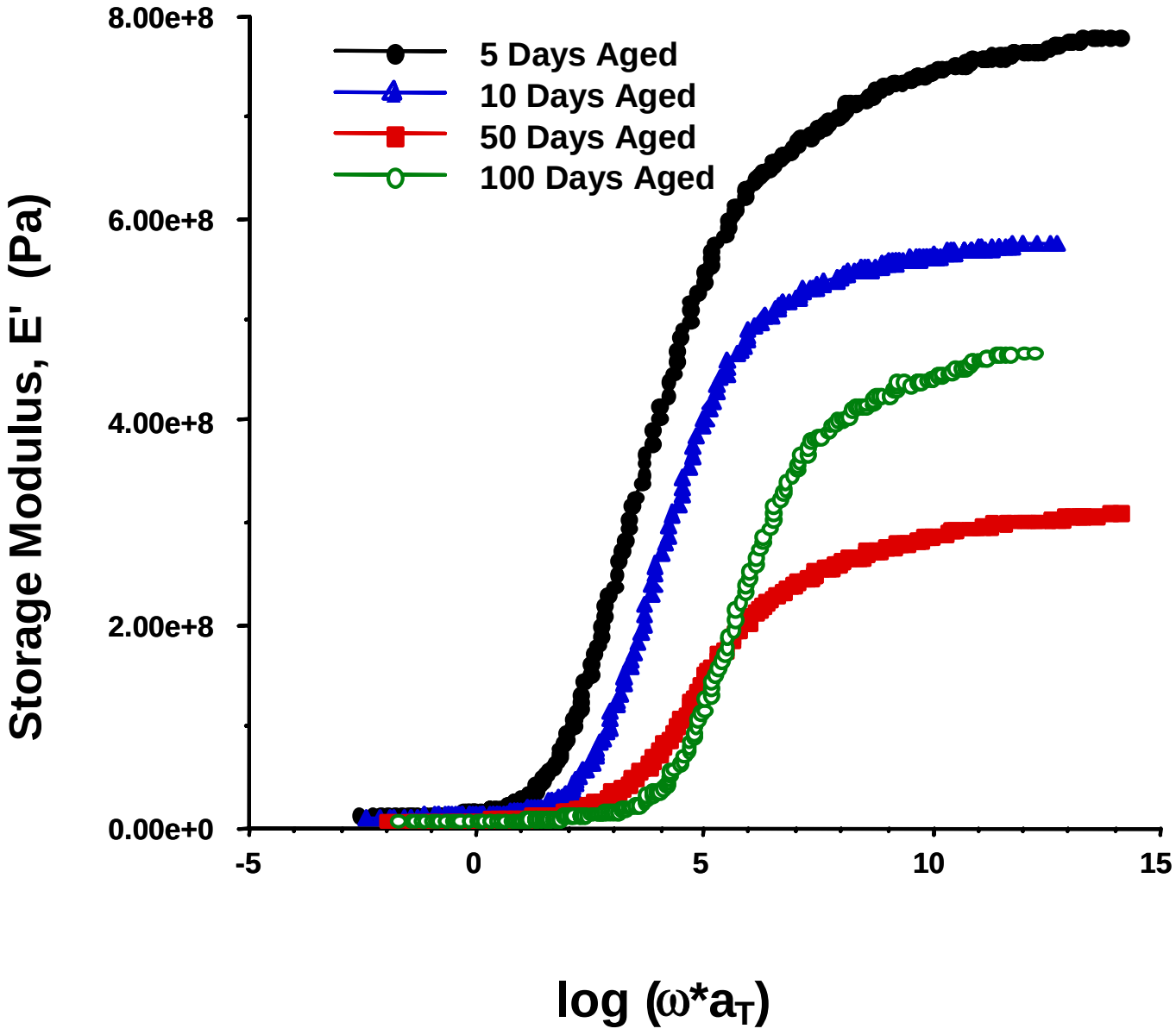

Figure 4-41. Storage modulus master curves for 25% thermoplastic toughened cyanate ester resins aged in an air atmosphere at 177°C for times shown. Cure schedule was one hour at 150°C and two hours at 250°C as a post-cure.

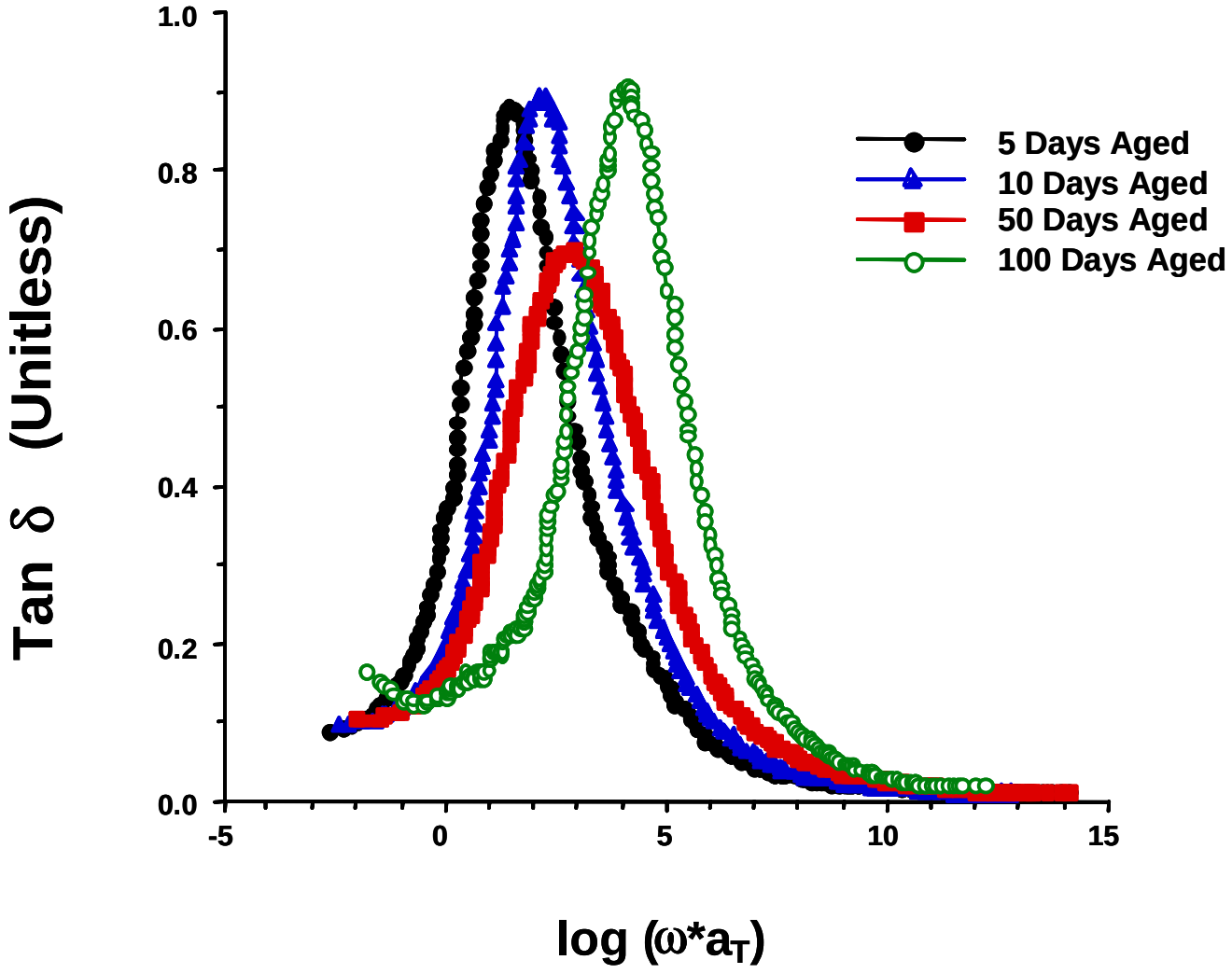

Figure 4-42. Tangent δ master curves for 25% thermoplastic toughened cyanate ester resins aged in an air atmosphere at 177°C for times shown. Cure schedule was one hour at 150°C and two hours at 250°C as a post-cure.

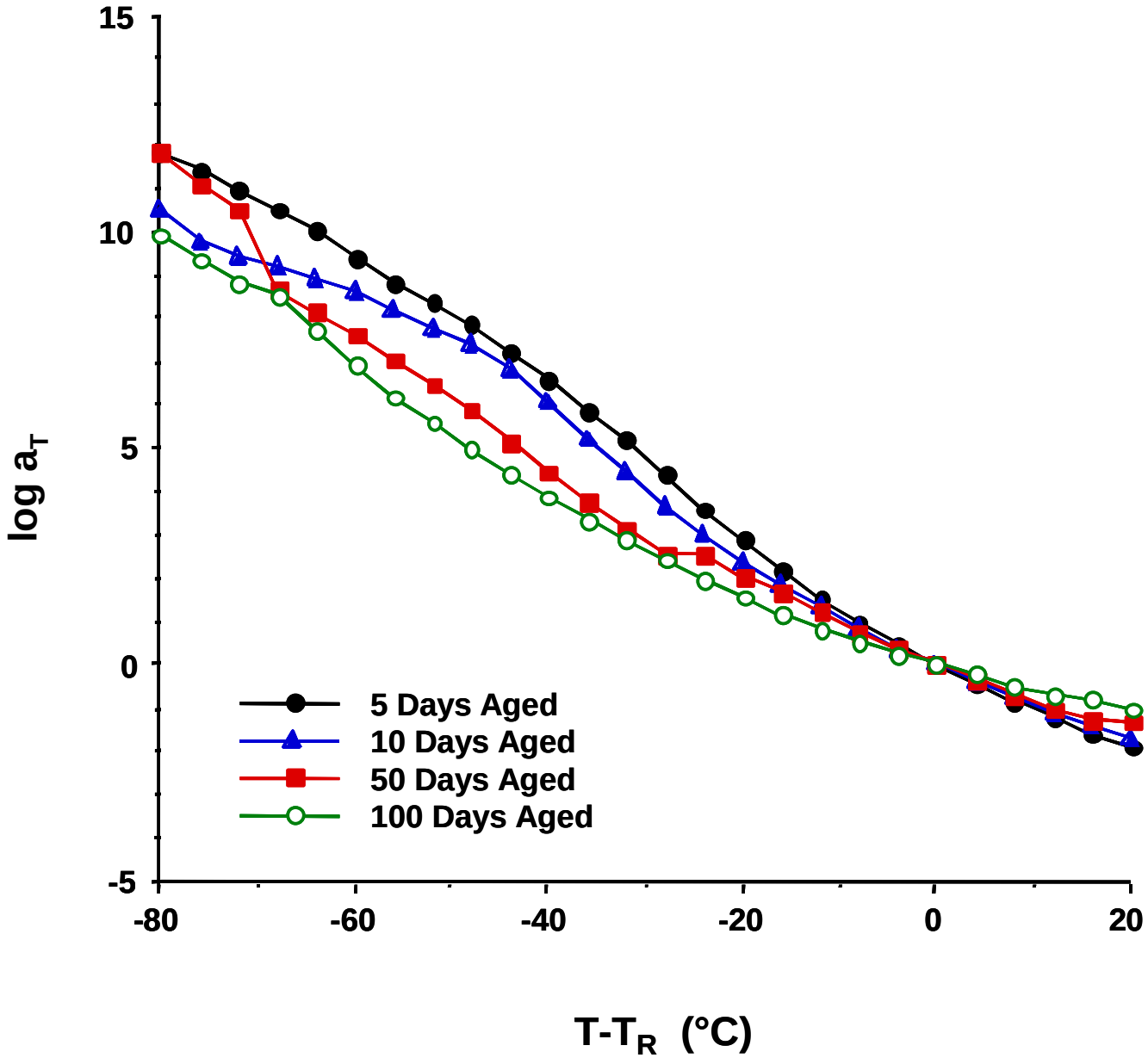

Figure 4-43. Shift factor plots for 25% thermoplastic toughened cyanate ester resins aged in an air atmosphere at 177°C for times shown. Plot corresponds to master curves displayed in Figure 4-41 and Figure 4-42.

4-44a)

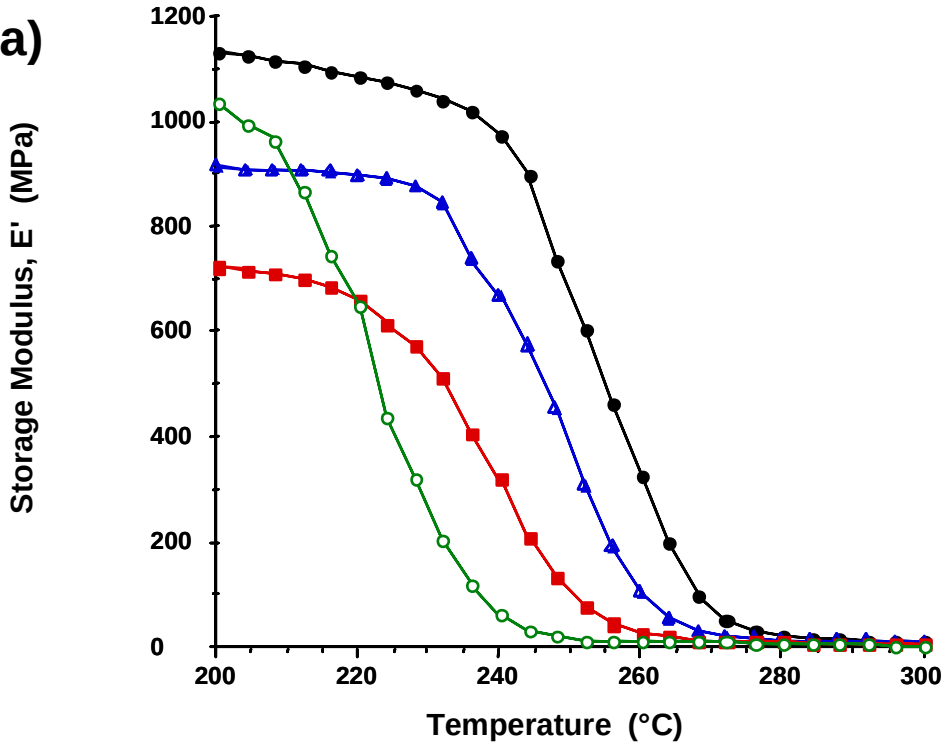

4-44b)

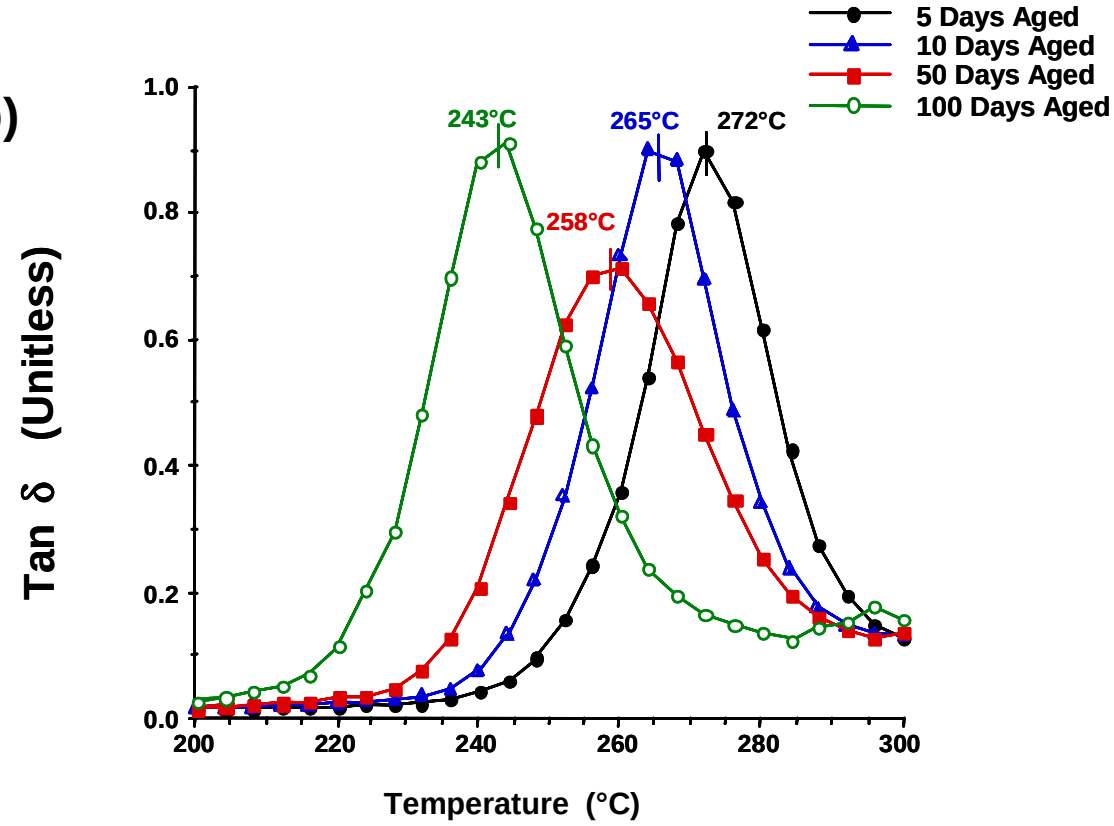

Figure 4-44. Rearranged mechanical data at a frequency of 1 Hz for examination on the temperature axis
a.) Storage Modulus, E'
b.) tan •δ

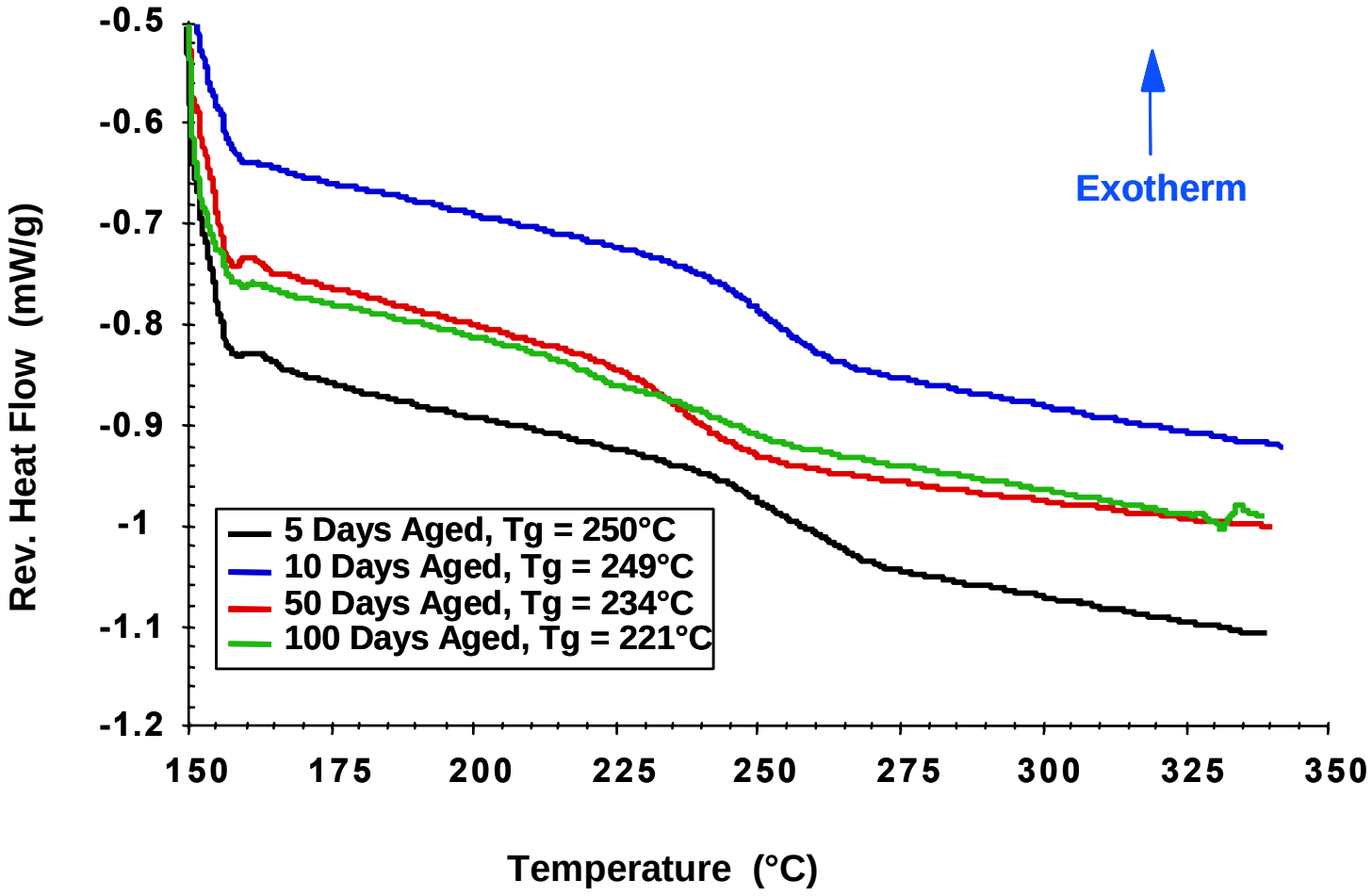

Figure 4-45. Modulated DSC scans of 25% thermoplastic toughened cyanate ester resin samples aged in an air atmosphere at 177°C for the times shown. Cure schedule was three hours at 250°C. T_g was determined using the TA Universal Analysis Software. The midpoint of change in the reversible heat flow was used as the measured value.

arises when comparing Figure 4-41 and Figure 4-44. Although the mechanical properties of the thermoplastic toughener begin to dominate the mechanical response (increase in high frequency modulus between fifty and one hundred days aged), the overall T_g of the material continues to decrease. Also, observed is the substantial decrease in T_g with respect to aging time, which occurs regardless of the phase morphology, suggesting the introduction of a mechanism other than physical aging (i.e. chemical degradation). It is difficult at best to attempt to quantify the chemical aging process in these materials due to the oxygen diffusion controlled nature of the mechanism. Any variation in thickness from sample to sample might defeat the quantitative aspect of the measurements. For example, it can be concluded that relating the behavior observed in the relatively thick samples would be greatly magnified in a thin film or small drop of this material.

4.3.3b 260°C Aging Study, Neat Resin

Aging the cyanate ester resin materials in an air atmosphere at 260°C for any length of time emphasized the deficiencies of these resins for such use. Figure 4-46 contains the results of such a harsh environment on the samples. The disintegration of the material due to chemical degradation as discussed earlier is obvious. As previously stated, it is believed that this degradation initiates at the triazine linkage, leading to volatile gas generation (ultimately NH_3 and CO_2). One of the physical effects of degradation is the decrease in the T_g of the

4-46a.) Nitrogen Aged Samples

0 Days **5 Days** **10 Days** **20 Days** **50 Days**

4-46b.) Air Aged Samples

0 Days **5 Days** **10 Days** **20 Days** **50 Days**

Figure 4-46. Visual Examination of neat cyanate ester resins aged at 260°C. Photographs of actual samples are displayed
a.) Materials aged in a nitrogen atmosphere
b.) Materials aged in an air atmosphere

material as a function of the network breakdown. As the T_g decreases to a temperature below the aging temperature, the volatile gases produced by the degradation cause an expansion in the material, ultimately resulting in the disintegration.

These specimens were so badly degraded after only five days at 260°C, that DMA aging studies could not be performed. Modulated DSC scans were obtained and are displayed in Figure 4-47. These scans show no detectable T_g that indicates the level of chemical degradation. These scans should be compared to those displayed in Figure 4-48 where the samples were aged at the same temperature but in a nitrogen atmosphere. With these latter samples, a T_g does exist and correlates with the DMA measurements displayed in Figure 4-14.

It is obvious from the data above that chemical degradation played a major role in the destruction of the high temperature air aged cyanate ester resins. Thermal gravimetric analyses were performed on these samples in an attempt to quantify the process of chemical degradation. Figure 4-49 displays the TGA thermal traces of weight loss in an air atmosphere for a) samples aged in nitrogen at 260°C and b) samples aged in air at 260°C.

It is clear that even though some discoloration occurred in the nitrogen aged samples (Figure 4-49a), very little difference was observed in the TGA traces as

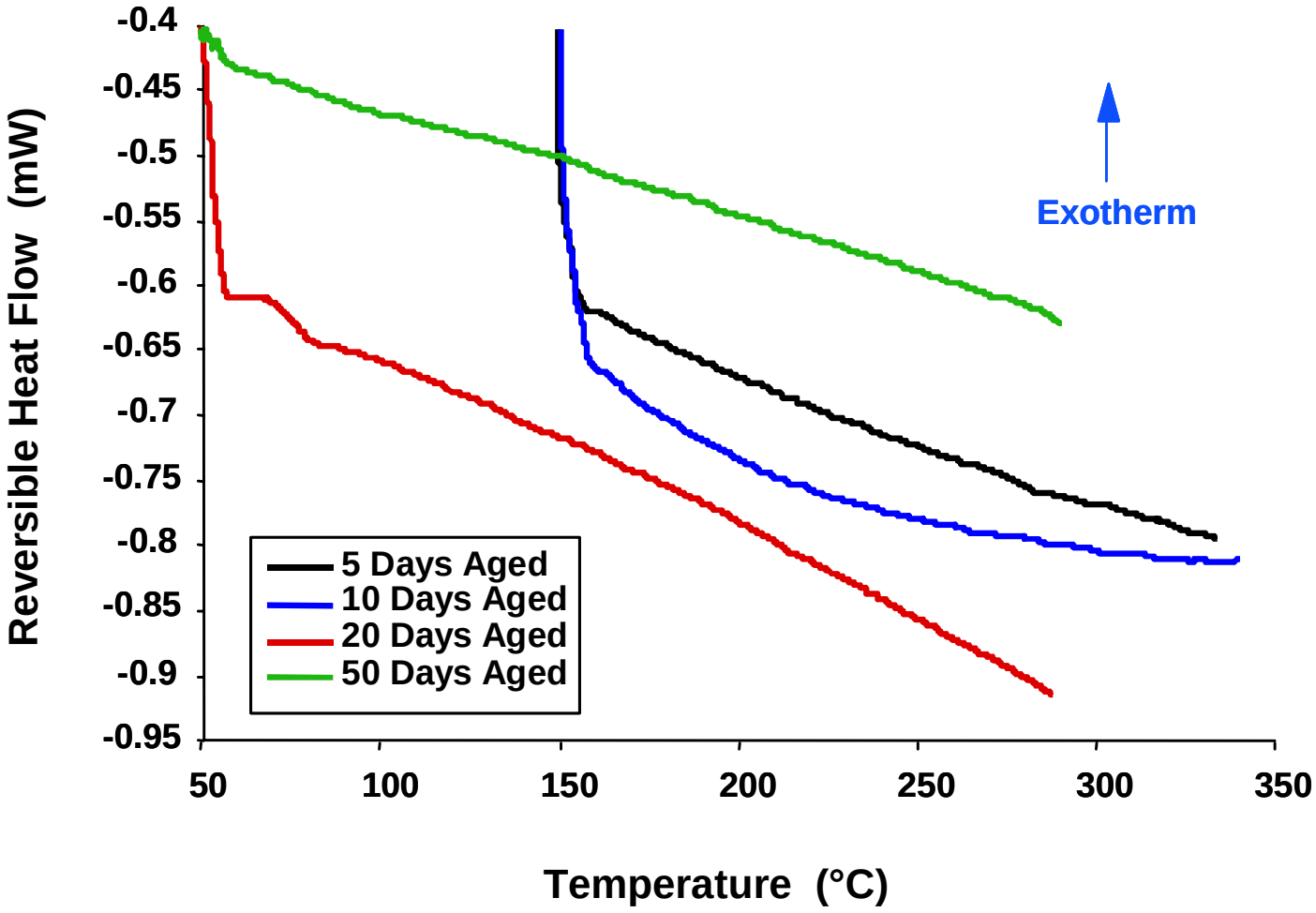

Figure 4-47. Modulated DSC scans of neat cyanate ester resin samples aged in an air atmosphere at 260°C for the times shown. No discernable T_g observed.

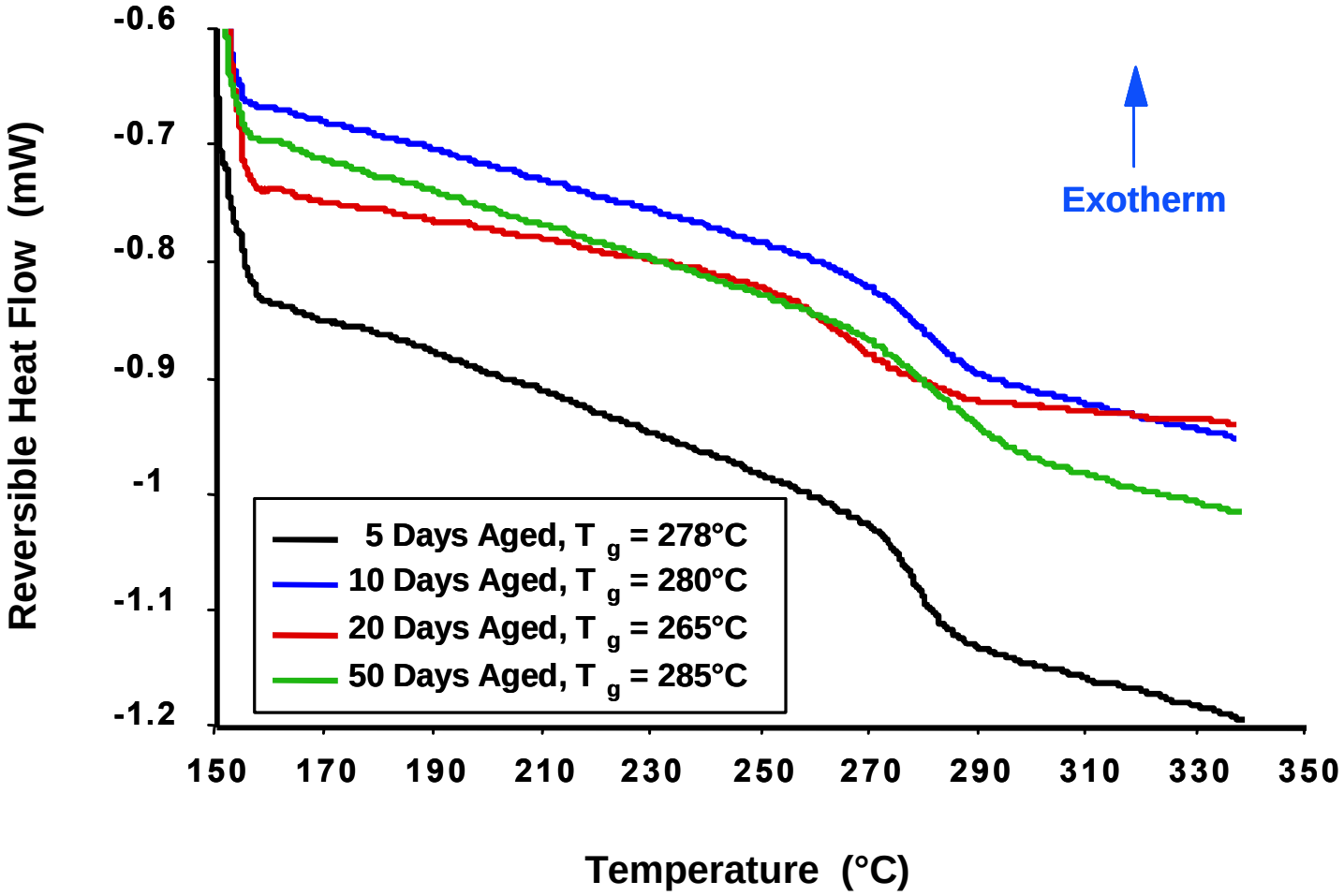

Figure 4-48. Modulated DSC scans of neat cyanate ester resin samples aged in a nitrogen atmosphere at 260°C for the times shown. T_g was determined using the TA Universal Analysis Software. The midpoint of change in the reversible heat flow was used as the measured value.

4-49a. Nitrogen Aged Samples

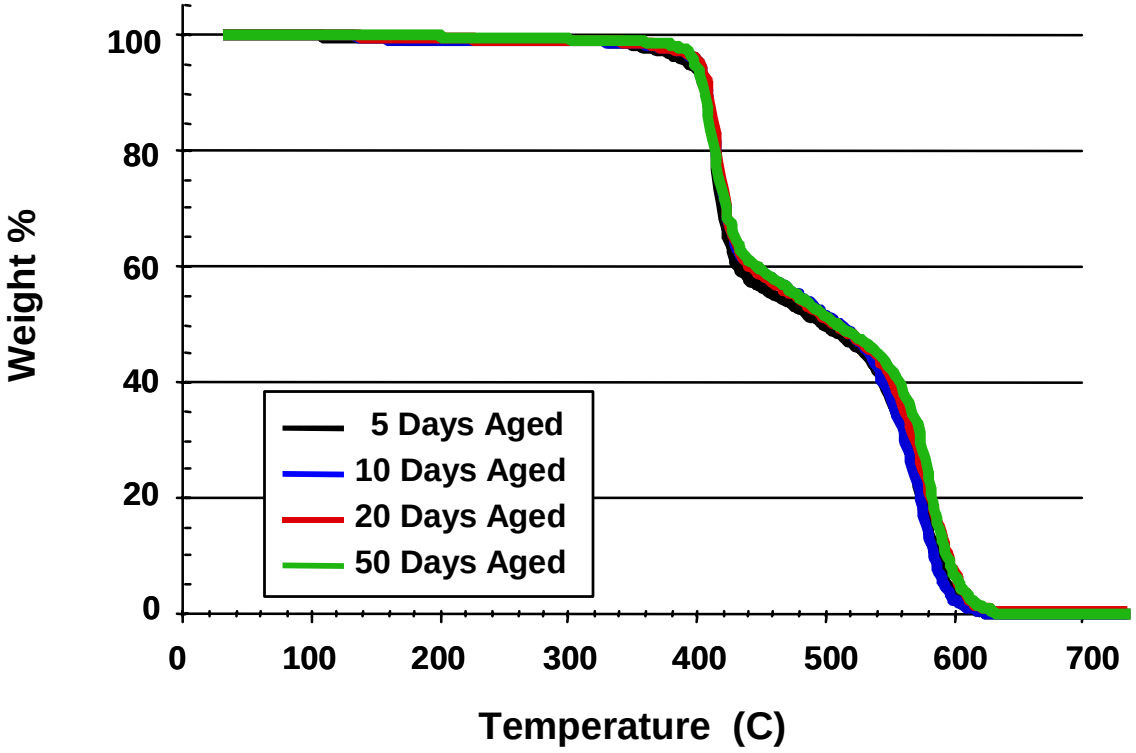

4-49b. Air Aged Samples

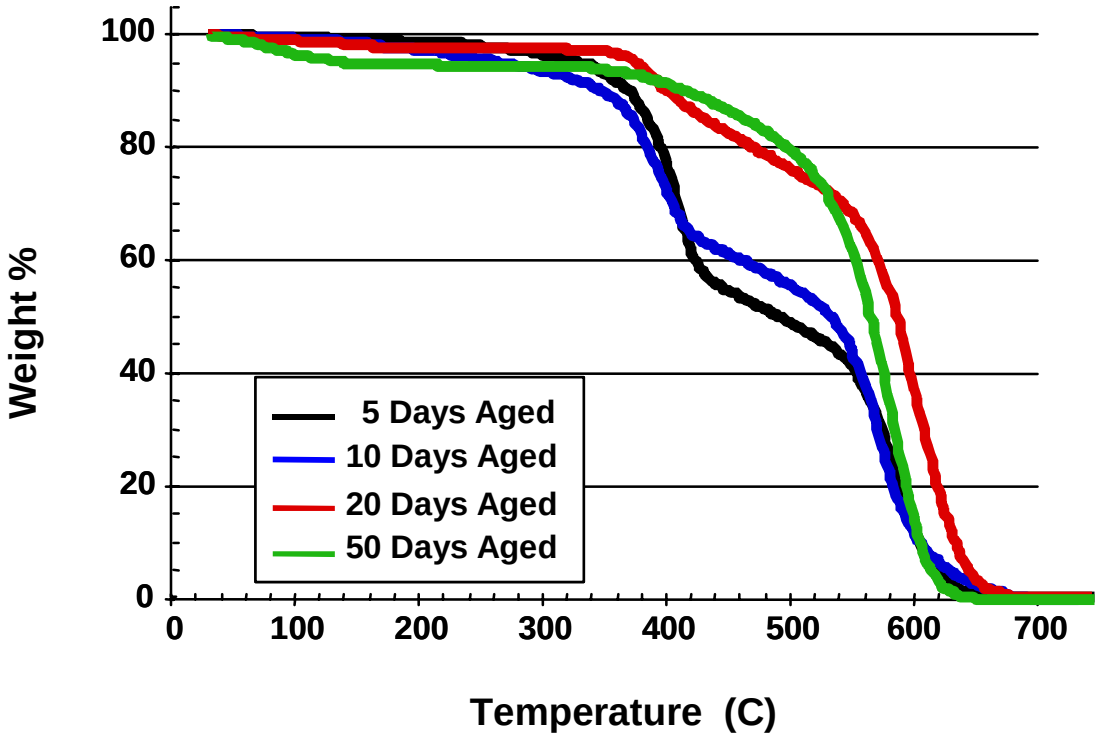

Figure 4-49. TGA thermal traces in air of neat cyanate ester resins aged at 260°C for times shown.
a.) Aged in nitrogen
b.) Aged in air

a result of aging. Therefore, physical aging in the resins aged in nitrogen, the remaining mechanism, is left to explain the results of Figure 4-11 and Figure 4-12.

The air-aged samples are quite different in their TGA analysis. Figure 4-50 displays an expanded view of the thermal traces for the air-aged samples. As is the case with many organic materials degraded in an oxygen rich atmosphere, there exists a two-step decomposition process. At some point during the degradation, oxygen in the atmosphere couples with the organic matter, crosslinking the material into an intermediate state. This is observed in the TGA thermal trace as a "knee" or plateau region. Increased temperatures force the breakdown of the crosslinked intermediate and ultimately turn the entire sample into gases, which are vented from the instrument. Focusing on the plateau regions displayed in Figure 4-50, it is clear that with increasing aging time, the plateau shifts dramatically to higher weight percent and to lower temperatures. This behavior indicates that an increased amount of chemical degradation has occurred in the samples that were aged for longer times in air prior to TGA testing.

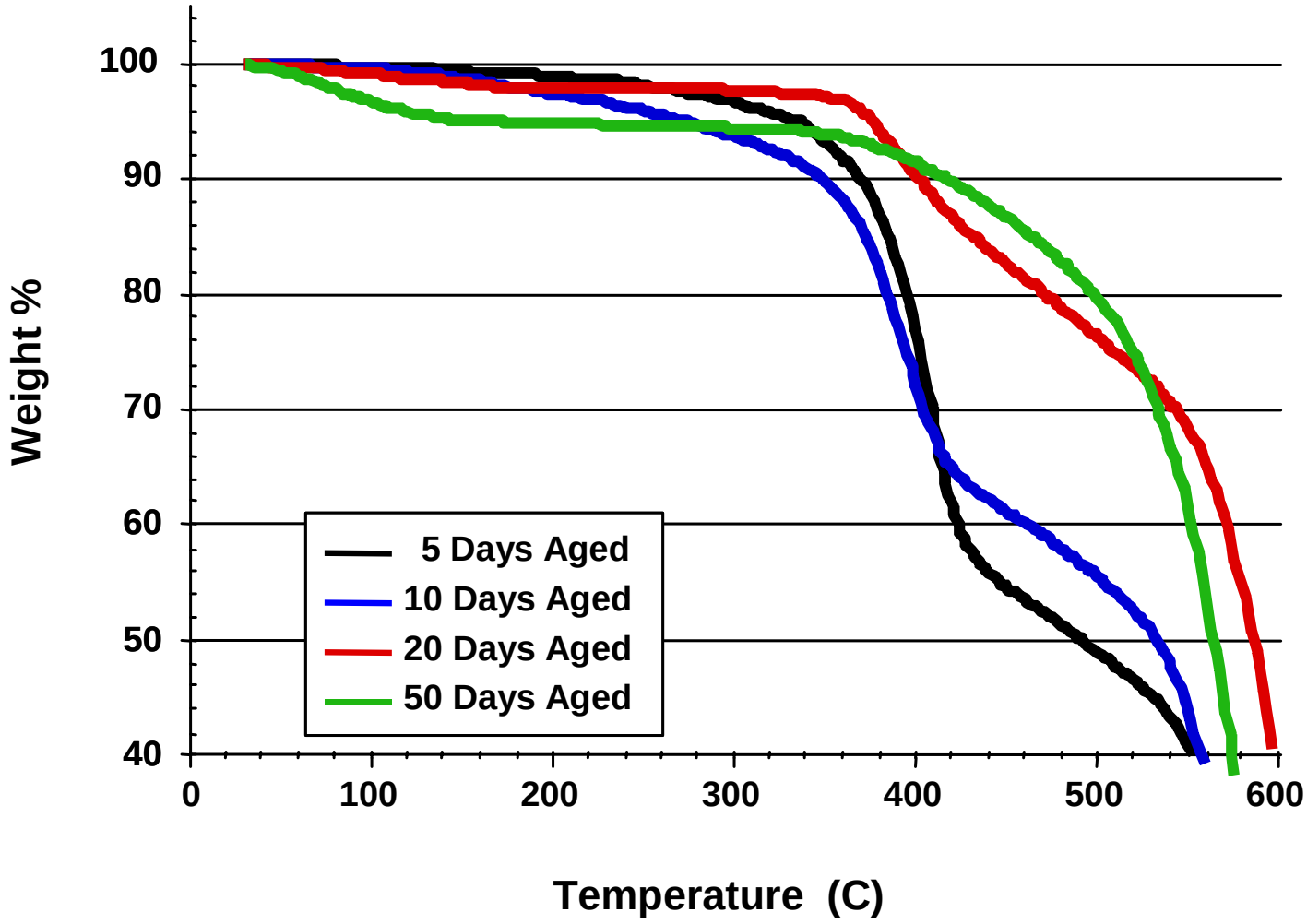

Figure 4-50. Expanded view of TGA thermal traces performed in air of neat cyanate ester resin samples aged in air at 260°C for times shown.

5.0 Summary and Conclusions

The research goal presented in this manuscript was to characterize the long term mechanical properties of cyanate ester resins, to develop a method for determining the effects of physical and chemical aging on the mechanical properties, and specifically to evaluate the AroCy B-10 cyanate ester resin for use in high temperature applications. A secondary goal was to see what influence a thermoplastic toughener had on the above results. A quench/ anneal study was first performed on the cured resins to develop an understanding of the density extremes available and to help the physical aging analysis. This study indicated that competing mechanisms of physical aging and chemical degradation were responsible for the observed variations in the measured mechanical data. An intermediate cooling cycle supported such a competing mechanism behavior.

Separation of chemical and physical aging was accomplished by aging the cyanate materials under different atmospheres and at different temperatures. Aging the cyanate ester resins in nitrogen at a temperature (260°C) very close to its T_g (280°C) yielded a family of storage modulus and tan • master curves, which efficiently pointed out the effects of physical aging alone on the cyanate ester resins. This conclusion as to the aging mechanism in nitrogen relied on an increase in the initial modulus with aging time as well as an increase in the T_g of the material with aging. Through TGA analyses, it was also determined that

chemical degradation was not a significant factor in the mechanical behavior of the nitrogen aged samples, even though slight sample discoloration occurred following the aging process and in an inert atmosphere.

A second nitrogen aging study was performed at a lower aging temperature (177°C). This temperature was chosen partially because it is an expected application temperature for this class of cyanate ester resins. The aged samples displayed some signs of physical aging, but to a much lesser extent. The initial storage modulus did increase with aging time. However, there was no change in the T_g of the samples. The conclusion is that the aging temperature was too far below the T_g of the material for any significant physical aging to occur over the time frame of the experiment.

Although the nitrogen atmosphere aging studies displayed the classic signs of physical aging, an important aspect of this research was to characterize the behavior of these resins closer to actual application conditions. Therefore, aging studies were performed in an air atmosphere at 260°C aging temperature. Severe chemical degradation progressed to the point of material disintegration and the loss of all structural integrity in such cases. Obviously, dynamic mechanical analyses could not be obtained from these weakened samples. MDSC scans displayed no discernable $T_{g,}$ and TGA analyses supported the severe oxidative degradation process that occurred in the specimens.

Samples aged in air at 177°C also displayed signs of chemical degradation, but to a much lesser extent. Samples were examined mechanically and families of master curves were generated. The mechanical property master curves as well as DMA temperature scans displayed a radical decrease in the initial modulus and a large decrease in T_g produced by increasing aging. The T_g shift was confirmed by MDSC analysis and was revealed to be well over 50°C lower after one hundred days under the aging conditions. The results discussed above are all obtained on the non-toughened, identically cured resins.

Two curing cycles were examined as a compliment to the aging studies performed on the thermoplastic toughened resins discussed below. Changes in the aging process due to cure cycle were negligible. This was confirmed by MDSC where little change in the T_g behavior was observed.

The aging studies in air at 177°C, performed on 25% thermoplastic toughened cyanate ester resins resulted in some interesting mechanical behavior. Before the aging study, distinct morphology variations were developed in the materials as a result of the cure cycle chosen. A low temperature cure cycle (1 hour at 150°C and 2 hours at 250°C) resulted in a micro-phase-separated morphology with the micro-phases being the thermoplastic toughener and the continuous support phase being the cyanate ester resin. When aged, this toughened material (cured with the low temperature cycle) displayed very little variation from the neat resins aged under similar conditions. A high temperature cure cycle (3 hours at 250°C) yielded a co-continuous phase morphology. When aged, in

contrast, this series of resins displayed a reversal in the mechanical trends, and this suggested the thermoplastic phase had started to dominate the mechanical properties. This reversal in behavior was confirmed by observing the T_g of the materials both by DMA and MDSC. The T_g trends in the co-continuous material were similar to the trends observed in the neat resin and the micro-phase-separated material. This would be expected considering that 75% of the material was cyanate ester resin.

Finally, it is important to give an overall conclusion to the research presented here and to comment on where the research may progress. From the results obtained on these samples' behavior at elevated temperatures in air, it is clear that such materials are unpredictable at these application temperatures. Other polymers should be sought for the desired applications in order to better withstand the harsh environments required of the application. According to some of the papers presented at the Cyanate Ester Symposium held during the Fall 1994 American Chemical Society Meeting in Washington D.C., major research efforts are underway to alleviate some of these problems. One of the most promising developments is the incorporation of halogenated compounds into the cyanate ester backbone.

This research has also uncovered areas in which new and useful projects could be developed. Development of an adequate normalization function, horizontally shifting the normalized data, and developing a master-master curve of aging or humidity with respect to time and temperature, would allow the prediction of

material behavior over several property axes simultaneously. Finally, it would be expected that the incorporation of antioxidants into the cyanate ester network structure would greatly alleviate some of the chemical degradation observed in this work.